Review Responses for: A global anthropogenic emission inventory of atmospheric pollutants from sector- and fuel-specific sources (1970–2017): An application of the Community Emissions Data System (CEDS)" *by* Erin E. McDuffie et al.

We thank both Reviewers for their comments, which have helped improve the quality and clarity of our manuscript describing the $CEDS_{GBD\text{-}MAPS}$ dataset. We have responded to each comment below. The original comments are in black, our responses are in blue and the changes to the manuscript text are in *blue italics*. Overall, the dataset remains unchanged, but we have added two additional supplemental figures and 1 supplemental table to address reviewer-specific concerns. All other manuscript changes are related to clarifying the CEDS methodology or descriptions of the final dataset. Changes were made to maintain a similar manuscript length, while providing improved clarity, context, and interpretation of major features. Line numbers in our responses below correspond to the re-submitted (non-tracked) version of the manuscript.

Anonymous Referee #1

McDuffie et al. Describe an update to the global emission inventory of atmospheric pollutants from the Community Emissions data System (CEDS). The updated dataset improves upon the earlier release of the CEDS inventory by adding additional emission sectors, separating emissions by fuel type, extending the timeseries to 2017, and updating the regional inventories used to "calibrate" the emissions corresponding regional sections of the global domain. The new CEDS inventory is currently the most up to date global emission inventory available to the community that is based on reported data. This fact, along with the new features provided with this data release, should make the inventory very attractive to global atmospheric chemistry modellers.
The manuscript describing the dataset is generally organised and written well. A lot of detail goes into such emission inventories, and the authors have found a good balance between including information in the manuscript, the supplement, and as references to other work. As well as describing the methodology of constructing the inventory, the resulting dataset itself is also presented and described, as well as compared to other global inventories, including the previous version of the CEDS inventory. Uncertainties are also discussed.
My only major comment on the manuscript concerns the calibration procedure. It is obviously a strength of the CEDS approach that regional emissions are scaled using detailed regional inventories where they are available. In this way, more detailed local information can be incorporated than would typically be the case for completely globally consistent inventories such as EDGAR or GAINS.

We thank this reviewer for their thoughtful comments and concerns. First, we note that per the suggestion of Reviewer #2, we have changed the terminology throughout the manuscript to now describe the original 'calibration' procedure as the 'scaling' procedure. We agree with Reviewer #2 that the term 'calibration' implies too great a level of certainty and accuracy in the regional and global inventories.

What is not clear to this reviewer is the necessity of also scaling the "default emission estimates" calculated in "Step 1" of the CEDS workflow to "existing, authoritative" global inventories (such as EDGAR and GAINS). Given the general uncertainties in emission inventories, would it not be valuable to have an additional semi-independent global inventory in addition to these two established inventories? Of course, a lot of the information used in constructing the CEDS inventory is shared with, or derived from the other global inventories, so a completely independent emissions inventory would be very difficult to compile.

The Reviewer is correct that regardless of default emission scaling, information from both EDGAR and GAINS global inventories are used to develop the $CEDS_{GBD\text{-}MAPS}$ (and core CEDS) inventory. The original aim of CEDS was not to generate a completely new independent inventory, but to use a consistent and reproducible methodology, while also leveraging information from regional and country-specific inventories to generate historical emission time series with consistent sectoral and fuel-type definitions across all years and all world countries. EDGAR already exists as a consistent, global inventory developed using consistent assumptions, so we do not need to re-invent that work.

This reviewer would however like to see some more discussion of why it is necessary to calibrate the total CEDS emissions using other global inventories.

Section 2.1 describes how the default CEDS combustions source emissions are estimated using a combination of energy consumption data from the International Energy Agency and Emission Factors from other inventories such as GAINS and the US NEI. The GAINS EFs are only available for more aggregate regions, whereas the EDGAR inventory has country-specific emission estimates for all countries. Scaling to the EDGAR inventory is therefore meant to better account for country-specific information in the CEDS combustion emission estimates in locations where country-specific information was not available for the default estimates. We do note however that for countries that are later scaled to other regional inventories (shown in Fig. 2), the initial scaling to the EDGAR inventory should have a limited effect on the final emission values. We have added the following text to the main manuscript to clarify this point.

Line 310– *For example, global $CEDS_{GBD\text{-}MAPS}$ combustion source emissions of NO_x, total NMVOCs, CO, and NH_3 are first scaled to EDGAR v4.3.2 country-level emissions as a means to incorporate additional country-specific information relative to default estimates derived using more regionally-aggregate EFs from GAINS.*

Related to this point, it would also be very interesting to know the size of the "scaling factors" which are applied in "Step 2" to calibrate the CEDS default emissions with the other global inventories. These numbers to not appear to be presented in the manuscript or the supplement.

Scaling factor limits are set following the original CEDS protocol so that these factors do not exceed the range of 1/100 to 100. For a select number of sectors and countries, these limits are extended to 1/1000 to 1000 to ensure better agreement between the final $CESD_{GBD\text{-}MAPS}$ emission totals and the regional inventories, as was described in Section S2.3.2. To clarify, we have added the following sentence to the Supplement.

Supplement - Line 170 - *Following original CEDS protocols, scaling factors are limited to values between 0.01 and 100, with select inventories and sectors expanded to a range of 0.001 and 1000, as described in Supplemental Section S2.3.2. As discussed in Hoesly et al. (2018), particularly small or large scaling factors may result for multiple reasons, including default CEDS estimates that are drastically different than regional emissions or imprecise mapping between CEDS and regional emission sectors.*

At the Reviewer's request, we have additionally provided a supplemental table of example scaling factors for a sub-set of African countries and years (Table S4). As stated in the main text, small and large scaling factors may result from largely different emission estimates in the default inventory relative to the regional inventories and/or imperfect mapping between the CEDS and regional inventory sectors.

Supplement - Line 169: *Example scaling factors for select years and countries in Africa, as a function of scaling sector are provided in Table S4. Data are included for illustrative purposes only.*

Table S4. Example BC scaling factors for select DICE-Africa countries and years.

Country (ISO)	Scaling Sector	Scaling Fuel	2006	2007	2008	2009	2010	2011	2012	2013	2014	2015
ago	residential	biomass	0.332	0.338	0.344	0.350	0.355	0.361	0.367	0.373	0.373	0.373
ago	residential	light oil	0.340	0.311	0.282	0.252	0.223	0.194	0.165	0.136	0.136	0.136
ago	road_ transport	gas_ diesel	0.307	0.293	0.278	0.264	0.250	0.235	0.221	0.207	0.207	0.207
nam	residential	biomass	0.297	0.320	0.342	0.364	0.386	0.409	0.431	0.453	0.453	0.453
nam	residential	light oil	44.71	44.72	44.72	44.72	44.73	44.73	44.73	44.74	44.74	44.74
nam	road_ transport	gas_ diesel	0.274	0.260	0.247	0.234	0.220	0.207	0.194	0.180	0.180	0.180

I also have one minor, and one extremely minor comment.
The minor comment relates to data availability. It is great that the CEDS inventory as well as the code is made available to the public. But what about the input data which are necessary for the CEDS code to run? While the data sources do all appear to be well referenced, it would be nice to see some comment in Section 5 on how freely available the input data sets are. This would of course influence the feasibility of other groups being able to reproduce the CEDS emissions using the CEDS code.

We have added the following sentence to section 5.
Line 858: *To run the CEDS system, users are required to first purchase the proprietary energy consumption data from the IEA (World Energy Statistics; https://www.iea.org/subscribe-to-data-services/world-energy-balances-and-statistics). The IEA is updated annually and provides the most comprehensive global energy statistics available to-date. All additional input data are available on the CEDS GitHub repository.*

The extremely minor comment relates to the presence or absence of seasonal cycles in the gridded emission data. While it seems clear that the gridded CEDS data do include a seasonal cycle, in two places (lines 250 and 790), these data are referred to as "annual" fluxes, implying strongly that they are annual averages. Perhaps this should be corrected to something like "seasonal cycles of annual . . . fluxes".

We have replaced the incorrect use of 'annual fluxes' on original lines 250 and 790 with 'monthly fluxes'. The seasonal profiles are primarily from the ECLIPSE project as mentioned in Section 2.1.

Line 257 - *Final products from the $CEDS_{GBD\text{-}MAPS}$ system include total annual emissions from 1970 - 2017 for each country, as well as monthly global gridded (0.5 °×0.5 °) emission fluxes…*

Line 862 - *Final products from the $CEDS_{GBD\text{-}MAPS}$ system include total annual emissions for each country as well as monthly global gridded (0.5 °×0.5 °) emission fluxes for the years 1970 – 2017.*

Reviewer #2 – Hugo Denier van der Gon

The paper describes an interesting new global emission Inventory (CEDSGBD-MAPS) for atmospheric pollutants (1970 – 2017) based on the so-called mosaic approach based on the Community Emissions Data System (CEDS). The paper is generally well-written and deserves to be published but I do have several concerns where I would ask for adjustment or further explanation. A problem with emission inventory papers is that one tries to describe a complete set for all pollutants, all source sectors, all countries and many years. It is impossible to write a paper on this that documents, explains & discusses all and is still readable. Choices have to be made. The intention of my review is not to be a dictate. Part of my comments will relate to choices made and I do not demand that all answers to my comments find their way into the paper. If the authors have good reasons for not adjusting something, they can explain themselves.

We thank the Reviewer for their thoughtful and detailed comments. We recognize the Reviewer's expertise and experience in this field and have addressed their comments accordingly. The changes and additions described below have greatly improved the quality and clarity of this manuscript.

The mosaic approach is not new and was previously successfully applied for example in the framework of HTAP by Janssens-maenhout et al (2015). This is an often used mosaic inventory. The approach by Janssens-maenhout et al differs from the approach taken in this paper and I think this should be briefly discussed in the introduction. Also to make clear that mosaic inventories are becoming a more frequently followed approach.

We have made adjustments to sentences in the Introduction and Methods sections to provide further context on the use of the 'mosaic' development strategy.

Line 95 - *In contrast to EDGAR and GAINS, the CEDS system implements an increasingly utilized mosaic approach, which, in this case, incorporates activity and emission input data from other sources such as EDGAR, GAINS, and regional/national-level inventories to produce global emissions that are both historically consistent and reflective of contemporary country-level estimates (Hoesly et al., 2018).*

Line 202 - As described in Hoesly et al. (2018), CEDS uses a "mosaic" scaling approach to retain detailed fuel- and sector-specific information across different inventories, while maintaining consistent methodology over space and time. The development and use of mosaic inventories has been recently increasing as they provide a means to utilize detailed local emissions, while harmonizing this information across large regional or global scales (Li et al., 2017;Janssens-Maenhout et al., 2015). The CEDS approach, however, differs from previous mosaic inventories, such as that developed for the HTAP project (Janssens-Maenhout et al., 2015), as local and regional inventories in $CEDS_{GBD\text{-}MAPS}$ *are used to scale sectoral emissions at the national-level, rather than merging together spatially distributed gridded estimates.*

A more fundamental problem is the term “calibration inventory” that is coined in the paper. Calibration is the comparison of measurement values delivered by a device under test (or a system) with those of a calibration standard of known accuracy. However, I think it is fair to say that the authors don’t know the accuracy of their calibration inventories. They motivate that regional or national inventories may include more national/regional knowledge and are therefore more accurate. This was also the motivation for e.g. the earlier HTAP_v2.2 mosaic inventory. It may well be true (and this reviewer firmly believes in the usefulness of mosaic inventories) but a) we don’t know for sure if the regional inventory is really better and b) we don’t know how accurate exactly. Good enough for calibration? In my opinion the term calibration adds too much certainty to a more empirical and intuitive solution for an operational problem. It reads well but in reality it is more fitting or scaling than calibrating. In e.g. line 213 is also stated that scaling factors are calculated in the calibration procedure . Apparently scaling is seen as calibrating. Should the authors really think that calibration is still the best terminology some additional clarification/disclaimer is needed to avoid “whitewashing” of something still uncertain (scaling) by calling it certain (calibrating). [see also the confusion created in line 360-365 between scaling and calibration and the remark that BC / OC are not scaled due to large uncertainties in EDGAR – but how well do you know that other inventories are much less uncertain?]

We appreciate this comment and in retrospect, agree that the term ‘calibration’ provides too much weight to the accuracy of the regional inventories. While the accuracies of some regional inventories have been quantified (e.g., Venkataraman et al., 2018), we agree that the term ‘calibration’ is not appropriate in this context. We have changed all instances and variations of the term ‘calibration’ to ‘scaling’ throughout the main text, supplement, and figure and table captions. Similarly, the ‘calibration inventories’ are changed to ‘scaling inventories’. These changes are now also in better alignment with the original CEDS description in Hoesly et al. (2018).

An advantage of the mosaic approach is the inclusion of more locally / nationally representative inventories in the global emission map. A disadvantage is that the emissions from different regions become apples and oranges. Obviously still the same species but the underlying choices are no longer necessary the same. It would be interesting for some of the more uncertain species like CO, NMVOC or BC to show a plot comparing some implied emission factors for certain source sectors for e.g. Africa, India, China, Former Soviet Union. What is the range in these implied EFs and based on expert judgement of the authors do these ranges seem plausible? This may be used to flag some of the pollutant / source sector / region combinations that may deserve further investigation in the future? It could also be connected to the paragraph starting at line 300.

We have added Figure S2 to the Supplement to provide an illustration of the time series of implied emission factors for each compound for the top 15 emitting countries. The panels in this figure show the implied emission factors (units of g g^{-1}) for the fuel and sector combinations that

dominantly contribute to emissions of each compound. For example, NO_x emissions are predominately from the combustion of oil and natural gas in the road-transport sector. We have used this figure to support several sections of our manuscript including the Methods and uncertainties discussion and have added the following sections to the main text.

Line 229 - *Figure S2 provides a time series of implied emission factors after the scaling procedure for select sector- and fuel- combinations that dominant emissions of each compound in the top 15 emitting countries.*

Line 336 - *Figure S2 shows that after scaling, the implied emission factors of CO from oil and gas combustion in the on-road transport sector for four African countries range from 0.19-0.28 g g^{-1}, slightly smaller than the range of 0.029 - 0.380 g g^{-1} used in the DICE-Africa inventory.*

Line 345 - *After scaling, the implied EFs for residential biofuel emissions of OC are ~0.001-0.002 g g^{-1} in three African countries (Figure S2), within the range of EFs of 0.0007 – 0.003 g g^{-1} implemented in the DICE-Africa inventory.*

Line 354 - *Figure S2 shows that the implied emission factor for NO_x emissions from oil & gas combustion in the on-road transport sector in India is ~0.015 g g^{-1} in 2015, which falls within the range of values of 0.0026 – 0.046 g g^{-1} used for various vehicles and fuel type in Venkataraman et al. (2018).*

Line 359 - *For SO_2, Figure S2 shows that the implied EF for coal combustion in the energy sector is ~0.004 g g^{-1}, slightly lower than the range of 0.0049 – 0.0073 g g^{-1} used for the SMoG-India inventory.*

Line 761 - *In addition to uncertainties in the scaling inventory emissions, uncertainties are also introduced by the $CEDS_{GBD\text{-}MAPS}$ scaling procedure. Uncertainties arise when mapping sectoral and fuel (when available) specific emissions between inventories (as discussed previously), as well as in the application of the calculated scaling factors outside the range of available scaling inventory years. For example, the implied CO EFs in Figure S2 highlight one case in China where the EFs for oil and gas combustion in the on-road transport sector peak in 1999 at a value over three times larger than EFs in all other top emitting countries. For China specifically, the calculated scaling factors for the year 2010 (earliest scaling inventory year) are applied to emissions from all years prior, which was calculated as a value of ~1.58 for the on-road transport sector. The implied EF of ~1.8 g g^{-1} for this sector in 2003 (Figure S2) suggests that the SF from 2010 may not be representative of emissions during this earlier time period. We do note, however, that the 1999 peak in total CO emissions in China (Figure S9) is driven by the IEA energy data and is consistent with the $CEDS_{Hoesly}$ inventory (Hoesly et al., 2018). In contrast, EFs from this sector in China after the year 2010 agree with the magnitude and trends found in other countries, further indicating that the scaling factors*

are most appropriate for years with overlapping inventory data. Other similar examples include coal energy emissions of SO_2 in Thailand (Figure S2). In this case, the REAS scaling inventory spans the years 2000 – 2008. The default EFs for the energy sector, however, independently decrease between 1997 and 2001. As a result, when the implied EF of 3.3 for the year 200 is applied to all historical energy emissions, the implied EFs prior to 1997 become an order of magnitude larger than those in nearly all other top emitting countries (Figure S2). Overall, the applicability of the scaling factors to emissions in years outside the available scaling inventory years remain uncertain due to real historical changes in activity, fuel-use, and emissions mitigation strategies. These uncertainties, however, vary by compound and sector as, for example, there are no similar peaks in on-road emissions for compounds other than CO in China.

Supplemental Line 202 - *To illustrate the outcome of the scaling procedure, implied emission factors for the top 15 emitting countries are additionally shown in Figure S2 for the select fuel-types and sectors that dominantly contribute to global emission of each compound. Various anomalies in the implied EFs can arise from multiple sources of uncertainty, including the underlying activity data or application of scaling factors outside the available scaling inventory years, as is the case with the on-road CO emission factor for China in 1999. These uncertainties are discussed further in Section 4.2 in the main text.*

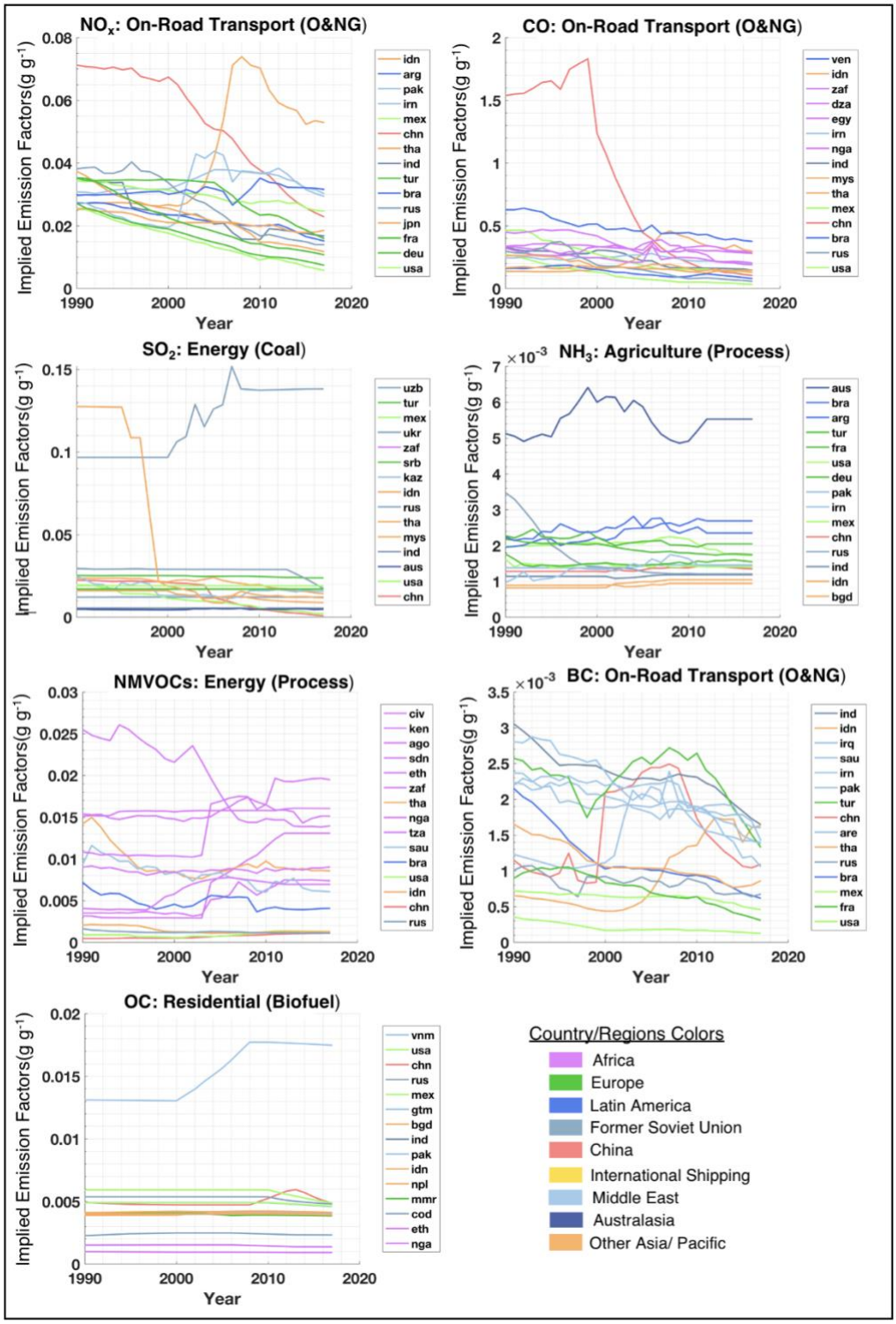

Figure S2. Time-series of implied (post-scaling) emission factors for select fuel and sector combinations that dominantly contribute to global emissions of each compounds. NOx, CO, and BC: oil & natural gas combustion in the on-road transport sector, SO_2: coal combustion in the energy sector, NH_3: agricultural emissions, NMVOCs: process-level energy sources, and OC: residential biofuel combustion. Time series are shown for the top 15 emitting countries, listed by their ISO codes to the right of each panel. Time series are colored by the region of each country.

From the methods section it was not clear to me where the shipping emissions come from. Are these based on AIS data or taken from EDGAR? Or another approach? Like with the regional inventories there may be ways to "scale/calibrate" these in recent years by using AIS based inventories. Was this considered?

We had not originally included an explicit description for international shipping emissions as these were not changed relative to the $CEDS_{Hoesly}$ inventory. To clarify the source of these emissions, we have added the following description to the Methods section.

Line 192 - *For International Shipping, IEA activity data is supplemented with consumption data and EFs from the International Maritime Organization (IMO), as described in Hoesly et al. (2018) and its supplement.*

The region "Other Asia/Pacific/Middle East region". This I find non-informative and I invite the authors to think of a solution possibly by breaking it up. The mix of countries (see Table S8 - e.g. Australia, Mongolia, Yemen, Saudi Arabia, Korea, New Zealand, Pakistan, Indonesia etc.) is such that any discussion of the trends for this group in the paper is pointless. Also graphs of such a group in my opinion do not add any information.

In an attempt to simplify the line plots and maintain consistency with Hoesly et al. (2018), we chose to aggregate many of the countries that were not central to the discussion in our manuscript (i.e., those countries that were not largely updated relative to the $CEDS_{Hoesly}$ inventory). To provide a more meaningful discussion, we have now broken the 'Other Asia / Pacific/ Middle East region into the Australasia, Middle East, and Other Asia / Pacific regions. The new definitions are in Table S9. We have also updated Fig 8 accordingly, as well as SI Fig's S10 and S17-S20. The following sections of text have been updated as well.

Line 441 - *Time series of regional contributions to global emissions in Fig. 8 additionally show that 50% of global 2017 NO_x emissions are from the combined Other Asia/Pacific region (Table S9) (13 Tg), China (24 Tg), International Shipping (25 Tg).*

Line 450 - *Fig. 8 shows that in 2017, China is the dominant source of global CO (144 Tg, 27% of global total), SO_2 (12 Tg, 15% of global total), NH_3 (12 Tg, 20% of global total), OC (2.7 TgC, 20% of global total), and BC (1.4 TgC, 24% of global total). In contrast, Africa is the dominant source of global NMVOCs in 2017 (48 TgC, 27% of global total) and International Shipping is the dominant source of global NO_x emissions (25 Tg, 20% of global total).*

Line 466 - *Despite, however, continued reductions in these regions, global emissions of CO slightly increase between 2002 and 2012 due to simultaneous increases among the energy, industry, and residential sectors in China, India, Africa, and the Other Asia/Pacific region (Fig. S9-S12).*

Line 480 - *While China is the largest global contributor to SO_2 emissions between 1994 and 2017, these large regional reductions, coupled with increasing SO_2 emissions in the Other Asia/Pacific region, African countries, and India (Fig. 8), indicate that future global SO_2 emissions will increasingly reflect activities in these other rapidly growing regions.*

Line 488 - *While more stringent vehicle emission standards result in more than a factor of 2 decrease in on-road transportation NO_x emissions in North America and Europe between 1992 and 2017 (Fig. S7-S8), on-road transport emissions in China, India, and the Other Asia/Pacific region simultaneously experience between a factor of 1.3 to 2.8 increase (Fig. S9-S11).*

Line 493 - *Global NO_x emissions from the energy and industry sectors increase by up to a factor of 6 between 1970 and 2011 due to regional increases in China, India, the Other Asia/Pacific region, and African countries, with reductions between 2011 and 2017, again largely from reductions in China from stricter emissions control policies for coal fired power plants and coal use in industrial processes (Zheng et al., 2018;Liu et al., 2015).*

Line 503 - *Though emissions of BC and OC have a higher level of uncertainty relative to other compounds (Sect. 4), emissions from African countries and the Other Asia/Pacific region experience growth in BC and OC emissions from these sectors.*

Line 509 – *Similar to trends in SO_2 emissions, increasing trends in total OC and BC emissions from Africa, India, Latin America, the Middle East, and the Other Asia/Pacific region, coupled with large decreases in emissions from China, North America, and Europe (Fig. 8) indicate that global emissions will increasingly reflect activities in these rapidly growing regions.*

Line 518- *Similarly, global NH_3 emissions from the waste sector increase by 77% between 1970 and 2017, driven by increases in Latin America, the Other Asia/Pacific region, Africa, and India (Fig. S6-S12).*

Line 525 - *Emissions from China are the second largest global NMVOC source between 1996 and 2017 (Fig. 8), while the Other Asia/Pacific region is the third largest source between 1999 and 2017.*

Line 540 - *Figure S17, however, also shows that emissions from coal combustion are simultaneously increasing in India, the Other Asia/Pacific region, and Africa.*

Line 544 - *In contrast, biofuel emissions from all other regions remain relatively flat or increase between 1970 and 2017, though biofuel emissions of NMVOCs, CO, SO_2, and OC in India, as well as SO_2 emissions in North America both decrease between 2010 and 2017 (Fig. S18). In 2017, biofuel*

emissions of all compounds are dominated by emissions from either Africa (NO_x, SO_2, NH_3, NMVOC, BC) or India (OC).

Line 550 - *In contrast to other combustion sectors and fuels, emissions of NO_x, CO, NMVOCs, BC, and OC from the combustion of liquid fuels and natural gas in China remain relatively flat or slightly decrease between 2010 and 2017. Dominant global regions vary by compound (Fig. S19) and include International Shipping (NOx, SO_2), Africa (OC), India (BC), North America (CO, NH_3), and the Other Asia/Pacific region (NMVOCs).*

Line 559 - *Dominant source regions in 2017 of these process level emissions include China (NO_x, CO, NH_3, BC, OC), India (SO_2), and African countries (NMVOCs) (Fig. S20).*

Line 903 - *Outside of international shipping, China is the largest regional source of global emissions of all compounds other than NMVOCs. As emissions in North America, Europe, and China continue to decrease, global emissions of NO_x, CO, SO_2, BC, and OC will increasingly reflect emissions in rapidly growing regions such as Africa, India, and countries throughout Asia, Latin America, and the Middle East. Lastly, in contrast to other compounds, global emissions of NMVOCs and NH_3 continuously increase over the entire time period. These increases are predominantly due to increases in agricultural NH_3 emissions in nearly all world regions, as well as NMVOCs from increased waste, energy sector, and solvent use emissions. In 2017, global emissions of these compounds have the largest regional contributions from India, China, and countries throughout Africa, Asia, and the Pacific.*

Compliments to the authors for all the line plots, they are generally really good to read and intercompare and thereby also reveal some issues that appear unlikely to be correct. That does not mean they have to (or even can be) solved in the current paper. There are a few individual cases that draw attention and possibly merit more comments. I like to share them but it is also up to the authors to think about what they feel is justified. I am not advocating to make the paper very anecdotical by discussing every detail. Like the drop in OC emissions for Industry in Figure S6; the CO peak from road transport and SO2 peak for energy in fig S8 (the latter is discussed in the text) - My suspicion is that what such abrupt peaks or drops have in common is most likely a change in legislation or methodology that "on paper" has almost immediate effect but in reality is smeared out over a longer time. For example the car fleet cannot be changed in 1-2 years, cleaner fuels (like low sulphur) generally take years to be completely adopted. NMVOCs from the Energy sector appear a special case (Fig S5) with a very large contribution but little explanation is given other than that these are process emissions. NMVOCs in general draw some attention – e.g. in line 630 there is a discrepancy of possibly missing NMVOC emissions as CEDS has no agricultural NMVOC emission? And, for example Fig3 India NOx emissions – almost a factor 2 difference between 2 CEDS versions. It is commented on in the text but would it also imply it is better not to use the previous CEDS version because of these large deviations? The difference is too large for both to be equally

plausible. This also applies to the discussion in line 568 and onward. As both inventories come from the CEDS team it seems logical to express some advice on to what extend you believe the new inventory replaces the old one. (Like the EDGAR team would advise to use v5 and v3 or v4.)

The Reviewer has highlighted some of the notable features in the region, fuel, and sector-specific line plots in the main text and supplement. These features highlight additional uncertainties in the CEDS system that were not explicitly discussed in the original text: 1) uncertainties and discontinuities in the IEA energy consumption data, and 2) uncertainties in the methodology of the CEDS scaling procedure. To provide a further analysis of some of these features, we have added two paragraphs to the main text that discuss these additional sources of uncertainty. We have chosen to discuss the specific features that the Review has noted as these are some of the most striking and provide a means to illustrate how these sources of uncertainty can impact the final emission estimates. We have added/edited the following text.

Line 676 - ***4.2.1 Uncertainties in Activity Data***

As discussed in Section 2.1, CEDS default emissions from combustion sources are largely informed by fuel consumption data from the IEA 2019 World Energy Statistics Product (IEA, 2019). While this database provides energy consumption data as a function of detailed source sector and fuel-type for most countries, the IEA data is uncertain and includes breaks in time-series data that can lead to abrupt changes in the $CEDS_{GBD\text{-}MAPS}$ emissions for select sectors, fuels, and countries. For example, Fig. S6 shows an order of magnitude decrease (0.1 TgC) in OC industrial emissions from North America between 1992 and 1993, which is driven by a break in IEA biofuel consumption data for the non-specified manufacturing industry sector (CEDS sector: 1A2g_Ind-Comb-other) in the United States. While the magnitude of this particular change is negligible on the global scale, this is not the case for all sectors. For example, as noted in Section S4, a known issue in the IEA data in China in the energy sector causes peaks in the associated NO_x and SO_2 $CEDS_{GBD\text{-}MAPS}$ emissions in 2004. These peak emissions may be over-estimated by up to 4 and 10 Tg, respectively, which is large enough to impact historical trends in both regional (Figure 8: NO_x and SO_2) and global (Figures6-7: SO_2) emissions. These point to areas where improvements could be made to the underlying driver data in future work.

Line 761 - *In addition to uncertainties in the scaling inventory emissions, uncertainties are also introduced by the $CEDS_{GBD\text{-}MAPS}$ scaling procedure. Uncertainties arise when mapping sectoral and fuel (when available) specific emissions between inventories (as discussed previously), as well as in the application of the calculated scaling factors outside the range of available scaling inventory years. For example, the implied CO EFs in Figure S2 highlight one case in China where the EFs for oil and gas combustion in the on-road transport sector peak in 1999 at a value over three times larger than EFs in all other top emitting countries. For China specifically, the calculated scaling factors for the year 2010 (earliest scaling inventory year) are applied to emissions from all years prior, which was calculated as a value of ~1.58 for the on-road transport sector. The implied EF of ~1.8 g g^{-1} for*

this sector in 2003 (Figure S2) suggests that the SF from 2010 may not be representative of emissions during this earlier time period. We do note, however, that the 1999 peak in total CO emissions in China (Figure S9) is driven by the IEA energy data and is consistent with the CEDS$_{Hoesly}$ inventory (Hoesly et al., 2018). In contrast, EFs from this sector in China after the year 2010 agree with the magnitude and trends found in other countries, further indicating that the scaling factors are most appropriate for years with overlapping inventory data. Other similar examples include coal energy emissions of SO_2 in Thailand (Figure S2). In this case, the REAS scaling inventory spans the years 2000 – 2008. The default EFs for the energy sector, however, independently decrease between 1997 and 2001. As a result, when the implied EF of 3.3 for the year 2000 is applied to all historical energy emissions, the implied EFs prior to 1997 become an order of magnitude larger than those in nearly all other top emitting countries (Figure S2). Overall, the applicability of the scaling factors to emissions in years outside the available scaling inventory years remain uncertain due to real historical changes in activity, fuel-use, and emissions mitigation strategies. These uncertainties, however, vary by compound and sector as, for example, there are no similar peaks in on-road emissions for compounds other than CO in China.

To answer the Reviewers other specific comments/questions, the CEDS$_{GBD-MAPS}$ inventory does not include agricultural emissions of NMVOCs, nor do the EDGAR or GAINS inventories. In the original Fig. S22, it appeared that the GAINS inventory included AGR NMVOC emissions and that the CEDS inventory did not. There was an error in the color scale of this figure that was displaying GAINS NMVOC solvent emissions as those from the AGR sector. This color scale has been corrected in the new Fig. S24.

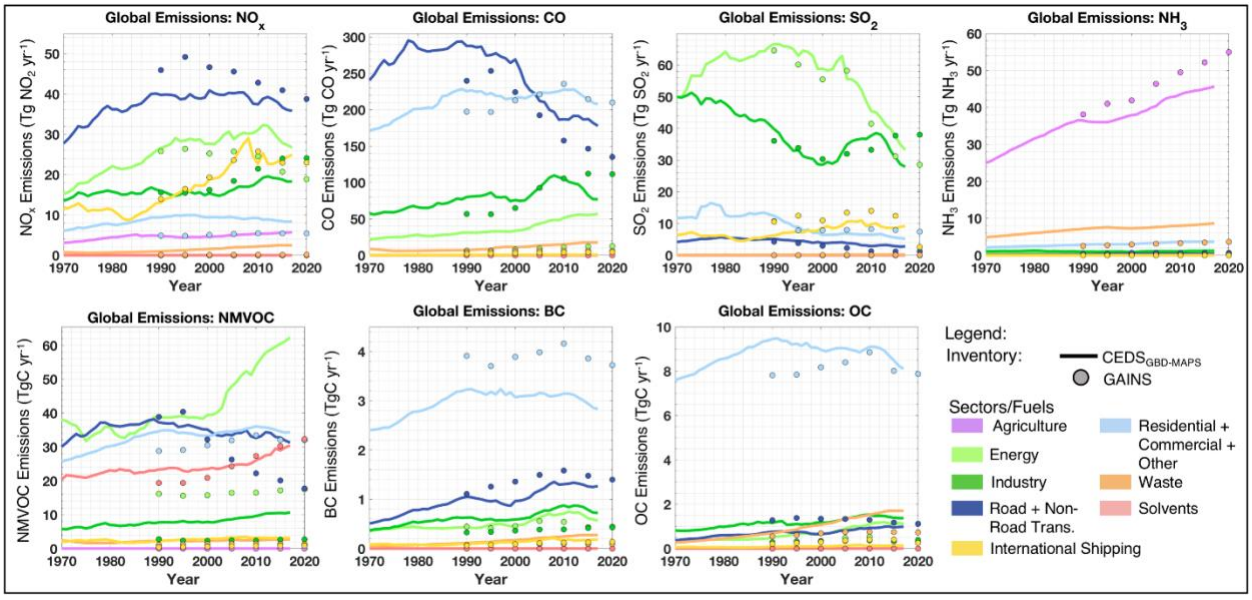

Figure S24.

The increase in energy NMVOC emissions noted by the Reviewer is largely associated with large increases in the Fugitive solid fuels sector in Africa between 2003 and 2017 in the EDGAR v4.3.2 inventory. As these emissions are assigned to the 'process' fuel-type in $CEDS_{GBD\text{-}MAPS}$, these emissions are taken directly from the EDGAR inventory. For instance, NMVOC emissions from this sector in EDGAR increased by nearly a factor of 5 in Nigeria during this time period. The source of the increase in this sector has been clarified on the following lines.

Line 347 - *Total $CEDS_{GBD\text{-}MAPS}$ emissions of NMVOCs are larger, primarily due to increased contributions from solvent use and the energy sector associated with changes in the EDGAR v4.3.2 inventory, while total emissions of CO, SO_2, and NH_3 are relatively consistent between the two CEDS versions.*

Line 524 - *Increases in energy sector emissions after 2003 are largely driven by increases in fugitive emissions from select African countries, including Nigeria, Kenya, and Angola, and Mozambique.*

For NO_x emissions in India, the original Fig. 3 shows that $CEDS_{GBD\text{-}MAPS}$ emissions are reduced by ~40%, due largely to road emissions. This sector is particularly uncertain in India due to uncertainties in the vehicle fleet. As discussed in Section 2, however, the road emissions in India are scaled to match the recent SMoG-India inventory. As previously discussed in Section 2.2, major difference between the two CEDS inventories for this sector are due to differences in the employed emission factors. We have added additional discussion that note that the scaled implied emission factors are within the range used for the road transport sector in the SMoG-India inventory, further suggesting that the large decrease in road emissions in India are resulting from the smaller NOx emissions factor. As the $CEDS_{GBD\text{-}MAPS}$ inventory presented in this manuscript was developed for the GBD-MAPS project (and not an updated release of the core CEDS system) we have discussed the differences between the two inventories in this manuscript, but refrain from making more specific recommendations. We have clarified this point in the Methods section.

Line 159 - *The $CEDS_{GBD\text{-}MAPS}$ inventory is developed for the GBD-MAPS project and is not an updated release of the core CEDS emissions inventory.*

Line 648 – "decreasing uncertainties": Here I do not by definition agree. If for example the (more uncertain) emissions from Africa and India become dominant and e.g. the more certain emissions from the US & EU go down, than the overall uncertainty might also increase in future years.

The reviewer raises a good point and we have updated the relevant text accordingly.

Line 695- *While improvements in data collection and reporting standards may decrease the uncertainty in some underlying sources overtime, the most recent years of $CEDS_{GBD\text{-}MAPS}$ emissions are still subject to high levels of uncertainty. For instance, the degree of local and national*

compliance with control measures is often variable or unknown (e.g., Wang et al., 2015;Zheng et al., 2018), recent activity and regional emissions data are often updated as new information becomes available, and emissions in generally more uncertain regions, including India and Africa are becoming an increasingly large fraction of global totals. Additionally, from a methodological standpoint, default CEDS emissions after 2010 also currently rely on the projection of emission factors from the GAINS EMF30 data release for sectors and countries where contemporary regional scaling inventories are not available.

A good assessment of uncertainty from a mosaic inventory is very challenging and simply stating that the uncertainty is similar to the other inventories (e.g. line 655) is an unsatisfactory answer. Moreover, there may also be considerable uncertainty in the spatial distribution. The authors, however, announce that in the near future a more robust uncertainty analysis is planned. And a much longer paper would not be helpful for the community. So separating this is an acceptable solution.

As this Reviewer points out, it is challenging to quantify uncertainties in emission estimates, especially for those derived using a mosaic approach. Core CEDS system uncertainties have been previously described in Hoesly et al. (2018), and a more robust uncertainty analysis is planned for an upcoming release of the core CEDS system, as mentioned on line 788. We have provided a summary of the sources of uncertainties in this inventory, including uncertainties in global bottom up inventories (Section 4.2.2), regional-level inventories (including the reported uncertainties in the few studies where they were reported) (Section 4.2.3), sectoral and fuel contributions (Section 4.2.4), as well as those in the gridded emission files (Section 4.2.5). We have also added two additional paragraphs to the uncertainties section as well as an addition supplemental figure of implied emission factors in order to provide a further discussion and analysis of inventory uncertainties.

Additional suggestions for final discussion: Recently Huneeus et al. (2020) published an evaluation of emission inventories for South America which included EDGSAR, ECLIPSE and CEDS. It would be interesting to comment on how the new inventory presented here would have an impact on SA estimates and compares to the CEDS version used in that paper?

In Section 2, we highlight the major updates implemented in this work relative to the previous $CEDS_{Hoesly}$ inventory. These updates will result in differences at the global level (discussed explicitly in Section 4.1.1), regional level (discussed for China, India, and Africa in Sections 2.2-2.3 and throughout Section 4), and in the gridded emission products. From a global perspective, we discuss on line 615 about how differences reflect the different activity data and scaling inventories. Per the Reviewer's question/comment, the updated CEDS emissions in Latin American countries will therefore largely reflect the changes between the EDGARv4.3.1 (used to derived $CEDS_{Hoesly}$) and EDGARv4.3.2 (used for $CEDS_{GBD\text{-}MAPS}$), except for in Argentina (see Fig. 2). The Reviewer, however,

has highlighted an important point that we had not provided a comparison to the previous $CEDS_{Hoesly}$ inventory across all regions. Therefore, we have added Figure S22 to the supplement to highlight the regional inventory differences. Based on this figure, the $CEDS_{GBD-MAPS}$ emissions in Latin America are slightly lower than $CEDS_{Hoesly}$, which would indicate a slight improvement in the agreement with other inventories shown for select Latin American countries in Figure 4 of Huneeus et al. (2020).

We have added the following text to the end of Section 4.1.1: Comparison to $CEDS_{Hoesly}$ Inventory.

Line 609 - *Similar to the total global emissions, changes between the two CEDS versions for the national-level and 0.5 °×0.5 °gridded products will also result from updates to the energy consumption data, scaling inventories (Section 2.2-2.3) and spatial distribution proxies from EDGARv4.3.2 (Section 2.1). Time series of differences between the $CEDS_{Hoesly}$ and $CEDS_{GBD-MAPS}$ inventories for 11 world regions are shown for each compound in Fig. S22. In recent years, Figure S22 shows that $CEDS_{GBD-MAPS}$ emissions are generally lower in each region, with the greatest differences in Africa, India and China. The relative changes in Africa and India are discussed previously in Section 2. For China, the $CEDS_{GBD-MAPS}$ emissions are generally lower than the $CEDS_{Hoesly}$ estimates after the year 2010 as a result of the updated scaling inventory. Regional differences between inventories are also greater for OC and BC emissions relative to other compounds due to the added scaling procedure discussed in Section 2. Differences in spatial distributions are not discussed here as changes represent differences in the spatial proxies, which are largely from updates to the EDGAR inventory.*

We have added Figure S22.

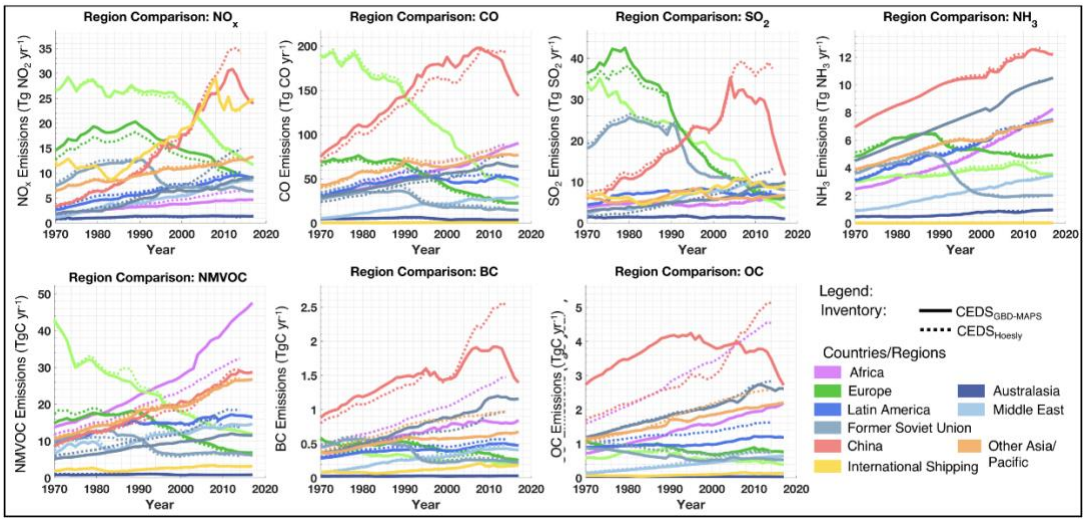

Figure S22. *Comparison of $CEDS_{Hoesly}$ and $CEDS_{GBD-MAPS}$ emissions as a function of 11 world regions.*

SI Line 385 - *Figures S21 and S22 compare $CEDS_{GBD-MAPS}$ and $CEDS_{Hoesly}$ emissions.*

Small editorial remarks

Line 42 – from "waste" combustion (otherwise strange to have carb aerosol from waste.)

To keep consistent terminology throughout the text, we have changed to '*the waste sector*'.
Line 39 - *Dominant sources of global CO emissions in 2017 include on-road transportation and residential biofuel combustion. Dominant global sources of carbonaceous aerosol in 2017 include residential biofuel combustion, on-road transportation (BC only), as well as emissions from the waste sector.*

Line 78 – as inputs to solve for? Not clear to me, maybe reformulate slightly?

Updated as follows.
Line 76 - *For example, spatially gridded emission inventories are used as inputs in general circulation/climate (GCM) and chemical transport models (CTM), which are used to predict the evolution of atmospheric constituents over space and time.*

Line 108 – "emission" reduction of coal-fired etc.

Changed

Line 181 – explain the term "working sector"
This terminology is from Hoesly et al. (2018) and refers to the sub-sectors that are carried through the CEDS system calculations and later aggregated for the final reported CEDS sectors. This term was first used 4 lines prior and is now further defined there.

Line 176- *In Eq. (1), emissions are calculated using relevant activity (A) and emission factor (EF) data for each country (c) and year (y), as a function of 52 detailed working sectors (s) (sub-sectors used for intermediate steps in the CEDS system) and nine working fuel-types (f) (Table 2).*

Line 410 – you mean Section S4.

Changed

Line 481 Global emissions of NOx from waste "combustion".

Changed

Line 680 I don't see how satellites will aid in fuel-type recognition.

In this case, we were considering examples such as from McLinden et al. (2016), where top-down estimates from specific point sources could be identified and/or better quantified by incorporating satellite-derived estimates. We did not mean to say that satellite-retrievals will aid in identifying the fuel used by various point sources, but rather that they can aid in reducing the uncertainties for point sources where fuel-type is already known.

Line 684 "emissions" – should be "uncertainties"?

We have clarified this sentence.
Line 732- *The inventories with the largest impact on the $CEDS_{GBD\text{-}MAPS}$ emission uncertainties relative to the $CEDS_{Hoesly}$ inventory will be those from China from Zheng et al. (2018), the DICE-Africa emission inventory from Marais and Wiedinmyer (2016), and the SMoG-India inventory from Venkataraman et al. (2018).*

Line 786 – but not for the latest years? And these will not be scaled ("calibrated") so not consistent?

We clarified this sentence.
Line 854 - *These compounds were previously included through 2014 in the $CEDS_{Hoesly}$ inventory.*

Line 791 – it seems the reference of (McDuffie et al., 2020c) here and in the ref list is redundant because this sis the dataset connected to the present paper? So won't the reference to that data not be simply this paper instead of (McDuffie et al., 2020c).

Yes, the dataset is connected to the paper. However, the dataset is also publicly available at Zenodo, which has a unique data doi and is not directly tied to this manuscript. Therefore, the data doi (McDuffie t al., 2020c) is for the dataset. The description of the dataset is provided in this manuscript, which will have a unique doi. Having a data-specific doi will also allow for the creation of new doi's on Zenodo when there are future updates to the CEDS_GBD-MAPS dataset.

Line 836 in agricultural "NH3" emissions

Changed

Line 867 – what is fuel abatement?

Changed.

Line 936 - *Due to the direct and secondary contribution of these reactive gases and carbonaceous aerosol to ambient air pollution, contemporary gridded and country-level emissions with both sector and fuel-type information can provide new insights necessary to motivate and develop effective strategies for emission reductions and air pollution mitigation around the world.*

There is an error in Table S8 – Other Asia includes Montenegro and I assume Chinese Taipei is Taiwan?

Changed both (Table S8 now Table S9)

There is an error in Table S9 – in the column for EDGAR "solvent use" and "waste" are swapped.

Changed. (Table S9 now Table S10)

References

Janssens-Maenhout, G., Crippa, M., Guizzardi, D., Dentener, F., Muntean, M., Pouliot, G., Keating, T., Zhang, Q., Kurokawa, J., Wankmüller, R., Denier van der Gon, H., Kuenen, J. J. P., Klimont, Z., Frost, G., Darras, S., Koffi, B., and Li, M.: HTAP_v2.2: a mosaic of regional and global emission grid maps for 2008 and 2010 to study hemispheric transport of air pollution, Atmos. Chem. Phys., 15, 11411–11432, https://doi.org/10.5194/acp-15-11411-2015, 2015.

Huneeus, N., Denier van der Gon, H., Castesana, P., Menares, C., Granier, C., Granier, L., ... & Gomez, D., Evaluation of anthropogenic air pollutant emission inventories for South America at national and city scale, Atmospheric Environment 235 (2020) https://doi.org/10.1016/j.atmosenv.2020.117606

Elguindi, N., Granier, C., Stavrakou, T., Darras, S., Bauwens, M., Cao, H., et al. (2020). Intercomparison of magnitudes and trends in anthropogenic surface emissions from bottomâĂŘup inventories, topâĂŘdown estimates and emission scenarios. Earth's Future, 8, e2020EF001520. https://doi.org/10.1029/2020EF0015202020.

Review Response References

Hoesly, R. M., Smith, S. J., Feng, L., Klimont, Z., Janssens-Maenhout, G., Pitkanen, T., Seibert, J. J., Vu, L., Andres, R. J., Bolt, R. M., Bond, T. C., Dawidowski, L., Kholod, N., Kurokawa, J. I., Li, M., Liu, L., Lu, Z., Moura, M. C. P., O'Rourke, P. R., and Zhang, Q.: Historical (1750–2014) anthropogenic emissions of reactive gases and aerosols from the Community Emissions Data System (CEDS), Geosci. Model Dev., 11, 369-408, 10.5194/gmd-11-369-2018, 2018.

Huneeus, N., Denier van der Gon, H., Castesana, P., Menares, C., Granier, C., Granier, L., Alonso, M., de Fatima Andrade, M., Dawidowski, L., Gallardo, L., Gomez, D., Klimont, Z., Janssens-Maenhout, G., Osses, M., Puliafito, S. E., Rojas, N., Ccoyllo, O. S., Tolvett, S., and Ynoue, R. Y.: Evaluation of anthropogenic air pollutant emission inventories for South America at national and city scale, Atmos. Environ., 235, 117606, https://doi.org/10.1016/j.atmosenv.2020.117606, 2020.

IEA: World Energy Statistics 2019 Edition, Database Documentation, http://wds.iea.org/wds/pdf/WORLDBES_Documentation.pdf (last access: 17 September 2019), 2019.

Janssens-Maenhout, G., Crippa, M., Guizzardi, D., Dentener, F., Muntean, M., Pouliot, G., Keating, T., Zhang, Q., Kurokawa, J., Wankmüller, R., Denier van der Gon, H., Kuenen, J. J. P., Klimont, Z., Frost, G., Darras, S., Koffi, B., and Li, M.: HTAP_v2.2: a mosaic of regional and global emission grid maps for 2008 and 2010 to study hemispheric transport of air pollution, Atmos. Chem. Phys., 15, 11411-11432, 10.5194/acp-15-11411-2015, 2015.

Li, M., Zhang, Q., Kurokawa, J. I., Woo, J. H., He, K., Lu, Z., Ohara, T., Song, Y., Streets, D. G., Carmichael, G. R., Cheng, Y., Hong, C., Huo, H., Jiang, X., Kang, S., Liu, F., Su, H., and Zheng, B.: MIX: a mosaic Asian anthropogenic emission inventory under the international collaboration framework of the MICS-Asia and HTAP, Atmos. Chem. Phys., 17, 935-963, 10.5194/acp-17-935-2017, 2017.

Liu, Z., Guan, D., Wei, W., Davis, S. J., Ciais, P., Bai, J., Peng, S., Zhang, Q., Hubacek, K., Marland, G., Andres, R. J., Crawford-Brown, D., Lin, J., Zhao, H., Hong, C., Boden, T. A., Feng, K., Peters, G. P., Xi, F., Liu, J., Li, Y., Zhao, Y., Zeng, N., and He, K.: Reduced carbon emission estimates from fossil fuel combustion and cement production in China, Nature, 524, 335-338, 10.1038/nature14677, 2015.

Marais, E. A., and Wiedinmyer, C.: Air Quality Impact of Diffuse and Inefficient Combustion Emissions in Africa (DICE-Africa), Environ. Sci. Technol., 50, 10739-10745, 10.1021/acs.est.6b02602, 2016.

McLinden, C. A., Fioletov, V., Shephard, M. W., Krotkov, N., Li, C., Martin, R. V., Moran, M. D., and Joiner, J.: Space-based detection of missing sulfur dioxide sources of global air pollution, Nature Geoscience, 9, 496, 10.1038/ngeo2724 https://www.nature.com/articles/ngeo2724#supplementary-information, 2016.

Venkataraman, C., Brauer, M., Tibrewal, K., Sadavarte, P., Ma, Q., Cohen, A., Chaliyakunnel, S., Frostad, J., Klimont, Z., Martin, R. V., Millet, D. B., Philip, S., Walker, K., and Wang, S.: Source influence on emission pathways and ambient $PM_{2.5}$ pollution over India (2015–2050), Atmos. Chem. Phys., 18, 8017-8039, 10.5194/acp-18-8017-2018, 2018.

Wang, S., Zhang, Q., Martin, R. V., Philip, S., Liu, F., Li, M., Jiang, X., and He, K.: Satellite measurements oversee China's sulfur dioxide emission reductions from coal-fired power plants, Environmental Research Letters, 10, 114015, 10.1088/1748-9326/10/11/114015, 2015.

Zheng, B., Tong, D., Li, M., Liu, F., Hong, C., Geng, G., Li, H., Li, X., Peng, L., Qi, J., Yan, L., Zhang, Y., Zhao, H., Zheng, Y., He, K., and Zhang, Q.: Trends in China's anthropogenic emissions since 2010 as the consequence of clean air actions, Atmos. Chem. Phys., 18, 14095-14111, 10.5194/acp-18-14095-2018, 2018.

A global anthropogenic emission inventory of atmospheric pollutants from sector- and fuel-specific sources (1970-2017): An application of the Community Emissions Data System (CEDS)

Erin E. McDuffie[1,2], Steven J. Smith[3], Patrick O'Rourke[3], Kushal Tibrewal[4], Chandra Venkataraman[4], Eloise A. Marais[5], Bo Zheng[6], Monica Crippa[7], Michael Brauer[8,9], Randall V. Martin[2,1]

[1]Department of Physics and Atmospheric Science, Dalhousie University, Halifax, NS, Canada
[2]Department of Energy, Environmental, and Chemical Engineering, Washington University in St. Louis, St. Louis, MO, USA
[3]Joint Global Change Research Institute, Pacific Northwest National Laboratory, College Park, MD, USA
[4]Department of Chemical Engineering, Indian Institute of Technology Bombay, Mumbai, Maharashtra, India
[5]School of Physics and Astronomy, University of Leicester, Leicester, UK
[6]Laboratoire des Sciences du Climat et de l'Environnement, CEA-CNRS-UVSQ, UMR8212, Gif-sur-Yvette, France
[7]European Commission, Joint Research Centre (JRC), Via E. Fermi 2749 (T.P. 123), 21027 Ispra, Varese, Italy
[8]School of Population and Public Health, University of British Columbia, Vancouver, BC, Canada
[9]Institute for Health Metrics and Evaluation, University of Washington, Seattle, WA, USA

Correspondence to: Erin McDuffie (erin.mcduffie@wustl.edu)

Deleted: State Key Joint Laboratory of Environment Simulation and Pollution Control, School of Environment, Tsinghua University, Beijing 100084, People's Republic of China…

Deleted: erin.mcduffie@dal.ca

Abstract. Global anthropogenic emission inventories remain vital for understanding the fate and transport of atmospheric pollution, as well as the resulting impacts on the environment, human health, and society. Rapid changes in today's society require that these inventories provide contemporary estimates of multiple atmospheric pollutants with both source sector and fuel-type information to understand and effectively mitigate future impacts. To fill this need, we have updated the open-source Community Emissions Data System (CEDS) (Hoesly et al., 2019) to develop a new global emission inventory, $CEDS_{GBD\text{-}MAPS}$. This inventory includes emissions of seven key atmospheric pollutants (NO_x, CO, SO_2, NH_3, NMVOCs, BC, OC) over the time period from 1970 – 2017 and reports annual country-total emissions as a function of 11 anthropogenic sectors (agriculture, energy generation, industrial processes, transportation (on-road and non-road), residential, commercial, and other sectors (RCO), waste, solvent use, and international-shipping) and four fuel categories (total coal, solid biofuel, and the sum of liquid fuels and natural gas combustion, plus remaining process-level emissions). The $CEDS_{GBD\text{-}MAPS}$ inventory additionally includes global gridded (0.5°×0.5°) emission fluxes with monthly time resolution for each compound, sector, and fuel-type to facilitate their use in earth system models. $CEDS_{GBD\text{-}MAPS}$ utilizes updated activity data, updates to the core CEDS default scaling procedure, and modifications to the final procedures for emissions gridding and aggregation to retain sector and fuel-specific information. Relative to the previous CEDS data released for CMIP6 (Hoesly et al., 2018), these updates extend the emission estimates from 2014 to 2017 and improve the overall agreement between CEDS and two widely used global bottom-up emission inventories. The $CEDS_{GBD\text{-}MAPS}$ inventory provides the most contemporary global emission estimates to-date for these key atmospheric pollutants and is the first to provide global estimates for these species as a function of multiple fuel-types across multiple source sectors. Dominant sources of global NO_x and SO_2 emissions in 2017 include the combustion of oil, gas, and coal in the energy and industry sectors, as well as on-road transportation and international shipping for NO_x. Dominant sources of global CO emissions in 2017 include on-road transportation and residential biofuel combustion. Dominant global sources of carbonaceous aerosol in 2017 include residential biofuel combustion, on-road transportation (BC only), as well as emissions from the waste sector. Global emissions of NO_x, SO_2, CO, BC, and OC all peak in 2012 or earlier, with more recent emission reductions driven by large changes in emissions from China, North America, and Europe. In contrast, global emissions of NH_3 and NMVOCs continuously increase between 1970 and 2017, with agriculture serving as a major source of global NH_3 emissions and solvent use, energy, residential, and the on-road transport sectors as major sources of global NMVOCs. Due to similar development methods and underlying datasets, the $CEDS_{GBD\text{-}MAPS}$ emissions are expected to have consistent sources of uncertainty as other bottom-up inventories, including uncertainties in the underlying activity data and sector- and region-specific emission factors. The $CEDS_{GBD\text{-}MAPS}$ source code is publicly available online through GitHub: https://github.com/emcduffie/CEDS/tree/CEDS_GBD-MAPS. The $CEDS_{GBD\text{-}MAPS}$ emission inventory dataset (both annual country-total and monthly global gridded files) is publicly available and registered under: https://doi.org/10.5281/zenodo.3754964 (McDuffie et al., 2020c).

Deleted: calibration

Deleted: monthly

1 Introduction

Human activities emit a complex mixture of chemical compounds into the atmosphere, impacting air quality, the environment, and population health. For instance, direct emissions of nitric oxide (NO) rapidly oxidize to form nitrogen dioxide (NO_2) and can lead to net ozone (O_3) production in the presence of sunlight and oxidized volatile organic compounds (VOCs) (e.g., Chameides, 1978;Crutzen, 1970). In addition, direct emissions of organic and black carbon-containing particles (OC, BC), as well as secondary reactions involving gaseous sulfur dioxide (SO_2), NO, ammonia (NH_3), and VOCs can lead to atmospheric fine particulate matter less than 2.5 μm in diameter ($PM_{2.5}$) (e.g., Mozurkewich, 1993;Jimenez et al., 2009;Saxena and Seigneur, 1987;Brock et al., 2002). $PM_{2.5}$ concentrations were estimated to account for nearly 3 million deaths worldwide in 2017 (Stanaway et al., 2018), while surface O_3 concentrations were associated with nearly 500,000 deaths in 2017 (Stanaway et al., 2018) and significant global crop losses, valued at $11 billion ($USD_{2000}$) in 2000 (Avnery et al., 2011;Ainsworth, 2017). In addition, atmospheric O_3 and aerosol both impact Earth's radiative budget (e.g., Bond et al., 2013;Haywood and Boucher, 2000;US EPA, 2018). Other pollutants, including carbon monoxide (CO), NO_2, and SO_2 are also directly hazardous to human health (US EPA, 2018), while NO_2 and SO_2 can additionally contribute to acid rain (Saxena and Seigneur, 1987;US EPA, 2018) and indirectly impact human health via their contributions to secondary $PM_{2.5}$ formation. In addition, NH_3 deposition and nitrification can also cause nutrient imbalances and eutrophication in terrestrial and marine ecosystems (e.g., Behera et al., 2013;Stevens et al., 2004). While these reactive gases and aerosol have both anthropogenic and natural sources, dominant global sources of NO_x (= NO + NO_2), SO_2, CO, and VOCs include fuel transformation and use in the energy sector, industrial activities, and on-road and off-road transportation (Hoesly et al., 2018). Global NH_3 emissions are predominantly from agricultural activities such as animal husbandry and fertilizer application (e.g., Behera et al., 2013) and OC and BC have large contributions from incomplete or uncontrolled combustion in residential and commercial settings (e.g., Bond et al., 2013). Emissions of these compounds and the distribution of their chemical products vary spatially and temporally, with atmospheric lifetimes that allow for their transport across political boundaries, continuously driving changes in the composition of the global atmosphere.

Global emission inventories of these major atmospheric pollutants, with both sectoral, and fuel-type information are paramount for 1) understanding the range of emission impacts on the environment and human health and 2) for developing effective strategies for pollution mitigation. For example, spatially gridded emission inventories are used as inputs in general circulation/climate (GCM) and chemical transport models (CTM), which are used to predict the evolution of atmospheric constituents over space and time. By perturbing emission sources or historical emission trends, such models can quantify the impact of emissions on the environment, economy, and human health (e.g., Mauzerall et al., 2005;Lelieveld et al., 2019;IPCC, 2013;Liang et al., 2018;Lacey and Henze, 2015), provide mitigation-relevant information for polluted regions (e.g., GBD MAPS Working Group, 2016, 2018;RAQC, 2019;Lacey et al., 2017), and anchor future projections (e.g., Shindell and Smith, 2019;Venkataraman et al., 2018;Gidden et al., 2019;Mickley et al., 2004).

Deleted: use

Deleted: spatially gridded emission inventories as inputs to solve for atmospheric transport and chemical processes, and to…

Three global emission inventories have been widely used for these purposes, including the Emissions Database for Global Atmospheric Research (EDGAR) from the European Commission Joint Research Centre (Crippa et al., 2018), the ECLIPSE (Evaluating the Climate and Air Quality Impacts of Short-Lived Pollutants) inventory from the Greenhouse Gas – Air Pollution Interactions and Synergies (GAINS) model at the International Institute for Applied Systems Analysis (IIASA) (Amann et al., 2011;Klimont et al., 2017), and the CEDS (v2016-07-26) inventory from the newly developed Community Emissions Data System (CEDS), from the Joint Global Change Research Institute at the Pacific Northwest National Laboratory and University of Maryland (Hoesly et al., 2018). All three inventories are derived using a bottom-up approach where emissions are estimated using reported activity data (e.g., amount of fuel consumed) and source- and regionally- (where available) specific emission factors (mass of emitted pollutant per mass of fuel consumed) for each emitted compound. All three inventories are similar in that they use this bottom-up approach to provide historical, source-specific gridded emission estimates of major atmospheric pollutants (NO_x (as NO_2) SO_2, CO, NMVOCs, NH_3, BC, and OC). Table 1 provides a comparison of the key features between these inventories, which provide emissions from multiple source sectors over the collective time period from 1750-2014. In contrast to EDGAR and GAINS, the CEDS system implements an increasingly utilized mosaic approach, which, in this case, incorporates activity and emission input data from other sources such as EDGAR, GAINS, and regional/national-level inventories to produce global emissions that are both historically consistent and reflective of contemporary country-level estimates (Hoesly et al., 2018). The CEDS source code has been publicly released (https://github.com/JGCRI/CEDS/tree/master), increasing both the reproducibility and public accessibility to quality emission estimates of global and national-level air pollutants.

Due to the long development times of global bottom-up inventories, current versions of the EDGAR, ECLIPSE, and CEDS inventories are limited in their ability to capture emission trends over recent years (Table 1), particularly the last 6 – 10 years in regions undergoing rapid change such as China, North America, Europe, India, and Africa. For example, China implemented the Action Plan on the Prevention and Control of Air Pollution in 2013, which has targeted specific emission sectors, fuels, and species and resulted in reductions of ambient $PM_{2.5}$ concentrations by up to 40% in metropolitan regions between 2013 and 2017 (reviewed in Zheng et al., 2018). Similarly, over the past 10-20 years in the US and Europe, the reduction of coal-fired power plant emissions and phase-in of stricter vehicle emission standards have resulted in emission reductions of SO_2 and NO_x across these regions (Krotkov et al., 2016;Duncan et al., 2013;Castellanos and Boersma, 2012;de Gouw et al., 2014). Over this same time period, however, oil and gas production in key regions in the US has more than tripled between 2007 and 2017 (EIA, 2020). In addition, the absence of widespread regulations targeting NH_3 from agricultural practices has led to continuous increases in global NH_3 emissions (Behera et al., 2013). Global energy consumption also increased by an average of 1.5% each year between 2008 and 2018 (BP, 2019) and the global consumption of coal increased for the first time in 2017 since its peak in 2013 (BP, 2019). Many of these energy changes have been attributed to the growth of energy generation in rapidly growing regions, such as India (BP, 2019). Africa is also experiencing rapid growth, with increasing emissions from diffuse and inefficient combustion sources, which may not be accurately accounted for in current global inventories (Marais and Wiedinmyer, 2016). Therefore, to capture recent trends around the globe, quantify the resulting

Deleted: that uses

Deleted: in order

Deleted: also

Deleted: s

economic, health, and environmental impacts, and mitigate future burdens, computational models require emission inventories with regionally accurate estimates, global coverage, and the most up-to-date information possible. Though global bottom-up inventories can lag in time due to data collection and reporting requirements, the incorporation of smaller regional inventories provides the opportunity to improve the timeliness and regional accuracy of global estimates.

To further increase the policy-relevance of such data, it is also important that global emission inventories not only provide contemporary estimates, but report emissions as a function of detailed source sector and fuel type. For example, the recent air quality policies in China have included emission reductions targeting coal-fired power plants within the larger energy generation sector (e.g., Zheng et al., 2018). Decisions to implement such policies require accurate predictions of the air quality benefits, which in turn depend on simulations that use accurate estimates of contemporary sector- and fuel-specific emissions. While the EDGAR, ECLIPSE, and CEDS inventories all provide varying degrees of sectoral information (Table 1), there are no global inventories to-date that provide public datasets of multiple atmospheric pollutants with both detailed source sector and fuel-type information. Crippa et al. (2019) do describe estimates of biofuel use from the residential sector in Europe using emissions from the EDGARv4.3.2 inventory (EC-JRC, 2018), but do not report global estimates or regional emissions from other fuel-types. Similarly, Hoesly et al. (2018) describe fuel-specific activity data and emission factors used to develop the global CEDSv2016-07-26 inventory, but do not publicly report final global emissions as a function of fuel-type. In contrast, a limited number of regional inventories have provided both fuel- and sector-specific emissions. These inventories, for example, have been applied to earth system models to attribute the mortality associated with outdoor air pollution to dominant sources of ambient $PM_{2.5}$ mass, such as residential biofuel combustion in India and coal combustion in China (GBD MAPS Working Group, 2018, 2016). As countries undergo rapid changes that impact fluxes of their emitted pollutants, including population, emission capture technologies, and the mix of fuels used, fuel and source-specific estimates are vital for capturing these contemporary changes and understanding the air quality impacts across multiple scales.

As part of the Global Burden of Disease - Major Air Pollution Sources (GBD-MAPS) project, which aims to quantify the disease burden associated with dominant country-specific sources of ambient $PM_{2.5}$ mass (https://sites.wustl.edu/acag/datasets/gbd-maps/), we have updated and utilized the CEDS open source emissions system to produce a new global anthropogenic emission inventory ($CEDS_{GBD\text{-}MAPS}$). $CEDS_{GBD\text{-}MAPS}$ includes country-level and global gridded (0.5°×0.5°) emissions of seven major atmospheric pollutants (NO_x (as NO_2), CO, NH_3, SO_2, NMVOCs, BC, OC) as a function of 11 detailed emission source sectors (agriculture, energy generation, industry, on-road transportation, non-road/off-road transportation, residential energy combustion, commercial combustion, other combustion, solvent use, waste, and international shipping) and four fuel groups (emissions from the combustion of total coal, solid biofuel, liquid fuels and natural gas, plus all remaining process-level emissions) for the time period between 1970 – 2017. Similar to the prior CEDS inventory released for CMIP6 (Hoesly et al., 2018), $CEDS_{GBD\text{-}MAPS}$ provides surface level emissions from all sectors, including fertilized soils, but does not include emissions from open burning. In the first two sections we provide an overview of the $CEDS_{GBD\text{-}MAPS}$ system and describe the updates that have allowed for the extension to the year 2017 and the added fuel-type information. These include updates to the underlying activity data and input emission inventories used for default estimates and scaling

Deleted: calibration

procedures (including the use of two new inventories from Africa and India), the additional scaling of default BC and OC emissions, as well as the use of updated spatial gridding proxies, and adjustments to the final gridding and aggregation steps that retain detailed sub-sector and fuel-type information. The third section presents global $CEDS_{GBD\text{-}MAPS}$ emissions in 2017 and discusses historical trends as a function of compound, sector, fuel-type, and world region. The final section provides a comparison of the global $CEDS_{GBD\text{-}MAPS}$ emissions with other global inventories, as well as a discussion of the magnitude and sources of uncertainty associated with the $CEDS_{GBD\text{-}MAPS}$ products.

Deleted: added
Deleted: calibration
Deleted: comparison n
Deleted: evaluation
Deleted: against with

2 Methods

The December 23, 2019 full release of the Community Emissions Data System (Hoesly et al., 2019) provides the core system framework for the development of the contemporary $CEDS_{GBD\text{-}MAPS}$ inventory. The $CEDS_{GBD\text{-}MAPS}$ inventory is developed for the GBD-MAPS project and is not an updated release of the core CEDS emissions inventory. As detailed in Hoesly et al. (2018), the original version of the CEDS system was used to produce the first CEDSv2016-07-26 inventory (hereafter called $CEDS_{Hoesly}$) (CEDS, 2017a, b), which provides global gridded (0.5°×0.5°) emissions of atmospheric reactive gases (NO_x (as NO_2), SO_2, NH_3, NMVOCs, CO), carbonaceous aerosol (BC, OC), and greenhouse gases (CO_2, CH_4) from eight anthropogenic sectors (Agriculture (AGR), Transportation (TRA), Energy (ENE), Industry (IND), Residential, Commercial, Other (RCO), Solvents (SLV), Waste (WST), International Shipping (SHP)) over the time period from 1750 - 2014. Here we provide a brief overview of the Community Emissions Data System with detailed descriptions of the major updates that have been implemented to produce the new $CEDS_{GBD\text{-}MAPS}$ inventory. This inventory has been extended to provide emissions from 1970 – 2017 for reactive gases and carbonaceous aerosol (NO_x, SO_2, NMVOCs, NH_3, CO, BC, OC) with increased fuel and sectoral information relative to the $CEDS_{Hoesly}$ inventory (Sect. 2.2.-2.3). Updates primarily include the use of updated input datasets (Sect. 2.1), new and updated global and regional scaling inventories (Sect. 2.2), added scaling of default BC and OC emissions (Sect. 2.3), and the disaggregation of emissions into contributions from additional source sectors and multiple fuel-types (Sect. 2.4).

Deleted: a similar
Deleted: calibration
Deleted: calibration

2.1. Overview of $CEDS_{GBD\text{-}MAPS}$ System

The CEDS system has five key procedural steps, illustrated in Fig. 1. After the collection of input data in Step 0, Step 1 calculates default global emission estimates (Em) for each chemical compound using a bottom-up approach shown in Eq. (1). In Eq. (1), emissions are calculated using relevant activity (A) and emission factor (EF) data for each country (c) and year (y), as a function of 52 detailed working sectors (s) (sub-sectors used for intermediate steps in the CEDS system) and nine working fuel-types (f) (Table 2). CEDS conducts these calculations for two types of emission categories: 1) fuel combustion sources (e.g., electricity production, industrial machinery, on-road transportation, etc.) and 2) process sources (e.g., metal production, chemical industry, manure management, etc.). We note that the distinction between these source categories is reflective of both sector definition and CEDS methodology, as described further in Sect. S2.1. This results in some working

sectors that include emissions from combustion, such as waste incineration and fugitive petroleum and gas emissions, to be characterized in the CEDS system as process-level sources (further details in Sect. S2.1). In contrast to CEDS combustion source emissions, which are calculated in Eq. (1) as a function of 8 fuel types, emissions from CEDS process-level sources are combined into a single 'process' category, as described in Sect. 2.4. Table 2 provides a complete list of $CEDS_{GBD\text{-}MAPS}$ working sectors and fuel-types, as well as source category distinctions.

$$\mathrm{Em}_{\mathrm{species}}^{\mathrm{country,\ sector,\ fuel,\ year}} = \mathrm{A}^{\mathrm{c,\ s,\ f,\ y}} \times \mathrm{EF}_{\mathrm{species}}^{\mathrm{c,\ s,\ f,\ y}} \quad (1)$$

For emissions from CEDS combustion sources, annual activity drivers in Eq. (1) primarily include country-, fuel-, and sector-specific energy consumption data from the International Energy Agency (IEA, 2019). Sector- and compound-specific emission factors are typically derived from energy use and total emissions reported from other inventories, including from the GAINS model (Klimont et al., 2017;IIASA, 2014;Amann et al., 2015), Speciated Pollutant Emission Wizard (SPEW) (Bond et al., 2007), and the US National Emissions Inventory (NEI) (NEI, 2013). For International Shipping, IEA activity data is supplemented with consumption data and EFs from the International Maritime Organization (IMO), as described in Hoesly et al. (2018) and its supplement. In contrast, default emissions (Em) for CEDS process sources are directly taken from other inventories, including from the EDGAR v4.3.2 global emission inventory (EC-JRC, 2018;Crippa et al., 2018). "Implied emission factors" are then calculated for these process sources in Eq. (1) using global population data (UN, 2019, 2018) or pulp and paper consumption (FAOSTAT, 2015) as the primary activity drivers. For years without available emissions, default estimates for CEDS process sources are calculated in Eq. (1) from a linear interpolation of the "implied emission factors" and available activity data (A) for that year. Supplemental Sect. S2.1 and S2.2 provide additional details regarding the input datasets for activity drivers and emission factors used for both CEDS combustion and process source categories.

While CEDS Step 1 is designed to provide a complete set of historical emission estimates, CEDS Step 2 scales these total default emission estimates to existing, authoritative global, regional, and national-level inventories. As described in Hoesly et al. (2018), CEDS uses a "mosaic" scaling approach to retain detailed fuel- and sector-specific information across different inventories, while maintaining consistent methodology over space and time. The development and use of mosaic inventories has been recently increasing as they provide a means to utilize detailed local emissions, while harmonizing this information across large regional or global scales (Li et al., 2017c;Janssens-Maenhout et al., 2015). The CEDS approach, however, differs from previous mosaic inventories, such as that developed for the HTAP project (Janssens-Maenhout et al., 2015), as local and regional inventories in $CEDS_{GBD\text{-}MAPS}$ are used to scale sectoral emissions at the national-level, rather than merging together spatially distributed gridded estimates.

The first step in the scaling procedure is to derive a time series of scaling factors (SF) for each scaling inventory using Eq. (2), calculated as a function of chemical compound, country, sector, and fuel-type (where available). Due to persistent differences and uncertainties in the underlying activity data and sectoral definitions in each scaling inventory, CEDS emissions are scaled to total emissions within aggregate scaling sectors (and fuels, where applicable). These aggregate scaling groups are defined for each scaling inventory and are chosen to be broad in order to improve the overlap between CEDS emission

Deleted: calibrates (or scales)

Deleted: this

Deleted: calibration

Deleted: calibration

Deleted: calibration

Deleted: calibrated

Deleted: calibration

estimates and those reported in other inventories. For example, the sum of CEDS emissions from working sectors 1A4a_Commercial-institutional, 1A4b_Residential, and 1A4c_agriculture-forestry-fishing are scaled to the aggregate 1A4_energy-for-buildings sector in the EDGAR v4.3.2 inventory. Sections 2.2 and Supplemental Sect. S2.3 provide further details about this scaling procedure and the scaling inventories used to develop the 1970 – 2017 CEDS$_{GBD\text{-}MAPS}$ inventory.

$$SF_{species}^{c,\ s,\ f,\ y} = \frac{\text{scaling inventory } Em_{species}^{c,\ s,\ f,\ y}}{\text{default CEDS } Em_{species}^{c,\ s,\ f,\ y}} \quad (2)$$

After SFs are calculated in Eq. (2), the second step in the scaling procedure is to extend these SFs forward and backward in time to fill years with missing data. For these time periods, the nearest available SF is applied. If a particular sector or compound is not present in a scaling inventory, default CEDS estimates are not scaled. For BC and OC emissions, the default procedure in the CEDSv2019-12-23 system was to retain all default BC and OC emission estimates due to limited availability of historical BC and OC emissions. In the CEDS$_{GBD\text{-}MAPS}$ inventory, these species are now scaled to available regional and national-level inventories (further details in Sect. 2.2). For all other species, the CEDS$_{GBD\text{-}MAPS}$ system uses a sequential scaling methodology where total default emissions for each country are first scaled to available global inventories (primarily EDGAR v4.3.2) and second scaled to regional and national-level inventories, many of which have been updated in this work (Sect. 2.2 and Table 3). This process results in final CEDS$_{GBD\text{-}MAPS}$ emissions that reflect the inventory last used to scale the emissions for that country (Fig. 2). Figure S2 provides a time series of implied emission factors after the scaling procedure for select sector- and fuel- combinations that dominant emissions of each compound in the top 15 emitting countries. Sections 2.2 and S2.3 describe further details and updates to this scaling procedure.

CEDS Step 3 extends the scaled emission estimates from 1970 back in time to 1750. This process is necessary as reported emission estimates and energy data are not typically reported with the same level of sectoral and fuel-type detail prior to 1970. Hoesly et al. (2018) provides a detailed description of this historical extension procedure, which is used to derive pre-1970 emissions in the CEDS$_{Hoesly}$ inventory. The new CEDS$_{GBD\text{-}MAPS}$ inventory only reports more contemporary emissions after 1970 and therefore, does not utilize this historical extension.

CEDS Step 4 aggregates the scaled country-level CEDS$_{GBD\text{-}MAPS}$ emissions into 17 intermediate gridding sectors (defined in Table 2). In the CEDSv2019-12-23 system, Step 4 additionally aggregated sectoral emissions from all fuel-types. In contrast, the CEDS$_{GBD\text{-}MAPS}$ system retains sectoral emissions from the combustion of total coal (hard coal + coal coke + brown coal), solid biofuel, and the sum of liquid oil (light oil + heavy oil + diesel oil) and natural gas, as well as all CEDS process-level emissions (Table 2). Sections 2.4 and 4.2.4 describe the CEDS$_{GBD\text{-}MAPS}$ fuel-specific emissions in further detail.

Lastly, CEDS Step 5 uses normalized spatial distribution proxies to allocate annual country-level emission estimates on to a 0.5°×0.5° global grid. Annual emissions from the 17 intermediate gridding sectors and four fuel groups are first distributed spatially using compound-, sector-, and year-specific spatial proxies, primarily from the gridded EDGAR v4.3.2 inventory. Supplemental Table S7 provides a complete list of sector-specific gridding proxies, with additional details specific to the CEDS$_{GBD\text{-}MAPS}$ system in Sect. S2.5 and about the general CEDS gridding procedure in Feng et al. (2020). Second,

Deleted: calibrated
Deleted: calibration
Deleted: calibration
Deleted: calibration
Deleted: calibration
Deleted: calibrated
Deleted: calibrated
Deleted: calibrated second
Deleted: calibrate
Deleted:
Deleted: calibration
Deleted: calibrated
Deleted: calibrated
Deleted: 3
Deleted: 6

gridded emission fluxes (units: kg m^{-2} s^{-1}) are aggregated into 11 final sectors (Table 2) and distributed over 12 months using sectoral and spatially explicit monthly fractions from the ECLIPSE project (IIASA, 2015) and EDGAR inventory (international shipping only). Relative to CEDSv2019-12-23, the new $CEDS_{GBD\text{-}MAPS}$ inventory retains detailed sub-sector emissions from the aggregate RCO (now RCO-Residential, RC-Commercial, and RCO-Other) and TRA (now On-Road and Non-Road) sectors, separate sectoral emissions from process sources, as well as combustion sources that utilize coal, solid biofuel, and the sum of liquid fuels and natural gas. Table 2 contains a complete breakdown of the definitions of CEDS working, intermediate gridding, and final sectors. Gridded total NMVOCs are additionally disaggregated into 25 VOC classes following sector- and country-specific VOC speciation maps from the RETRO project (HTAP2, 2013), which are different from those used in the recent EDGARv4.3.2 inventory (Huang et al., 2017). Similar to the gridding procedure, the same VOC speciation and monthly distributions are applied to sectoral emissions associated with each fuel category.

Final products from the $CEDS_{GBD\text{-}MAPS}$ system include total annual emissions from 1970 - 2017 for each country, as well as monthly global gridded (0.5°×0.5°) emission fluxes, both as a function of 11 final source sectors and four fuel-categories (total coal, solid biofuel, liquid fuel + natural gas, and remaining process sources). Section 5 provides additional details on the dataset availability and file formats.

2.2 Default Emission Scaling Procedure – $CEDS_{GBD\text{-}MAPS}$ Update Details

As described above, default emission estimates for each compound are scaled in CEDS Step 2 to existing authoritative inventories as a function of emission sector and fuel type (where available). In the scaling procedure, annual emissions and EFs for each country are first scaled to available global inventories, then to available regional and national-level inventories, assuming that the latter use local knowledge to derive more accurate regional estimates. Final $CEDS_{GBD\text{-}MAPS}$ emission totals for each country therefore reflect the inventory last used to scale each compound and sector. Many of these inventories are updated annually and where available, have been updated in this work relative to the CEDSv2019-12-23 system (Table 3). For example, global $CEDS_{GBD\text{-}MAPS}$ combustion source emissions of NO_x, total NMVOCs, CO, and NH_3 are first scaled to EDGAR v4.3.2 country-level emissions as a means to incorporate additional country-specific information relative to default estimates derived using more regionally-aggregate EFs from GAINS. $CEDS_{GBD\text{-}MAPS}$ emissions from European countries are then scaled to available EMEP (European Monitoring and Evaluation Programme) (EMEP, 2019) and UNFCCC (United Nations Framework Convention on Climate Change) (UNFCCC, 2019) inventories that extend to 2017, while CO, NMVOCs, NO_x and SO_2 emissions from the US, Canada, and Australia are also scaled to emissions that extend to 2017 from the US NEI (US EPA, 2019), Canadian APEI (Air Pollutant Emissions Inventory) (ECCC, 2019), and Australian NPI (National Pollutant Inventory) (ADE, 2019), respectively. In addition, emissions of all 7 compounds from China are scaled to emissions for 2008, 2010, and 2012 from Li et al. (2017c), followed by subsequent scaling to emissions between 2010 and 2017 from Zheng et al. (2018). Relative to the CEDSv2019-23-13 system, regional inventories have also been added to scale $CEDS_{GBD\text{-}MAPS}$ emissions from India and Africa as described below. Updates to additional regional scaling inventories, including South Korea, Japan,

Deleted: as well as

Deleted: annual

Deleted: Calibration

Deleted: calibrated (or scaled)

Deleted: calibration

Deleted: calibrated

Deleted: calibrate

Deleted: calibrated

Deleted: that extend to 2012 for NO_x, total NMVOCs, CO, and NH_3.

Deleted: calibrated

Deleted: calibrated

Deleted: calibrated

Deleted: calibration

Deleted: calibrate

Deleted: calibration

and other European and Asian countries are not available relative to those used in the CEDSv2019-12-23 system. Table 3 provides a complete list of the inventories used to scale $CEDS_{GBD\text{-}MAPS}$ default emissions, with additional details in Sect. S2.3.

Relative to the CEDSv2019-12-23 system, the $CEDS_{GBD\text{-}MAPS}$ system adds scaling inventories for two rapidly changing regions, Africa and India. First, $CEDS_{GBD\text{-}MAPS}$ emissions from Africa for select sectors are now scaled to the Diffuse and Inefficient Combustion Emissions in Africa (DICE-Africa) inventory from Marais and Wiedinmyer (2016). This inventory provides gridded (0.1° × 0.1°) emissions for NO_x (= NO + NO_2), SO_2, 25 speciated VOCs, NH_3, CO, BC, and OC for 2006 and 2013 for select anthropogenic sectors and fuels. In this work, default CEDS emissions are scaled to total DICE-Africa emissions from each country and later re-gridded in CEDS Step 5 using source-specific spatial proxies described in Sect. 2.1. Following the CEDSv2019-12-23 scaling procedure (Supplemental Sect. S2.3), a set of aggregate scaling sectors and fuels are defined to ensure that $CEDS_{GBD\text{-}MAPS}$ emissions are scaled to emissions from consistent sectors and fuel types within the DICE-Africa inventory (Table S3). Briefly, $CEDS_{GBD\text{-}MAPS}$ 1A3b_Road and 1A4b_Residential emissions are scaled to DICE-Africa emissions from diesel and gasoline powered cars and motorcycles, as well as biomass and oil combustion associated with residential charcoal, crop residue, fuelwood, and kerosene use. The DICE-Africa inventory also includes emission estimates from gas flares across Africa and ad-hoc oil refining in the Niger Delta, fuelwood use for charcoal production and other commercial enterprises, and gas and diesel use in residential generators. Marais and Wiedinmyer (2016) state that these particular sources are missing or not adequately captured in existing global inventories. Therefore, depending on the source sector and inventory details, they recommend that these emissions be added to existing global inventories for formal industry and on-grid energy production in Africa (DICE-Africa, 2016). Due to uncertainties in the representation of these sectors in the default CEDS Africa emissions, these sources are not included in the scaling process here. Default $CEDS_{GBD\text{-}MAPS}$ emissions from the 1B2_fugitive_pert_gas (gas flaring) sector (derived from the ECLIPSE and EDGAR inventories) are larger than DICE-Africa gas flaring emissions in 2013, suggesting that this source may be accurately represented in the default $CEDS_{GBD\text{-}MAPS}$ estimates. As described in Sect. S2.3.2, however, residential generator and fuelwood use for charcoal production and other commercial activities are not explicitly represented in CEDS and will be accounted for only to the extent that these sources are included in the underlying IEA activity data and EDGAR process emission estimates. In the event that the DICE-Africa emissions from these sources are missing in the default CEDS estimates, total 2013 $CEDS_{GBD\text{-}MAPS}$ emissions from Africa for each compound may be underestimated by up to 11% (Sect. S2.3, Table S5). These values range from 0.7% for SO_2 to 11% for CO (Table S5) and all fall within the range of uncertainties typically reported from regional bottom-up inventories (>20%, Sect. 4.2.3). Final emissions from additional sectors or species in CEDS that are not included in the DICE-Africa inventory are set to $CEDS_{GBD\text{-}MAPS}$ default values.

Second, emissions from India for select sectors are now scaled to the Speciated Multi-pollutant Generator Inventory described by Venkataraman et al. (2018) (hereafter called SMoG-India). This inventory includes gridded emissions (0.25° × 0.25°) of NO_x (as NO_2), SO_2, total NMVOCs, CO, BC, and OC for the year 2015 from select anthropogenic sectors and fuels (SMoG-India, 2019). Similar to DICE-Africa emissions, the final spatial distribution in the SMoG-India and $CEDS_{GBD\text{-}MAPS}$ inventories will differ as country-level emissions are scaled to country totals and spatially re-allocated using CEDS proxies in

Deleted: calibrate
Deleted: calibration
Deleted: calibrated
Deleted: calibration
Deleted: calibrated
Deleted: calibrated
Deleted: calibration
Deleted: 4
Deleted: 4
Deleted: 2
Deleted: calibrated

Step 5. SMoG-India emissions for each compound are available for 17 sectors and nine fuel types (coal, fuel oil, diesel, gasoline, kerosene, naptha, gas, biomass, process/fugitive). Similar to the DICE-Africa inventory, aggregate scaling groups have been defined to scale consistent sectors and fuels between inventories, as described in Sect. S2.3. Briefly default $CEDS_{GBD\text{-}MAPS}$ emissions for 1A4c_Agriculture-forestry-fishing sector are scaled to the sum of SMoG-India emissions for agricultural pumps and tractors, 1A4b_Residential emissions are scaled to the sum of SMoG-India emissions from residential lighting, cooking, diesel generator use, space and water heating, 1A1a electricity and heat generation sectors are scaled to SMoG-India thermal power plant emissions, 1A3b road and rail sectors are scaled to the respective SMoG-India road and rail emissions, and $CEDS_{GBD\text{-}MAPS}$ industrial working sectors are allocated and scaled to four SMoG-India industrial sectors: light industry (e.g., mining and chemical production), heavy industry (e.g., iron and steel production), informal industry (e.g., food production), and brick production. Calculated scaling factors for these sectors are held constant before and after 2015. $CEDS_{GBD\text{-}MAPS}$ emissions do not include contributions from open burning and are not scaled to SMoG-India open burning emissions. In cases where SMoG-India emissions are not reported (e.g., power generation from oil combustion), default $CEDS_{GBD\text{-}MAPS}$ emissions are retained. Sect. S2.3.3 provides additional details.

To examine the changes in $CEDS_{GBD\text{-}MAPS}$ emissions associated with the incorporation of the SMoG-India and DICE-Africa scaling inventories, as well as the updated underlying input datasets, Fig. 3 compares the total and sectoral distribution of $CEDS_{GBD\text{-}MAPS}$ and $CEDS_{Hoesly}$ emissions for these two regions in 2014 (year with latest overlapping data). For the Africa comparison, the left plot in Fig. 3 shows that total NO_x, BC, and OC emissions are generally lower in the $CEDS_{GBD\text{-}MAPS}$ inventory than in $CEDS_{Hoesly}$. Lower NO_x and OC emissions are largely associated with smaller contributions from on-road transport and residential combustion, respectively, while lower BC emissions are associated with both lower residential and on-road transport contributions. Lower emissions of NO_x from the transport sector result from the lower EF used for diesel vehicles in the DICE-Africa inventory (Marais et al., 2019). Compared to GAINS (2010) and EDGAR v4.3.2 (2012), on-road emissions from African countries in $CEDS_{GBD\text{-}MAPS}$ are up to 2.5 Tg lower for NO_x, but within 0.1 Tg for BC. In contrast to NO_x, larger EFs in the DICE-Africa inventory for on-road emissions of CO and OC result in $CEDS_{GBD\text{-}MAPS}$ emissions that are up to 14.8 and 0.3 Tg higher, than previous estimates. Figure S2 shows that after scaling, the implied emission factors of CO from oil and gas combustion in the on-road transport sector for four African countries range from 0.19-0.28 g g^{-1}, slightly smaller than the range of 0.029 - 0.380 g g^{-1} used in the DICE-Africa inventory. Emissions from the residential/commercial sectors in Africa are generally lower in $CEDS_{GBD\text{-}MAPS}$ than in $CEDS_{Hoesly}$ due to both lower biofuel consumption and a lower assumed EF in the DICE-Africa inventory (Marais and Wiedinmyer, 2016). Residential BC and OC emission estimates are also lower than those from GAINS (Klimont et al., 2017). The difference in biofuel consumption is due to different data sources. The DICE-Africa inventory uses residential wood fuel consumption estimates from the UN while $CEDS_{Hoesly}$ uses data from the IEA. Both of these sources consist largely of estimates for African countries because there is little country-reported biofuel consumption data available. The estimation methodologies for both the UN and IEA estimates are not well documented, which adds to the uncertainty in these values (Sect. 4.2). After scaling, the implied EFs for residential biofuel emissions of OC are ~0.001-0.002 g g^{-1} in three African countries (Figure S2), within the range of EFs of 0.0007 – 0.003 g g

Deleted: calibration

Deleted: calibrate

Deleted: calibrated

Deleted: calibrated

Deleted: calibrated

Deleted: calibrated

Deleted: calibrated

Deleted: calibrated

Deleted: calibration

Deleted: , which reflects the use of inefficient combustion sources…

Deleted: due to

Deleted: ,

Deleted: respectively

Deleted: , in $CEDS_{GBD\text{-}MAPS}$

Deleted: In addition, Africa e

Deleted: These r

[1] implemented in the DICE-Africa inventory. Total $CEDS_{GBD\text{-}MAPS}$ emissions of NMVOCs are larger, primarily due to increased contributions from solvent use and the energy sector associated with changes in the EDGAR v4.3.2 inventory, while total emissions of CO, SO_2, and NH_3 are relatively consistent between the two CEDS versions.

For the India comparison, the right panel of Fig. 3 shows that total emissions of NO_x, CO, SO_2, NMVOCs, and OC are lower in $CEDS_{GBD\text{-}MAPS}$. Relative reductions in NO_x emissions are largely associated with on-road transport. Scaled $CEDS_{GBD\text{-}MAPS}$ transport emissions are 5 Tg smaller than NO_x emissions in $CEDS_{Hoesly}$, largely as a result of lower fuel consumption levels for gas, diesel, and CNG on-road vehicles used to develop SMoG-India estimates (Sadavarte and Venkataraman, 2014). Figure S2 shows that the implied emission factor for NO_x emissions from oil & gas combustion in the on-road transport sector in India is ~0.015 g g^{-1} in 2015, which falls within the range of values of 0.0026 – 0.046 g g^{-1} used for various vehicles and fuel type in Venkataraman et al. (2018). Similarly, NO_x transport emissions are also lower in $CEDS_{GBD\text{-}MAPS}$ relative to the EDGAR and GAINS inventories. Causes of other reductions are mixed. For example, lower emissions of SO_2 and NMVOCs are largely associated with the energy sector, while reductions in the industry sector contribute to reduced CO emissions. For SO_2, Figure S2 shows that the implied EF for coal combustion in the energy sector is ~0.004 g g^{-1}, slightly lower than the range of 0.0049 – 0.0073 g g^{-1} used for the SMoG-India inventory.

To further examine the $CEDS_{GBD\text{-}MAPS}$ inventory in these regions, Fig. 4 compares final $CEDS_{GBD\text{-}MAPS}$ and $CEDS_{Hoesly}$ emissions for India and Africa to total emissions from two widely used global inventories: GAINS (ECLIPSE v5a) and EDGAR (v4.3.2). First, Fig. 4 shows the percent difference between the $CEDS_{GBD\text{-}MAPS}$ inventory and the GAINS and EDGAR inventories on the y-axis, against the percent difference between the $CEDS_{Hoesly}$ inventory and GAINS and EDGAR emissions on the x-axis. Percent differences are calculated from total emissions from Africa (left) and India (right) for the year 2012 for the comparison with EDGAR and for 2010 for the comparison to GAINS (most recent years with overlapping data). The green shaded areas indicate regions where the updated $CEDS_{GBD\text{-}MAPS}$ inventory has improved agreement with EDGAR or GAINS relative to the $CEDS_{Hoesly}$ inventory. This comparison shows that the additional scaling of $CEDS_{GBD\text{-}MAPS}$ emissions to the SMoG-India inventory generally improves agreement with both the EDGAR and GAINS inventories relative to $CEDS_{Hoesly}$ for all species except black carbon (BC). Scaling to the DICE-Africa inventory generally improves $CEDS_{GBD\text{-}MAPS}$ agreement with the EDGAR inventory but not with GAINS (except for OC). Further comparisons to these two inventories are discussed in Sect. 4. While uncertainties in emissions from these inventories are expected to be at least 20% for each compound (discussed in Sect. 3.3), this comparison provides an illustration of the changes between the two CEDS versions relative to two widely used global inventories.

2.3 Default BC & OC Scaling Procedure – $CEDS_{GBD\text{-}MAPS}$ Update Details

Relative to the CEDSv2019-12-23 system, the second largest change to the $CEDS_{GBD\text{-}MAPS}$ system is the added scaling of BC and OC emissions in CEDS Step 2. In the v2019-12-23 system, OC and BC were not scaled due to a lack of historical BC and OC emission estimates in regional and global inventories. Due to the focus of the $CEDS_{GBD\text{-}MAPS}$ inventory on more recent years, these two compounds are now scaled to available regional and country-level estimates (Table 3), following the same

Deleted: in

Deleted: Calibrated

Deleted: Compared to EDGAR and GAINS inventories,

Deleted: .

Deleted: calibration

Deleted: Calibration

Deleted: Calibration

Deleted: calibration

scaling procedure described above for the reactive gases. Unlike the reactive gases, however, BC and OC emissions are not scaled to the global EDGAR v4.3.2 inventory due to the large reported uncertainties in this inventory (ranging from 46.8% to 153.2% (Crippa et al., 2018)).

To examine the impact of the new BC and OC emissions scaling, in addition to the updated IEA energy consumption data, Fig. 5 and Fig. S3-S4 show time series of global BC and OC emissions from $CEDS_{GBD\text{-}MAPS}$ compared to emissions from the $CEDS_{Hoesly}$ inventory. In 2014, respective global annual emissions of BC and OC are 21% and 28% lower than the $CEDS_{Hoesly}$ inventory and have total global annual emissions in 2017 of 6 and 13 TgC yr^{-1} for BC and OC, respectively. These reductions in global emissions are largely due to the added scaling of emissions from China, Africa, Japan, and other countries in Asia included in the REAS inventory (Fig. S3-S4). Figures 5 and S3-S4 additionally compare $CEDS_{GBD\text{-}MAPS}$ emissions to those from the GAINS (ECLIPSE v5a) and EDGAR (v4.3.2) inventories, which generally show improved agreement in BC and OC emissions with the GAINS inventory. $CEDS_{GBD\text{-}MAPS}$ emissions between 1990 and 2015 are now 7-14% lower than GAINS BC emissions, while $CEDS_{GBD\text{-}MAPS}$ emissions of OC remain 12-25% higher than GAINS estimates. Further discussion of $CEDS_{GBD\text{-}MAPS}$ BC and OC emissions and comparisons to EDGAR and GAINS inventories are below in Sect. 4.1.2. As an additional point of comparison, Bond et al. (2013) report global BC and OC values for the year 2000, derived from averages of energy-related burning emissions from SPEW and GAINS. Reported global estimates of BC and OC are 5 TgC and ~11-14 TgC (16 Tg organic aerosol/ organic mass: organic carbon ratio of 1.1 - 1.4), respectively (Bond et al., 2013). These also have improved agreement with the $CEDS_{GBD\text{-}MAPS}$ estimates of BC and OC in 2000 relative to those in the $CEDS_{Hoesly}$ inventory. Lastly, we note plans for an upcoming update to the core CEDS system to improve historical trends in carbonaceous aerosol by incorporating reported inventory values for total $PM_{2.5}$ and its ratio with BC and OC emissions.

2.4 Fuel Specific Emissions – $CEDS_{GBD\text{-}MAPS}$ Update Details

Prior to gridding, $CEDS_{GBD\text{-}MAPS}$ Step 4 combines total country-level emissions for each of the 52 working sectors and nine fuel groups into 17 aggregate sectors and 4 fuel-groups: total coal (hard coal + brown coal + coal coke), solid biofuel, the sum of liquid fuels (heavy oil + light oil + diesel oil) and natural gas, and all remaining 'process' emissions (Table 2). In contrast, the CEDSv2019-12-23 system aggregates all fuel-specific emissions and reports inventory values as a function of sector only. In $CEDS_{GBD\text{-}MAPS}$, country-total emissions from these aggregate sectors and fuel groups are distributed across a 0.5°×0.5° global grid using spatial gridding proxies, as discussed in Sect. 2.1 (Table S7). During gridding, the same spatial proxies are applied to all fuel groups within each sector. In practice, this requires that the gridding procedure be repeated four times for each of the fuel groups. After gridding in CEDS Step 5, both annual country-total and gridded emission fluxes from each fuel group are aggregated to 11 final sectors. Figure S5 demonstrates the level of detail available in the new $CEDS_{GBD\text{-}MAPS}$ gridded emission inventory by illustrating global BC emissions in 2017 from 1) all source sectors, 2) the residential sector only, 3) residential biofuel-use only, and 4) residential coal-use only. Additional uncertainties associated with the $CEDS_{GBD\text{-}MAPS}$ fuel-specific emissions in both the country-total and annual gridded products are discussed further in Sect. 4.2.4.

Deleted: calibration
Deleted: calibration
Deleted: 2
Deleted: 3
Deleted: calibration
Deleted: 2
Deleted: 3
Deleted: 2
Deleted: 3
Deleted: 6
Deleted: 4
Deleted: 3

3 Results

The new $CEDS_{GBD\text{-}MAPS}$ inventory provides global emissions of NO_x, SO_2, NMVOCs, NH_3, CO, OC, and BC for 11 anthropogenic sectors (agriculture, energy, industry, on-road, non-road transportation, residential, commercial, other, waste, solvents, international shipping) and four fuel groups (combustion of total coal, solid biofuel, and liquid fuels and natural gas, and process sources) over the time period between 1970 - 2017. Final country-level emissions are provided as annual time series in units of kilotons per year (kt yr^{-1}) for each sector and fuel-type and include NO_x as emissions of NO_2. Final global gridded (0.5° × 0.5°) emissions for each compound, sector, and fuel group have been converted to emission fluxes (kg m^{-2} s^{-2}), distributed over 12 months, and represent NO_x as NO to facilitate use in earth system models. Total NMVOCs in gridded products are additionally separated into 25 sub-VOC classes. Using a combination of updated energy consumption data and scaling procedures, $CEDS_{GBD\text{-}MAPS}$ provides the most contemporary bottom-up global emission inventory to-date, and is the first inventory to report global emissions of multiple atmospheric pollutants from multiple fuel groups and sectors using consistent methodology. The following results section presents an overview of the $CEDS_{GBD\text{-}MAPS}$ emission inventory, with particular focus on emissions in 2017 and historical trends as a function of compound, sector, fuel type, and world region. Section 4 compares these results to other global emission inventories and discusses the magnitudes and sources of inventory uncertainties. Known issues in the inventory data at the time of submission are detailed in Sect. S4.

3.1 Global Annual Total Emissions in 2017

Figures 6 and 7 show time series from 1970 – 2017 of global annual $CEDS_{GBD\text{-}MAPS}$ emissions for each emitted compound. Global $CEDS_{GBD\text{-}MAPS}$ emissions for reactive gases in 2017 are 122 Tg for NO_x (as NO_2), 538 Tg for CO, 79 Tg for SO_2, 175 TgC for total NMVOCs, and 61 Tg for NH_3. Global 2017 emissions of carbonaceous aerosol are 13 and 6 TgC for OC and BC, respectively. The time series in Fig. 6 and 7 additionally show the contributions to global emissions from each of the 11 source sectors (Fig. 6) and four fuel groups (Fig. 7). Each panel in Fig. 6 additionally shows a pie chart with the fractional contribution of each sector to total global emissions in 2017 (outside), while the inner pie chart shows the fractional contributions from each of the fuel groups to each source sector. Numerical values for these fractional contributions are in Table S8. Global totals for 2017 are provided in the center of each pie chart. Global emissions from each compound are additionally split into contributions from 11 world regions (defined in Table S9) in Fig. 8 to aid in the interpretation of global trends below.

For global 2017 emissions of NO_x, Fig. 6 and Table S8 show that 60% of NO_x emissions are associated with the energy generation (22%), industry (15%), and on-road transportation (23%) sectors. These sectors have the largest contributions from emissions from coal combustion (> 46% for the energy and industry emissions) and the combined combustion of liquid fuels (oil) and natural gas (with these two fuels accounting for 100% of NO_x on-road emissions). Time series of regional contributions to global emissions in Fig. 8 additionally show that 50% of global 2017 NO_x emissions are from the combined Other Asia/Pacific region (Table S9) (13 Tg), China (24 Tg), International Shipping (25 Tg). For global

Deleted: their

Deleted: calibration

Deleted: S5

Deleted: 7

Deleted: 9

Deleted: 8

Deleted: 7

Deleted: 59

Deleted: the combined Other Asia/Pacific/Middle East region (Table S8) (23 Tg), and

2017 emissions of remaining gas-phase pollutants, 67% of CO emissions are from the on-road (100%: oil + gas) and residential (86%: biofuel) sectors, 78% of SO_2 emissions are from the energy generation (63%: coal) and industry (38% coal, 36% process, 25% oil + gas) sectors, 89% of NH_3 emissions are from the agriculture (100%: process) and waste (100%: process) sectors, and emissions of NMVOCs have the largest single contribution (36%) from the energy sector, 99% of which are associated with $CEDS_{GBD\text{-}MAPS}$ process sources (Table 2). For carbonaceous aerosol in 2017, 58% of global BC emissions are from the residential (70%: biofuel) and on-road (100%: oil + gas) sectors, while 67% of global OC emissions are from the residential (92%: biofuel) and waste (100%: process) sectors. Fig. 8 shows that in 2017, China is the dominant source of global CO (144 Tg, 27% of global total), SO_2 (12 Tg, 15% of global total), NH_3 (12 Tg, 20% of global total), OC (2.7 TgC, 20% of global total), and BC (1.4 TgC, 24% of global total). In contrast, Africa is the dominant source of global NMVOCs in 2017 (48 TgC, 27% of global total) and International Shipping is the dominant source of global NO_x emissions (25 Tg, 20% of global total).

As discussed above in Sect. 2 and below in Sect. 4.2.4, the distinction between CEDS combustion and process-level source categories for all species may result in the underrepresentation of emissions from combustion sources relative to those from CEDS process-level sectors. As shown in Table 2, for example, some combustion emissions from the energy, industry, and waste sectors, such as fossil fuel fires and waste incineration are categorized as CEDS 'process-level' source categories (Table 2). These emissions are allocated to the final CEDS process category rather than the CEDS total coal, biofuel, or oil and gas categories.

3.2 Historical Trends in Annual Global Emissions

Historical emission trends between 1970 and 2017 in Fig. 6 and 7 indicate that global emissions of each compound generally follow three patterns: (1) global CO and SO_2 emissions peak prior to 1990 and generally decrease until 2017, (2) global emissions of NO_x, BC, and OC peak much later around 2010 and then decrease until 2017, and (3) global emissions of NH_3 and NMVOCs continuously increase throughout the entire time period. These trends generally reflect the sector-specific regulations implemented in dominant source regions around the world. For example, global emissions of CO generally decrease after the incorporation of catalytic converters in North America and Europe around 1990 (Fig. S7 and S8). Despite, however, continued reductions in these regions, global emissions of CO slightly increase between 2002 and 2012 due to simultaneous increases among the energy, industry, and residential sectors in China, India, Africa, and the Other Asia/Pacific region (Fig. S9-S12). Global CO emissions then decrease by 9% between 2012 and 2017, largely due to reductions in industrial coal, residential biofuel, and process energy sector emissions in China (S6, S9, S17-S18), associated with the implementation of emission control strategies (reviewed in Zheng et al., 2018), as well as continued reductions in on-road transport emissions in North America and Europe (Fig. S7-S8). Similarly, global SO_2 emissions decrease after peaking in 1979, largely due to emission control policies in the energy and industry sectors in North America and Europe (Fig. S7-S8). While simultaneous increases in emissions from coal use in the energy and industry sectors in China result in a brief increase in global SO_2 emissions between 1999 and 2004 (Fig. 6, S9), global SO_2 emissions decline by 32% between 2004 and 2017 due to the implementation of stricter emission standards for the energy and industry sectors after 2010 in China (Zheng et al., 2018), as

Deleted: By 2017, the combined Other Asia/Pacific/Middle East region surpasses China to become the largest source of global SO_2 (17 Tg, 22% of global total) and OC (3 TgC, 22% of global total).

Deleted: in 2017

Deleted: ,

Deleted: followed by the Other Asia/Pacific/Middle East region (42 TgC) and China (29 TgC).

Deleted: 3

Deleted: 6

Deleted: 7

Deleted: in

Deleted: combustion

Deleted: CO emissions

Deleted: 8

Deleted: 1

Deleted: 5

Deleted: 8

Deleted: 6

Deleted: 7

Deleted: that are

Deleted: 6

Deleted: 7

Deleted: 6

Deleted: 7

Deleted: 8

well as continued reductions in North America and Europe (Fig. S7- S8). Regional SO_2 emission trends are particularly large with a factor of 9.5 decrease in total SO_2 emissions in North America between 1973 and 2017, a factor of 6.9 decrease in Europe between 1979 and 2017, and a factor of 5.9 increase in China between 1970 and 2004, followed by a factor of 2.6 decrease after 2011 (Fig. 8). While China is the largest global contributor to SO_2 emissions between 1994 and 2017, these large regional reductions, coupled with increasing SO_2 emissions in the Other Asia/Pacific region, African countries, and India (Fig. 8), indicate that future global SO_2 emissions will increasingly reflect activities in these other rapidly growing regions.

In contrast to historical emissions of SO_2 and CO, global emissions of NO_x, BC, and OC peak later between 2011 and 2013. Global emissions then decrease by 7%, 9%, and 7%, respectively by 2017 (Fig. 6). These trends also reflect the sector-specific regulations implemented in dominant source regions. For NO_x for example, global emissions between 1970 and 2017 are dominated by the combustion of coal, oil, and gas in the on-road transportation, energy generation, industry, and international shipping sectors (Fig. 6, 8). Global on-road transportation emissions are generally flat between 1988 and 2013 due to competing trends across world regions. While more stringent vehicle emission standards result in more than a factor of 2 decrease in on-road transportation NO_x emissions in North America and Europe between 1992 and 2017 (Fig. S7-S8), on-road transport emissions in China, India, and the Other Asia/Pacific region simultaneously experience between a factor of 1.3 to 2.8 increase (Fig. S9-S11). Subsequent reductions between 2013 and 2017 in global on-road emissions correspond to a 12% reduction in on-road transportation emissions in China due to the phase in of stricter emission standards (Zheng et al., 2018), coupled with a continued decrease in emissions from North America and Europe. Global NO_x emissions from the energy and industry sectors increase by up to a factor of 6 between 1970 and 2011 due to regional increases in China, India, the Other Asia/Pacific region, and African countries, with reductions between 2011 and 2017, again largely from reductions in China from stricter emissions control policies for coal fired power plants and coal use in industrial processes (Zheng et al., 2018;Liu et al., 2015). Global emissions of NO_x from waste combustion and agricultural activities also increased by a factor of 2 and 65%, respectively, between 1970 and 2017, also contributing to the offset of recent reductions in emissions from regulated combustion sources (Fig. 6). Similar to global NO_x emissions, trends in historical BC and OC emissions reflect a balance between emission trends in North America, Europe and other world regions, with reduction between 2010 and 2017 largely driven by reductions in emissions from China (Fig. 8, S9). In contrast to NO_x emissions, however, BC and OC emissions are dominated by contributions from biofuel combustion in the residential sector, as well as on-road transportation, industry, and energy sectors for BC and the waste sector for global OC (Fig. 6). Though emissions of BC and OC have a higher level of uncertainty relative to other compounds (Sect. 4), emissions from African countries and the Other Asia/Pacific region experience growth in BC and OC emissions from these sectors. The exceptions are in China and India, both of which experience a plateau or reduction in BC and OC emissions from the residential, energy (China only), industry, and on-road transportation sectors between 2010 and 2017. In India, reductions in BC and OC emissions from the residential and informal industry sectors are expected to continue under policies to switch to cleaner residential fuels and energy sources, while BC emissions from on-road transport may increase due to increased transport demand (Venkataraman et al., 2018). Similar to trends in SO_2 emissions, increasing trends in total OC and BC emissions from Africa, India, Latin America, the Middle East,

Deleted: 6
Deleted: 2015
Deleted: 6
Deleted: 7
Deleted: 8
Deleted: 0
Deleted: processing
Deleted: 8
Deleted: steady

and the Other Asia/Pacific region, coupled with large decreases in emissions from China, North America, and Europe (Fig. 8) indicate that global emissions will increasingly reflect activities in these rapidly growing regions.

Trends in historical emissions of NMVOCs and NH_3 differ from other pollutants in that they continuously increase between 1970 and 2017. Global emissions of NH_3 increase by 81% between 1970 and 2017 and are largely associated with emissions from agricultural practices (75% in 2017) and waste disposal and handling (14% in 2017) (Fig. 6, Table S8). Unlike emissions from combustion sources, there are no largescale regulations outside of Europe targeting NH_3 emissions from agricultural activities, such as livestock manure management. As a result, global agricultural emissions of NH_3 increase between 1970 and 2017 by 82%, driven by increases in all regions other than Europe (Fig. 6, S6, S12). Similarly, global NH_3 emissions from the waste sector increase by 77% between 1970 and 2017, driven by increases in Latin America, the Other Asia/Pacific region, Africa, and India (Fig. S6, S12). Global emissions of NMVOCs increase by 40% between 1970 and 2017 and are largely associated with emissions from the on-road transport, residential, energy, industry, and solvent use sectors (Fig. 6). In contrast to other emitted pollutants, Africa is the largest global source of NMVOC emissions between 2010 and 2017, largely due to large contributions and continued increases in emissions from the residential (factor of 2.7) and energy (factor of 4) sectors (Fig. S12). Increases in energy sector emissions after 2003 are largely driven by increases in fugitive emissions from select African countries, including Nigeria, Kenya, and Angola, and Mozambique. Emissions from China are the second largest global NMVOC source between 1996 and 2017 (Fig. 8), while the Other Asia/Pacific region is the third largest source between 1999 and 2017. Total NMVOCs in China increase by a factor of 3.4 between 1970 and 2017 due to activity increases in the solvent, energy, and industry sectors (Zheng et al., 2018), while targeted emission controls for the residential and on-road transport sectors result in their reduced contributions to NMVOC emissions between 2012 and 2017 (Fig. S9). Total emissions of NMVOCs in Europe and North America decrease by up to a factor of 2.4 between 1970 and 2017, due to reductions in all source sectors, except for energy emissions in North America, which increase between 2007 and 2011 and remain flat through 2017 (Fig. S7).

To provide a fuel-centric perspective of global historical emissions trends, Fig. 7 illustrates the contributions from the combustion of coal, solid biofuel, the sum of liquid fuel and natural gas, as well as all remaining CEDS 'process-level' sources (Table 2) to total global emissions between 1970 and 2017. Reductions discussed above between 2010 and 2017 for global emissions of NO_x, CO, SO_2, BC and OC, are largely associated with reductions in coal combustion from the energy, industry, and residential sectors associated with emission control policies and residential fuel replacement in China, as well as coal-fired power plant reductions in North America and Europe (Fig. 7, S13, S17). Despite large reductions in emissions, China is still the single largest source of global emissions from coal combustion in 2017 (23-64% for each compound except NH_3). Figure S17, however, also shows that emissions from coal combustion are simultaneously increasing in India, the Other Asia/Pacific region, and Africa. Specifically, SO_2 emissions from coal combustion in India are set to surpass those from China by 2018 if recent $CEDS_{GBD\text{-}MAPS}$ trends hold. For biofuel combustion, global emissions of all compounds are primarily associated with the residential sector (Fig. S14), with recent reductions in biofuel CO, SO_2, BC, and OC emissions largely from reductions in China (Fig. S18). In contrast, biofuel emissions from all other regions remain relatively flat or increase

Deleted: 7
Deleted: 5
Deleted: 1
Deleted: 5
Deleted: 1
Deleted: 1
Deleted: the Other Asia region
Deleted: in 2017 and the dominant source
Deleted: 1989
Deleted: to
Deleted: 2010
Deleted: . China
Deleted: of global NMVOCs
Deleted: 1996
Deleted: 8
Deleted: 6
Deleted: 2
Deleted: 6
Deleted: 6
Deleted: Other Asia/Pacific/Middle East
Deleted: 3
Deleted: 7

between 1970 and 2017, though biofuel emissions of NMVOCs, CO, SO_2, and OC in India, as well as SO_2 emissions in North America both decrease between 2010 and 2017 (Fig. S18). In 2017, biofuel emissions of all compounds are dominated by emissions from either Africa (NO_x, SO_2, NH_3, NMVOC, BC) or India (OC). For oil and gas combustion, global emissions of all compounds are primarily associated with on-road transportation, international shipping, and energy and industry (SO_2 only) sectors, with general decreases in associated emissions in North America and Europe between 1970 and 2017 and increases in other regions (Fig. S19). In contrast to other combustion sectors and fuels, emissions of NO_x, CO, NMVOCs, BC, and OC from the combustion of liquid fuels and natural gas in China remain relatively flat or slightly decrease between 2010 and 2017. Dominant global regions vary by compound (Fig. S19) and include International Shipping (NO_x, SO_2), Africa (OC), India (BC), North America (CO, NH_3), and the Other Asia/Pacific region (NMVOCs). Global CEDS process source emissions, which include contributions from some fuel combustion processes (Table 2), decrease between 2010 and 2017 for CO, SO_2, BC, and OC. These trends are primarily associated with reductions in emissions from the energy and industry sectors. In contrast, process source contributions to NO_x, NH_3, and NMVOCs increase over this same time period due to increases in non-combustion agricultural and solvent use emissions, as well as emissions from waste disposal and energy generation and transformation. Increases in emissions from these sectors between 1970 – 2017 drive the continuous increases in NH_3 and NMVOCs, discussed above. Dominant source regions in 2017 of these process level emissions include China (NO_x, CO, NH_3, BC, OC), India (SO_2), and African countries (NMVOCs) (Fig. S20).

Deleted: and Europe
Deleted: 7
Deleted: ,
Deleted: , or the Other Asia/Pacific/Middle East region
Deleted: 8
Deleted: Similar
Deleted: 8
Deleted: , but are generally either the Other Asia/Pacific/Middle East region, Africa, or International Shipping…
Formatted: Subscript
Deleted: the combined Other Asia/Pacific/Middle East region, and Africa
Deleted: are all dominant sources of process level emissions in 2017 …
Deleted: 19

4 Discussion

4.1 Comparison to Global Inventories

4.1.1 Comparison to $CEDS_{Hoesly}$ Inventory

As a result of the similar methodologies, Fig. 6 shows that $CEDS_{GBD\text{-}MAPS}$ and $CEDS_{Hoesly}$ emission inventories predict similar magnitudes and historical trends in global emissions of each compound between 1970 and 2014. The two inventories, however, diverge in recent years due to the incorporation of updated activity data and both updated and new scaling emission inventories included in the $CEDS_{GBD\text{-}MAPS}$ system. For global emissions of NO_x, CO, and SO_2, the $CEDS_{GBD\text{-}MAPS}$ emissions are smaller than the $CEDS_{Hoesly}$ emissions after 2006 and show a faster decreasing trend. By 2014, global emissions of these compounds are between 7 and 21% lower than previous $CEDS_{Hoesly}$ estimates. These differences are largely associated with large emission reductions in China as a result of the updated national-level scaling inventory from Zheng et al. (2018), along with the added DICE-Africa (Marais and Wiedinmyer, 2016) and SMoG-India (Venkataraman et al., 2018) scaling inventories. Differences in emissions from India and Africa in the two CEDS inventories are discussed in Sect. 2 (Fig. 3) and combined, account for ~60% of the reduction in global NO_x emissions, 23% of the reduction in global CO, and 14% of the reduction in global SO_2. The largest differences between these two inventories in India and Africa are the reduced NO_x emissions from the transport sector, as well as reduced energy emissions of SO_2 in India. Remaining differences between NO_x and SO_2 emissions in the

Deleted: calibration
Deleted: calibration
Deleted: calibration

two CEDS inventories are largely associated with the updated China emission inventory from Zheng et al. (2018), which reports lower emissions in 2010 and 2012 than a previous version of the MEIC inventory that was used to scale China emissions in the $CEDS_{Hoesly}$ inventory (Li et al., 2017c). These emission reductions are largely associated with the industrial and residential sectors in China and are partially offset by a simultaneous increase in transportation emissions of all compounds relative to $CEDS_{Hoesly}$.

For global emissions of NH_3 and NMVOCs, these species remain relatively unchanged between the $CEDS_{Hoesly}$ and $CEDS_{GBD\text{-}MAPS}$ inventories. In 2014 $CEDS_{GBD\text{-}MAPS}$ emissions are 5% higher than $CEDS_{Hoesly}$ emissions for NMVOCs and 2% lower than $CEDS_{Hoesly}$ global NH_3 emissions. Emissions of NH_3 remain relatively unchanged (within <2%) from dominant source regions, including India, Africa (Fig. 3), and China. In contrast, emissions of NMVOCs from Africa and China in the DICE-Africa and Zheng et al. (2018) scaling inventories are larger than those in the $CEDS_{Hoesly}$ inventory. Global emissions of NMVOCs are also higher in EDGARv4.3.2 inventory relative to the previous version used in the $CEDS_{Hoesly}$ inventory. NMVOCs are particularly large from the process energy sector emissions in Africa (Figure S12), which primarily include fugitive emissions from oil and gas operations (Table 2). Default energy sector emissions from 'non-combustion' processes are taken from the EDGAR inventory and are not scaled to DICE-Africa inventory. Therefore, the large increase in these emissions in Africa relative to $CEDS_{Hoesly}$ are largely driven by changes in the EDGAR v4.3.2 inventory, with emissions from the 1B2_Fugitive_Fossil fuels sector, increasing for example by a factor of 5 in Nigeria between 2003 and 2017.

Global emissions of OC and BC have the largest differences between the two CEDS inventories, with $CEDS_{GBD\text{-}MAPS}$ emissions consistently smaller than $CEDS_{Hoesly}$ emissions between 1970 and 2014. By 2014, $CEDS_{GBD\text{-}MAPS}$ emissions of BC and OC are 24 and 33% smaller than corresponding $CEDS_{Hoesly}$ emissions. In the $CEDS_{Hoesly}$ inventory, default emissions of BC and OC are not scaled and therefore these differences are largely associated with the added scaling inventories, discussed in Sect. 2 and shown in Table 3. As shown in Fig. S3-S4, the added scaling of BC and OC emissions leads to a reduction in global $CEDS_{GBD\text{-}MAPS}$ emissions of OC in all scaled regions, and a reduction in BC emissions in all regions other than India. In India, increases in industry and residential BC emissions from the SMoG-India scaling inventory result in a slight increase in BC emissions relative to the $CEDS_{Hoesly}$ inventory (Fig. 3). Waste emissions of OC and BC are also reduced in the $CEDS_{GBD\text{-}MAPS}$ inventory due to updated assumptions for the fraction of waste burned (Sect. S1.1). As discussed in Hoesly et al. (2018) and further below, BC and OC emissions typically have the largest uncertainties of all the emitted species and their recent changes in the residential and waste sectors are particularly uncertain.

The relative contributions of each source sector to emissions in the two CEDS versions are additionally shown in Fig. S21. This comparison shows that the fractional sectoral contributions to global emissions in 2014 are the same to within 10% in the two CEDS inventories. The largest differences are a 9% increase in the relative contribution of on-road transportation emissions of CO and reductions in the relative contribution of waste emissions across all compounds. These trends reflect the large update to default waste emissions described above as well as changes associated with the DICE-Africa and national China scaling inventories.

Deleted: calibrate
Deleted: calibration
Deleted: calibrated
Deleted: calibration
Deleted: 2
Deleted: 3
Deleted: calibration
Deleted: calibrated
Deleted: calibration
Deleted: 0
Deleted: calibration

Similar to the total global emissions, changes between the two CEDS versions for the national-level and 0.5°×0.5° gridded products will also result from updates to the energy consumption data, scaling inventories (Section 2.2-2.3) and spatial distribution proxies from EDGARv4.3.2 (Section 2.1). Time series of differences between the $CEDS_{Hoesly}$ and $CEDS_{GBD\text{-}MAPS}$ inventories for 11 world regions are shown for each compound in Fig. S22. In recent years, Figure S22 shows that $CEDS_{GBD\text{-}MAPS}$ emissions are generally lower in each region, with the greatest differences in Africa, India and China. The relative changes in Africa and India are discussed previously in Section 2. For China, the $CEDS_{GBD\text{-}MAPS}$ emissions are generally lower than the $CEDS_{Hoesly}$ estimates after the year 2010 as a result of the updated scaling inventory. Regional differences between inventories are also greater for OC and BC emissions relative to other compounds due to the added scaling procedure discussed in Section 2. Differences in spatial distributions are not discussed here as changes represent differences in the spatial proxies, which are largely from updates to the EDGAR inventory.

4.1.2 Comparison to Other Global Inventories (EDGAR & GAINS)

Figure 6 additionally provides a comparison of the $CEDS_{GBD\text{-}MAPS}$ global emissions to those from two widely used inventories: EDGAR v4.3.2 (Crippa et al., 2018;EC-JRC, 2018) and ECLIPSE v5a (GAINS) (IIASA, 2015;Klimont et al., 2017). For a comparison of global emissions across similar emission sectors, the EDGAR v4.3.2 inventory in Fig. 6 includes emissions from all reported sectors (including international shipping), except for those from agricultural waste burning and domestic and international aviation. Similarly, the GAINS ECLIPSE v5a baseline scenario inventory in Fig. 6 includes all reported emissions, other than those from agricultural waste burning. These include contributions from aggregate residential and commercial combustion sources ('dom'), energy generation ('ene'), industrial combustion processes ('ind'), road and non-road transportation ('tra'), agricultural practices ('agr'), and waste disposal ('wst'). GAINS ECLIPSE v5a baseline estimates for international shipping emissions are also included in Fig. 6. A table with sectoral mappings of the $CEDS_{GBD\text{-}MAPS}$, EDGAR v4.3.2, and GAINS inventories in provided in Table S10.

The comparison in Fig. 6 shows that global emissions of all compounds in the $CEDS_{GBD\text{-}MAPS}$ inventory are consistently larger than in the EDGAR v4.3.2 inventory (Crippa et al., 2018). Global $CEDS_{GBD\text{-}MAPS}$ emissions of NO_x, SO_2, CO, and NMVOCs are at least 27% larger, while global emissions of NH_3, BC, and OC are within 52%. Figure S23 indicates that differences in global BC and OC emissions are largely due to higher waste and residential and commercial emissions in the $CEDS_{GBD\text{-}MAPS}$ inventory. Figure 6, however also shows that the trends in global emissions are similar between EDGAR v4.3.2 and $CEDS_{GBD\text{-}MAPS}$ for most compounds. For example, between 1970 and 2012, global emissions of SO_2, NH_3, NMVOCs, and BC peak in the same years. Global CO and NO_x emissions both peak one year earlier in the $CEDS_{GBD\text{-}MAPS}$ inventory, but otherwise follow similar historical trends. Trends in OC emissions are the most different between the two inventories with a peak in emissions in 1988 in the EDGAR inventory, compared to 2012 in the $CEDS_{GBD\text{-}MAPS}$ inventory. A comparison of relative sectoral contributions in Fig. S23 shows that these differences in OC emissions are largely due to the residential and commercial sectors, which may be underestimated in the EDGAR v4.3.2 inventory relative to GAINS (Crippa et al., 2018) and $CEDS_{GBD\text{-}MAPS}$. Both inventories also show a net increase in global emissions of all compounds other than

Deleted: 9

Deleted: 1

Deleted: 1

SO_2 between 1970 and 2012. Global SO_2 emissions follow a similar trend until 2007, after which, the emissions in $CEDS_{GBD\text{-}MAPS}$ decrease at a faster rate than in EDGAR v4.3.2. These differences are largely due to the energy sector, which increase between 2006 and 2012 in EDGAR, and decrease as a result of emission reductions in China in the $CEDS_{GBD\text{-}MAPS}$ inventory (Fig. S23). For all other compounds, the rate of increase in emissions between 1970 and 2012 is also slightly different between the two inventories. For example, NH_3 emissions in the $CEDS_{GBD\text{-}MAPS}$ inventory increase by 74% compared to a 139% increase in EDGAR. In contrast, BC and OC emissions increase at a faster rate in the $CEDS_{GBD\text{-}MAPS}$ inventory. Due to similar sources of uncertainty and the additional scaling of $CEDS_{GBD\text{-}MAPS}$ emissions to EDGAR (except for BC and OC), levels of uncertainty between the two inventories are expected to be similar, as discussed further in Sect. 4.2.

Similar to the comparison with EDGAR emissions, Fig. 6 also shows that global emissions in the $CEDS_{GBD\text{-}MAPS}$ inventory are generally larger than emission estimates from the GAINS model, published as part of the ECLIPSE v5a inventory (referred to here as GAINS) (Klimont et al., 2017). Two exceptions are for SO_2 emissions, which are up to 6% lower than GAINS in select years, and BC emissions, which are consistently 5-15% lower than GAINS for all years. While the sectoral definitions may slightly differ between these inventories, Fig. S24 shows that these differences are largely due to different trends in energy and industry SO_2 emissions between 2005 and 2015 and consistently lower BC emissions from the residential and commercial sector in the $CEDS_{GBD\text{-}MAPS}$ inventory. For all years with overlapping data between 1990 and 2015, the absolute magnitude of global emissions are within ±15% for NO_x, SO_2, NH_3, and BC, within 22% for CO and OC, and within 50% for NMVOCs. Historical trends in each inventory are also similar for all compounds other than CO and NMVOCs (Fig. 6). Peak global emissions occur between 2010 and 2012 for NO_x, BC, and OC, while both inventories show a net decrease in emissions in SO_2 and a net increase in emissions of NH_3. In contrast, GAINS emissions of CO peak in 2010, while $CEDS_{GBD\text{-}MAPS}$ emissions peak in 1990. The largest differences in historical trends are for global NMVOC emissions with GAINS showing a 3% decrease between 1990 and 2010, while $CEDS_{GBD\text{-}MAPS}$ NMVOC emissions increase by 13% over this same time period (Fig. 6). Sectoral contributions between the two inventories in Fig. S24 indicates that these differences are largely due differences in the energy, industry, and on-road transport emissions of NMVOCs. Uncertainties in the GAINS model have been previously estimated to fall between 10% and 30% in Europe for gas-phase species (Schöpp et al., 2005) and within the uncertainty estimates for BC and OC of other global bottom-up inventories (Klimont et al., 2017;Bond et al., 2004), as discussed in the following section.

4.2 Uncertainties

The level and sources of uncertainty in the $CEDS_{GBD\text{-}MAPS}$ inventory are similar to those in the $CEDS_{Hoesly}$ inventory, which are largely a function of uncertainty in the activity data, emission factors, and country-level inventories. As these uncertainties have been previously discussed in Hoesly et al. (2018), we have not performed a formal uncertainty analysis here, but rather provide a brief summary of the sources of uncertainty associated with this work. We note plans for a robust uncertainty analysis in an upcoming release of the CEDS core system. While this section highlights many of the challenges associated with

Deleted: 1

Deleted: calibration

Deleted: 2

Deleted: 2

Deleted: agricultural

estimating comprehensive and accurate global bottom-up emission inventories, such inventories remain vital for their use in chemistry and climate models and for the development and evaluation of future control and mitigation strategies.

4.2.1 Uncertainties in Activity Data

As discussed in Section 2.1, CEDS default emissions from combustion sources are largely informed by fuel consumption data from the IEA 2019 World Energy Statistics Product (IEA, 2019). While this database provides energy consumption data as a function of detailed source sector and fuel-type for most countries, the IEA data is uncertain and includes breaks in time-series data that can lead to abrupt changes in the $CEDS_{GBD\text{-}MAPS}$ emissions for select sectors, fuels, and countries. For example, Fig. S7 shows an order of magnitude decrease (0.1 TgC) in OC industrial emissions from North America between 1992 and 1993, which is driven by a break in IEA biofuel consumption data for the non-specified manufacturing industry sector (CEDS sector: 1A2g_Ind-Comb-other) in the United States. While the magnitude of this particular change is negligible on the global scale, this is not the case for all sectors. For example, as noted in Section S4, a known issue in the IEA data in China in the energy sector causes peaks in the associated NO_x and SO_2 $CEDS_{GBD\text{-}MAPS}$ emissions in 2004. These peak emissions may be over-estimated by up to 4 and 10 Tg, respectively, which is large enough to impact historical trends in both regional (Figure 8: NO_x and SO_2) and global (Figures 6-7: SO_2) emissions. These point to areas where improvements could be made to the underlying driver data in future work.

4.2.2 Uncertainties in Global Bottom-Up Inventories

Uncertainties in bottom-up emission inventories vary as a function of space, time, and compound, making total uncertainties difficult to quantify. Default emission estimates in the CEDS system are subject to uncertainties in underlying activity data, such as IEA energy consumption data, as well as activity drivers for process-level emissions. Knowledge of accurate emission factors also drive inventory uncertainties as these are not often available for all sectors in countries with emerging economies, and are heavily dependent on the use, performance, and enforcement of control technologies within each sector and country (e.g., Zhang et al., 2009;Wang et al., 2015). While improvements in data collection and reporting standards may decrease the uncertainty in some underlying sources overtime, the most recent years of $CEDS_{GBD\text{-}MAPS}$ emissions are still subject to considerable uncertainty. For instance, the degree of local and national compliance with control measures is often variable or unknown (e.g., Wang et al., 2015;Zheng et al., 2018). recent activity and regional emissions data are often updated as new information becomes available, and emissions in generally more uncertain regions, including India and Africa are becoming an increasingly large fraction of global totals. Additionally, from a methodological standpoint, default CEDS emissions after 2010 also currently rely on the projection of emission factors from the GAINS EMF30 data release for sectors and countries where contemporary regional scaling inventories are not available.

As the CEDS system uses a "mosaic" approach and incorporates information from other global and national-level inventories, the final $CEDS_{GBD\text{-}MAPS}$ emissions will also be subject to the same sources and levels of uncertainty as these external inventories. For example, as discussed in Sect. 2.1, default process-level emissions in $CEDS_{GBD\text{-}MAPS}$ are derived using

Deleted: 1

Deleted: In general,

Deleted: these uncertainties are expected to decrease in recent years with the

Deleted: of

Deleted: . T

Deleted: in

Deleted: ,

Deleted: however,

Deleted: to increased levels of uncertainty as

Deleted: are

Deleted: and

Deleted: in each version release

Deleted: In addition

Deleted: model

emissions from the EDGAR v4.3.2 inventory, with many countries additionally scaled to this inventory during Step 2. As reported and discussed in Crippa et al. (2018), EDGAR v4.3.2 emissions for 2012 at the regional level are estimated to have the smallest uncertainties for SO_2, between 14.4% and 47.6%, with uncertainties of NO_x between 17.2% and 69.4% (up to 124% for Brazil), CO between 25.9% and 123% (lower for industrialized countries), and NMVOCs between 32.7% and 148% (lower for industrialized countries). Emissions of NH_3 are highly uncertain in all inventories (186% to 294% in EDGAR) due to uncertainties in the reporting of agricultural statistics and emission factors that will depend on individual farming practices, biological processes, and environmental conditions (e.g., Paulot et al., 2014). As noted in Crippa et al. (2018) and Klimont et al. (2017), EDGAR v4.3.2 and GAINS uncertainty estimates for BC and OC fall within the factor of two range that has been previously estimated by the seminal work of Bond et al. (2004). While $CEDS_{GBD\text{-}MAPS}$ emissions are not scaled to EDGAR v4.3.2 BC and OC emissions, estimates are derived from similar sources and are therefore expected to be consistent with uncertainties in both EDGAR and other global bottom-up inventories. It should also be noted that these reported uncertainty estimates from EDGAR only reflect the uncertainties associated with the emission estimation process and do not account for the potential of missing emissions sources or super-emitters within a given sector (Crippa et al., 2018).

To evaluate and improve the accuracy of these bottom-up emission estimates, inventories are increasingly using information from high-resolution satellite retrievals, particularly for major cities, large area and natural sources, and large point sources (e.g., Li et al., 2017a;McLinden et al., 2016;Streets et al., 2013;van der Werf et al., 2017;Beirle et al., 2011;McLinden et al., 2012;Lamsal et al., 2011;Zheng et al., 2019;Elguindi et al., 2020). For example, both the $CEDS_{Hoesly}$ and $CEDS_{GBD\text{-}MAPS}$ inventories incorporate SO_2 emission estimates derived using satellite retrievals in McLinden et al. (2016) to account for previously missing SO_2 point sources in the CEDS 1B2_Fugitive-petr-and-gas sector (described further in the supplement of Hoesly et al. (2018)), with additional use of satellite data planned for a future CEDS core release. With the continued advancement of satellite-retrievals, the development of source and sector-specific inventories, such as $CEDS_{GBD\text{-}MAPS}$, will continue to provide new opportunities for the application of new satellite-based inventories, which will aid in the quantification of spatial and temporal emissions from distinct sources associated with specific sectors and fuel-types that may not be accurately estimated using conventional-bottom up approaches.

4.2.3. Uncertainties in Regional-Level Scaling Inventories

Similar to the $CEDS_{Hoesly}$ inventory, the $CEDS_{GBD\text{-}MAPS}$ emissions will also reflect the uncertainties associated with the inventories used for the scaling procedure. The inventories with the largest impact on the $CEDS_{GBD\text{-}MAPS}$ emission uncertainties relative to the $CEDS_{Hoesly}$ inventory will be those from China from Zheng et al. (2018), the DICE-Africa emission inventory from Marais and Wiedinmyer (2016), and the SMoG-India inventory from Venkataraman et al. (2018). While formal uncertainty analyses were not performed for all of these inventories, similar bottom-up methods used in these studies will result in similar sources of uncertainties (activity and emission factors) as the global inventories. For example, Zheng et al. (2018) state that the largest sources of uncertainties are the accuracy and availability of underlying data (reviewed in Li et al. (2017b)) and that the levels of uncertainty for China emissions between 2010 and 2017 are expected to be similar to previous

Deleted: calibrated

Deleted: calibrated

Deleted: 2

Deleted: Calibration

Deleted: calibration

Deleted: s

national-level bottom-up inventories derived using similar data sources and methodology, such as Zhao et al. (2011), Lu et al. (2011), and Zhang et al. (2009). Similar to global inventories, these previous regional studies estimate much lower levels of uncertainty for SO_2 and NO_x (±16% and -13 to +37% respectively) than for CO (70%) and OC and BC emissions (-43 to +258% and -43 to +208%, respectively). Some sectors in China and other regions are particularly uncertain, as discussed further below.

Regional and national inventories, however, have the added benefit of using local knowledge to reduce potential uncertainties in emission factors and missing emission sources. For example, Marais and Wiedinmyer (2016) note that the DICE-Africa emissions are uncertain due to gaps in fuel consumption data, however, this inventory also includes sources frequently missing in global inventories such as widespread diesel/petrol generator use, kerosene use, and ad-hoc oil refining, and have used emission factors for on-road car and natural gas flaring that are more representative of the inefficient fuel combustion conditions in Africa (Marais and Wiedinmyer, 2016;Marais et al., 2019). As discussed in Sect. 2, the $CEDS_{GBD-MAPS}$ inventory may still underestimate total emissions from some of these sources (up to 11% in 2013; Sect. 2.2.3), but otherwise will have uncertainties for total Africa emissions similar to the DICE-Africa inventory. For emissions in India, uncertainties also arise from missing fuel consumption data and the application of non-local or uncertain emission factors. Venkataraman et al. (2018), however, is one of the few studies to present a detailed uncertainty analysis of their inventory and use the propagation of source-specific activity data and emission factors to estimate that total emission uncertainties are smaller for SO_2 (-20 to 24%), than for NO_x (-65 to 125%) and NMVOCs (-44 to +66%). While uncertainties are not explicitly reported for OC and BC emissions, Fig. 1 in Venkataraman et al. (2018) indicates that uncertainties in these emissions are between -60% to + 95%, consistent with BC and OC uncertainties reported in other bottom-up inventories. We also note the ongoing work to improve the accuracy of highly uncertain emission sectors in a future release of the SMoG-India inventory, through the CarbOnaceous AerosoL Emissions, Source apportionment and ClimatE impacts (COALESCE) project (Venkataraman et al., 2020).

In addition to uncertainties in the scaling inventory emissions, uncertainties are also introduced by the $CEDS_{GBD-MAPS}$ scaling procedure. Uncertainties arise when mapping sectoral and fuel (when available) specific emissions between inventories (as discussed previously), as well as in the application of the calculated scaling factors outside the range of available scaling inventory years. For example, the implied CO EFs in Figure S2 highlight one case in China where the EFs for oil and gas combustion in the on-road transport sector peak in 1999 at a value over three times larger than EFs in all other top emitting countries. For China specifically, the calculated scaling factors for the year 2010 (earliest scaling inventory year) are applied to emissions from all years prior, which was calculated as a value of ~1.58 for the on-road transport sector. The implied EF of ~1.8 g g^{-1} for this sector in 2003 (Figure S2) suggests that the SF from 2010 may not be representative of emissions during this earlier time period. We do note, however, that the 1999 peak in total CO emissions in China (Figure S9) is driven by the IEA energy data and is consistent with the $CEDS_{Hoesly}$ inventory (Hoesly et al., 2018). In contrast, EFs from this sector in China after the year 2010 agree with the magnitude and trends found in other countries, further indicating that the scaling factors are most appropriate for years with overlapping inventory data. Other similar examples include coal energy emissions of SO_2 in

Thailand (Figure S2). In this case, the REAS scaling inventory spans the years 2000 – 2008. The default EFs for the energy sector, however, independently decrease between 1997 and 2001. As a result, when the implied EF of 3.3 for the year 2000 is applied to all historical energy emissions, the implied EFs prior to 1997 become an order of magnitude larger than those in nearly all other top emitting countries (Figure S2). Overall, the applicability of the scaling factors to emissions in years outside the available scaling inventory years remain uncertain due to real historical changes in activity, fuel-use, and emissions mitigation strategies. These uncertainties, however, vary by compound and sector as, for example, there are no similar peaks in on-road emissions for compounds other than CO in China.

Though the inclusion of these regional inventories can improve the accuracy of the global CEDS system (particularly during years with overlapping data), Hoesly et al. (2018) note that large uncertainties may still persist, even in developed countries with stringent reporting standards. In the US for example, it has been suggested that compared to the US National Emissions Inventory (US NEI), total NO_x emissions from on-road and industrial sources in some regions may be overestimated by up to a factor of two (e.g., Travis et al., 2016). In addition, NH_3 emissions in agricultural regions in winter may be underestimated by a factor of 1.6 to 4.4 (Moravek et al., 2019), and national and regional emissions of NMVOCs from oil and gas extraction regions, solvents, and the use of personal care products may also be underestimated by up to a factor of 2 (McDonald et al., 2018;Ahmadov et al., 2015).

4.2.4 Uncertainties in Sectoral and Fuel Contributions

Deleted: 3

Emissions reported as a function of individual source sectors are typically considered to have higher levels of uncertainty than those reported as country totals, due to the cancelation of compounding errors (Schöpp et al., 2005). Source sectors with the largest levels of uncertainty in $CEDS_{GBD\text{-}MAPS}$ estimates are generally consistent with other inventories, which include waste burning, residential emissions, and agricultural processes (Hoesly et al., 2018). This higher level of sectoral uncertainty is reflected in the relatively larger uncertainties discussed above in global emissions of OC, BC, and NH_3 relative to other gas-phase species. In general, uncertainties from these sources are larger due the difficulty in accurately tracking energy consumption statistics and uncertainties in the variability of source-specific emission factors, which will depend on local operational and environmental conditions. For example, residential emission factors from heating and cooking vary depending on technology-used and operational conditions (e.g, Venkataraman et al., 2018;Carter et al., 2014;Jayarathne et al., 2018), while soil NO_x emissions and NH_3 from wastewater and agriculture result from biological processes that depend on local practices and environmental conditions (e.g., Chen et al., 2012;Paulot et al., 2014). While uncertainties are not always reported at the sectoral level, Venkataraman et al. (2018) do report that industry emissions of NO_x and NMVOCs in the SMoG-India inventory actually have larger uncertainties than those from the transportation, agriculture, and residential (NMVOCs only) sectors, while the relative uncertainties for SO_2 emissions follow the opposite trend. For total fine particulate matter emissions, Venkataraman et al. (2018) estimate that the sectors with the largest uncertainties are the residential and industry emissions. Similarly, Lei et al. (2011) estimate that BC and OC emissions from the residential sector in China have the largest inventory uncertainties, while Zhang et al. (2009) and Zheng et al. (2018) also report relatively smaller uncertainties from power plants

and heavy industry in China due to known activity data, local emission factors, pollution control technologies, and direct emissions monitoring. Overall, the mosaic scaling procedure in the CEDS system will result in similar levels of uncertainties as these regional scaling inventories.

With the release of fuel-specific information in the $CEDS_{GBD\text{-}MAPS}$ inventory, additional uncertainties in the allocation of fuel types is expected. In this work, activity data at the detailed sector and fuel level are taken from the IEA World Energy statistics (IEA, 2019) and are subject to the same sources of uncertainty. Emission factors for CEDS working sectors and fuels (Table S2) are derived from GAINS. In general, emissions from solid biofuel combustion are considered to be less certain than fossil fuel consumption due to large uncertainties in both fuel consumption and EFs, particularly in the residential and commercial sectors. For example, by combining information from EDGAR v4.3.2 (Crippa et al., 2018) and a recent TNO-RWC (Netherland Organization for Applied Scientific Research, Residential Wood Combustion) inventory from Denier van der Gon et al. (2015), Crippa et al. (2019) estimated that uncertainties in emissions from wood combustion in the residential sector in Europe are between 200 to 300% for OC, BC, and NH_3. Crippa et al. (2019) also report that these uncertainties are largely driven by uncertainties in regional emission factors, as uncertainties in biofuel consumption are estimated to be between 38.9 and 59.5%. These uncertainties, however, are still larger than those estimated for fossil fuel consumption in many countries. As noted in Hoesly et al. (2018), increased levels of uncertainty in fossil fuel emissions are also expected in some countries, including the consumption and emission factors related to coal combustion in China (e.g., Liu et al., 2015;Guan et al., 2012;Hong et al., 2017), which will have the largest impacts on $CEDS_{GBD\text{-}MAPS}$ emissions of NO_x, SO_2, and BC. Specific to the $CEDS_{GBD\text{-}MAPS}$ fuel inventory, additional uncertainties may arise from the potential underestimation of total coal, oil and gas, and biofuel emissions associated with fugitive emissions and gas flaring in the energy sector, as well as waste incineration in the waste sector. As discussed above and in Hoesly et al. (2018), fugitive emissions are highly uncertain. The degree of underestimation in combustion-fuel contributions will be dependent on the fractional contribution of process level emissions in these sectors relative to those from coal, biofuel, and oil and gas combustion (Table S8). Additional uncertainties in the gridded fuel-specific products are discussed in the following section.

4.2.5 Uncertainties and limitations in gridded emission fluxes

As noted in Sect. 2.1, global gridded $CEDS_{GBD\text{-}MAPS}$ emission fluxes are provided to facilitate their use in earth system models. Relative to the reported country-total emission files, additional uncertainties are introduced in the 0.5°×0.5° global gridded $CEDS_{GBD\text{-}MAPS}$ emission fluxes through the use of source-specific spatial gridding proxies in CEDS Step 5. Historical spatial distributions within each country are largely based on normalized gridded emissions from the EDGAR v4.3.2 inventory. These spatial proxies are held constant after 2012, which serves to increase the uncertainties in spatial allocation in large countries in recent years. The magnitude of this uncertainty will depend on the specific compound and sector. For example, gridded emissions from the energy sector will not reflect the closure or fuel-switching of individual coal-fired power stations after 2012. Changes in total country-level emissions from this sector and fuel-type, however, will be accurately reflected in the total country-level emission files. This source of uncertainty is also present in the $CEDS_{Hoesly}$ inventory. An additional source of

Deleted: calibration

Deleted: calibration

Deleted: 7

Deleted: 4

Deleted: As noted in Sect. 2.1, hH

uncertainty in the gridded emissions is that the same spatial allocations are applied uniformly across emissions of all three fuel-types within each source sector. This may lead to additional uncertainties if, for example, emissions from the use of coal, biofuel, and 'other' fuels within each sector are spatially distinct. These uncertainties, however, do not impact the final country-level $CEDS_{GBD\text{-}MAPS}$ products because they are not gridded.

Lastly, while $CEDS_{GBD\text{-}MAPS}$ emissions provide a global inventory of key atmospheric pollutants, this inventory does not include a complete set of sources or species required for GCM or CTM simulations of atmospheric chemical processes. As noted in Sect. 2, neither $CEDS_{Hoesly}$ nor $CEDS_{GBD\text{-}MAPS}$ estimates include emissions from large or small open fires, which must be supplemented with additional open-burning inventories, such as the Global Fire Emissions Database (GFED, 2019;van der Werf et al., 2017) or Fire INventory from NCAR (FINN, 2018;Wiedinmyer et al., 2011). In addition, simulations of atmospheric chemistry require emissions from biogenic sources, typically supplied from inventories, such as the Model of Emissions of Gases and Aerosols from Nature (MEGAN, 2019;Guenther et al., 2012). Other sources to consider in atmospheric simulations include volcanic emissions, sea spray, and windblown dust. In addition, the CEDS system does not include dust emissions from windblown and anthropogenic sources such as roads, combustion, or industrial process. Anthropogenic dust sources may contribute up to ~10% of total fine dust emissions in recent years and are important to consider when simulating concentrations of total atmospheric particulate matter (Philip et al., 2017). Lastly, the $CEDS_{GBD\text{-}MAPS}$ inventory also excludes emissions of greenhouse gases such as methane and carbon dioxide (CH_4, CO_2). These compounds were previously included through 2014 in the $CEDS_{Hoesly}$ inventory.

Deleted: are

5 Data availability

The source code for the $CEDS_{GBD\text{-}MAPS}$ system is available on GitHub (https://github.com/emcduffie/CEDS/tree/CEDS_GBD-MAPS and https://doi.org/10.5281/zenodo.3865670 (McDuffie et al., 2020a). To run the CEDS system, users are required to first purchase the proprietary energy consumption data from the IEA (World Energy Statistics; https://www.iea.org/subscribe-to-data-services/world-energy-balances-and-statistics). The IEA is updated annually and provides the most comprehensive global energy statistics available to-date. All additional input data are available on the CEDS GitHub repository.

Deleted:)

Final products from the $CEDS_{GBD\text{-}MAPS}$ system include total annual emissions for each country as well as monthly global gridded (0.5°×0.5°) emission fluxes for the years 1970 – 2017. Both products are available on Zenodo (https://doi.org/10.5281/zenodo.3754964) (McDuffie et al., 2020c) and report total emissions and gridded fluxes as a function of 11 final source sectors and four fuel categories (total coal, solid biofuel, oil + gas, process). Time series of annual country-total emissions from 1970 – 2017 are provided in units of kt yr^{-1} and provide NO_x emissions as NO_2. These data do not speciate total NMVOCs into sub-VOC classes. In these .csv files, total anthropogenic emissions for each country are calculated as the sum of all sectors and fuel-types within each country. For the global gridded products, emission fluxes of each compound as a function of 11 sectors and four fuel types are available for each year in individual netCDF files. These data are in units of kg m^{-2} s^{-1} and provide NO_x emissions as NO. Total NMVOCs are speciated into 25 sub-VOC classes as described in Sect. 2. For

Deleted: annual

consistency with the CEDS data released for CMIP6 (CEDS, 2017a, b), gridded anthropogenic fluxes for 1970-2017 are additionally available in the CMIP6 format. Note that NO_x is in units of NO_2 in this format. Additional file format details are in the README.txt file in the Zenodo repository (https://doi.org/10.5281/zenodo.3754964).

To provide an example of the products and file formats available for download from the full $CEDS_{GBD\text{-}MAPS}$ repository, we have also prepared an additional data 'snapshot' inventory that provides emissions in all three file formats described above, for the 2014 – 2015 time period (McDuffie et al., 2020b). The gridded data are provided as monthly averages for the Dec 2014 – Feb 2015 time period, while the annual data include total emissions from both 2014 and 2015. These data can be downloaded from https://doi.org/10.5281/zenodo.3833935, and are further described in the associated README.txt file.

6 Summary and Conclusions

We described the new $CEDS_{GBD\text{-}MAPS}$ global emission inventory for key atmospheric reactive gases and carbonaceous aerosol from 11 anthropogenic emission sectors and four fuel types (total coal, solid biofuel, and liquid fuel and natural gas combustion and remaining process-level emissions) over the time period from 1970 – 2017. The $CEDS_{GBD\text{-}MAPS}$ inventory was derived from an updated version of the Community Emissions Data System, which incorporates updated activity data for combustion and process-level emission sources, updated scaling inventories, the added scaling of BC and OC emissions, and adjustments to the aggregation and gridding procedures to enable the extension of emission estimates to 2017 while retaining sectoral and fuel-type information. We incorporated new regional scaling inventories for India and Africa; as a result default $CEDS_{GBD\text{-}MAPS}$ emissions are now lower than previous $CEDS_{Hoesly}$ estimates for all compounds in these regions other than NMVOCs in Africa and BC in India. These updates improve the agreement of $CEDS_{GBD\text{-}MAPS}$ Africa emissions with those from EDGAR v4.3.2, as well as the agreement of all India emissions other than BC with both the EDGAR (2012) and GAINS (2010) inventories. Scaling default BC and OC estimates reduces these global emissions by up to 21% and 28%, respectively, relative to the $CEDS_{Hoesly}$ inventory. This reduction improves $CEDS_{GBD\text{-}MAPS}$ agreement with both GAINS and EDGAR global estimates of BC and OC, particularly in recent years. The resulting $CEDS_{GBD\text{-}MAPS}$ inventory provides the most contemporary global emission inventory to-date for these key atmospheric pollutants and is the first to provide their global emissions as a function of both detailed source sector and fuel type.

Global 2017 emissions from the $CEDS_{GBD\text{-}MAPS}$ inventory suggest that the combustion of coal and oil and gas in the energy and industry sectors are the largest global sources of SO_2 emissions, while CO is primarily from on-road transportation and biofuel combustion in the residential sector. Global emissions of both compounds peak by 1990 and decrease until 2017 as a result of continuous reductions in on-road transport emissions in Europe, North America as well as reductions in coal combustion emissions from the energy and industry sectors across these regions and in China. In contrast, global NO_x, BC, and OC emissions peak later between 2010 and 2012, but also decrease until 2017 due to reductions in North America, Africa, and China. Dominant sources of NO_x in 2017 are from international shipping energy, industry and on-road transportation sectors. Major sources of BC emissions are from residential biofuel combustion and on-road transportation, while dominant

Deleted: calibration
Deleted: calibration
Deleted: We
Deleted:
Deleted: ed
Deleted: calibration
Deleted: ;
Deleted: as a result
Deleted: The added calibration
Deleted: of
Deleted: also

OC sources are from the residential biofuel and the waste sector. Outside of international shipping, China is the largest regional source of global emissions of all compounds other than NMVOCs. As emissions in North America, Europe, and China continue to decrease, global emissions of NO_x, CO, SO_2, BC, and OC will increasingly reflect emissions in rapidly growing regions such as Africa, India, and countries throughout Asia, Latin America, and the Middle East. Lastly, in contrast to other compounds, global emissions of NMVOCs and NH_3 continuously increase over the entire time period. These increases are predominantly due to increases in agricultural NH_3 emissions in nearly all world regions, as well as NMVOCs from increased waste, energy sector, and solvent use emissions. In 2017, global emissions of these compounds have the largest regional contributions from India, China, and countries throughout Africa, Asia, and the Pacific.

Historical global emission trends in the $CEDS_{GBD\text{-}MAPS}$ inventory are generally similar to those in three other global inventories, $CEDS_{Hoesly}$, EDGAR v4.3.2, and ECLIPSE v5a (GAINS). Relative to the $CEDS_{Hoesly}$ inventory, however, $CEDS_{GBD\text{-}MAPS}$ emissions diverge in recent years, particularly for NO_x, CO, SO_2, BC, and OC emissions. In addition to the use of updated underlying activity in the $CEDS_{GBD\text{-}MAPS}$ inventory, emissions of these compounds were most impacted by the updated CEDS scaling inventories, including those for China, India, and Africa. These same updates also contribute to the different trends in global NO_x, CO, and SO_2 emissions after 2010 between $CEDS_{GBD\text{-}MAPS}$ and the GAINS and EDGAR inventories. Global emissions between 1970 and 2017 from the $CEDS_{GBD\text{-}MAPS}$ inventory are generally smaller than the $CEDS_{Hoesly}$ emissions for all compounds other than NMVOCs and are consistently higher than all emissions from EDGAR v4.3.2. Global $CEDS_{GBD\text{-}MAPS}$ emissions are also larger than GAINS emissions, except for BC and select years of SO_2 emissions.

Due to similar bottom-up methodologies and the use of EDGAR v4.3.2 data in the CEDS system, country-level $CEDS_{GBD\text{-}MAPS}$ emissions are expected to have similar sources and magnitudes of uncertainty as those in the $CEDS_{Hoesly}$, EDGAR v4.3.2, GAINS, and scaling emission inventories. These inventories consistently predict the smallest uncertainties in emissions of SO_2 and the largest for emissions of NH_3, OC, and BC. The latter three compounds largely depend on accurate knowledge of activity data and emission factors for small scattered sources that vary by location, combustion technologies used, and environmental conditions. Uncertainties in the sectoral and fuel allocations in $CEDS_{GBD\text{-}MAPS}$ emissions will also generally follow the uncertainties in the CEDSv2019-12-23 system and will largely depend on the accuracy of the fuel allocations for combustion sources in the underlying IEA activity data. Gridded $CEDS_{GBD\text{-}MAPS}$ emissions also have uncertainties associated with the accuracy of the normalized spatial emission distributions from EDGAR v4.3.2, which are equally applied to all the four fuel categories and are held constant after 2012.

Contemporary global emission estimates with detailed sector and fuel-specific information are vital for quantifying the anthropogenic sources of air pollution and mitigating the resulting impacts on human health, the environment, and society. While bottom-up methods can provide sectoral-specific emission estimates, previous global inventories of multiple compounds and sources have lagged in time and do not provide fuel-specific emissions for multiple compounds at the global scale. To address this community need, the $CEDS_{GBD\text{-}MAPS}$ inventory utilizes the CEDS system (v2019-12-23) to provide emissions of seven key atmospheric pollutants with detailed sectoral and fuel-type information, extended to the year 2017. Due to the direct

Deleted: Besides

Deleted: NO_x and BC emissions in 2017, while countries across Asia and Middle East contribute more than other regions to global OC emissions.

Formatted: Subscript

Deleted: India,

Deleted: in

Deleted: and

Deleted: e

Deleted: Africa,

Deleted: countries in Asia and the Middle East

Deleted: calibration

Deleted: larger

Deleted: calibration

and secondary contribution of these reactive gases and carbonaceous aerosol to ambient air pollution, contemporary gridded and country-level emissions with both sector and fuel-type information can provide new insights necessary to motivate and develop effective strategies for emission reductions and air pollution mitigation around the world. The CEDS$_{GBD-MAPS}$ source code is publicly available (https://github.com/emcduffie/CEDS/tree/CEDS_GBD-MAPS and https://doi.org/10.5281/zenodo.3865670) and both country total and global gridded emissions from the 2020_v1 version of this dataset are publicly available at Zenodo with the following doi: https://doi.org/10.5281/zenodo.3754964.

Deleted: fuel

Deleted: abatement

Deleted: strategies

Information about the Supplement

The supplement for this article describes a list of known inventory issues at the time of submission, as well as a number of additional CEDS$_{GBD-MAPS}$ details, tables and figures, and data sources, including the following: (Boden et al., 2016, 2017;BP, 2015;Doxsey-Whitfield et al., 2015;EC-JRC/PBL, 2012, 2016;EIA, 2019;IEA, 2015;Klein Goldewijk et al., 2011;Sharma et al., 2019;Stohl et al., 2015;The World Bank, 2016;UN, 2014, 2015;Wiedinmyer et al., 2014;Commoner et al., 2000;Reyna-Bensusan et al., 2018;Nagpure et al., 2015;Meidiana and Gamse, 2010;US EPA, 2006).

Author Contributions

EEM prepared the manuscript with contributions from all co-authors. RVM, MB, and SSJ supervised the scientific content of this publication. EEM led the development of the CEDS$_{GBD-MAPS}$ source code and CEDS$_{GBD-MAPS}$ dataset, with significant contributions from SSJ and PO, as well as supplemental data from KT, CV, and EAM.

Competing Interests

The authors declare that they have no conflict of interest.

Acknowledgements

This work was supported by the Health Effects Institute (HEI), Global Burden of Disease – Major Air Pollution Sources project. We thank Christine Wiedinmyer and Qiang Zhang for their respective contributions to the DICE-Africa and updated China nation-level inventories, used here for scaling CEDS$_{GBD-MAPS}$ emissions. CEDS utilizes many sources of input data and we are grateful for these contributions from a large number of research teams.

Deleted: calibration of

References

ADE: Australian Department of the Environment: National Pollution Inventory, 2017/2018, http://www.npi.gov.au/npidata/action/load/advance-search(last access: 15 August 2019), 2019.

Ahmadov, R., McKeen, S., Trainer, M., Banta, R., Brewer, A., Brown, S., Edwards, P. M., de Gouw, J. A., Frost, G. J., Gilman, J., Helmig, D., Johnson, B., Karion, A., Koss, A., Langford, A., Lerner, B., Olson, J., Oltmans, S., Peischl, J., Pétron, G., Pichugina, Y., Roberts, J. M., Ryerson, T., Schnell, R., Senff, C., Sweeney, C., Thompson, C., Veres, P. R., Warneke, C., Wild, R., Williams, E. J., Yuan, B., and Zamora, R.: Understanding high wintertime ozone pollution events in an oil- and natural gas-producing region of the western US, Atmos. Chem. Phys., 15, 411-429, 10.5194/acp-15-411-2015, 2015.

Ainsworth, E. A.: Understanding and improving global crop response to ozone pollution, The Plant Journal, 90, 886-897, 10.1111/tpj.13298, 2017.

Amann, M., Bertok, I., Borken-Kleefeld, J., Cofala, J., Heyes, C., Höglund-Isaksson, L., Klimont, Z., Nguyen, B., Posch, M., Rafaj, P., Sandler, R., Schöpp, W., Wagner, F., and Winiwarter, W.: Cost-effective control of air quality and greenhouse gases in Europe: Modeling and policy applications, Environmental Modelling & Software, 26, 1489-1501, https://doi.org/10.1016/j.envsoft.2011.07.012, 2011.

Amann, M., Bertok, I., Borken-Kleefeld, J., Cofala, J., Heyes, C., Hoglund-Isaksson, L., Kiesewetter, G., Klimont, Z., Schopp, W., Vellinga, N., and Winiwarter, W.: Adjusted historic emission data, projections, and optimized emission reduction targets for 2030 - a comparison with COM data 2013, IIASA, Laxenburg, Austria, http://ec.europa.eu/environment/air/pdf/review/TSAP_16a.pdf (last access: 15 January 2018), 2015.

Argentina UNFCCC Submission: Argentinian Inventory 1990-2012, Submitted to UNFCCC, 2016.

Avnery, S., Mauzerall, D. L., Liu, J., and Horowitz, L. W.: Global crop yield reductions due to surface ozone exposure: 1. Year 2000 crop production losses and economic damage, Atmos. Environ., 45, 2284-2296, https://doi.org/10.1016/j.atmosenv.2010.11.045, 2011.

Behera, S. N., Sharma, M., Aneja, V. P., and Balasubramanian, R.: Ammonia in the atmosphere: a review on emission sources, atmospheric chemistry and deposition on terrestrial bodies, Environmental Science and Pollution Research, 20, 8092-8131, 10.1007/s11356-013-2051-9, 2013.

Beirle, S., Boersma, K. F., Platt, U., Lawrence, M. G., and Wagner, T.: Megacity Emissions and Lifetimes of Nitrogen Oxides Probed from Space, Science, 333, 1737, 10.1126/science.1207824, 2011.

Boden, T. A., Marland, G., and Andres, R. J.: Global, Regional, and National Fossil-Fuel CO_2 Emissions, Carbon Dioxide Information Analysis Center, U.S. Department of Energy, Oak Ridge, Tenn., U.S.A., 2016.

Boden, T. A., Marland, G., and Andres, R. J.: Global, Regional, and National Fossil-Fuel CO_2 Emissions, Carbon Dioxide Information Analysis Center, U.S. Department of Energy, Oak Ridge, Tenn., U.S.A., doi: 10.3334/CDIAC/00001_V2017, 2017.

Bond, T. C., Streets, D. G., Yarber, K. F., Nelson, S. M., Woo, J.-H., and Klimont, Z.: A technology-based global inventory of black and organic carbon emissions from combustion, J. Geophys. Res. Atmos., 109, 10.1029/2003JD003697, 2004.

Bond, T. C., Bhardwaj, E., Dong, R., Jogani, R., Jung, S., Roden, C., Streets, D. G., and Trautmann, N. M.: Historical emissions of black and organic carbon aerosol from energy-related combustion, 1850–2000, Global Biogeochemical Cycles, 21, 10.1029/2006GB002840, 2007.

Bond, T. C., Doherty, S. J., Fahey, D. W., Forster, P. M., Berntsen, T., DeAngelo, B. J., Flanner, M. G., Ghan, S., Kärcher, B., Koch, D., Kinne, S., Kondo, Y., Quinn, P. K., Sarofim, M. C., Schultz, M. G., Schulz, M., Venkataraman, C., Zhang, H., Zhang, S., Bellouin, N., Guttikunda, S. K., Hopke, P. K., Jacobson, M. Z., Kaiser, J. W., Klimont, Z., Lohmann, U., Schwarz, J. P., Shindell, D., Storelvmo, T., Warren, S. G., and Zender, C. S.: Bounding the role of black carbon in the climate system: A scientific assessment, J. Geophys. Res. Atmos., 118, 5380-5552, 10.1002/jgrd.50171, 2013.

BP: BP Statistical Review of World Energy, bp.com/statisticalreview (last access: 15 January 2018), 2015.

BP: Statistical Review of World Energy: 2019, https://www.bp.com/content/dam/bp/business-sites/en/global/corporate/pdfs/energy-economics/statistical-review/bp-stats-review-2019-full-report.pdf (last access: January 23, 2020), 2019.

Brock, C. A., Washenfelder, R. A., Trainer, M., Ryerson, T. B., Wilson, J. C., Reeves, J. M., Huey, L. G., Holloway, J. S., Parrish, D. D., Hübler, G., and Fehsenfeld, F. C.: Particle growth in the plumes of coal-fired power plants, J. Geophys. Res. Atmos., 107, AAC 9-1-AAC 9-14, 10.1029/2001JD001062, 2002.

Carter, E. M., Shan, M., Yang, X., Li, J., and Baumgartner, J.: Pollutant Emissions and Energy Efficiency of Chinese Gasifier Cooking Stoves and Implications for Future Intervention Studies, Environ. Sci. Technol., 48, 6461-6467, 10.1021/es405723w, 2014.

Castellanos, P., and Boersma, K. F.: Reductions in nitrogen oxides over Europe driven by environmental policy and economic recession, Scientific Reports, 2, 265, 10.1038/srep00265, 2012.

CEDS: v2017_08_30, https://esgf-node.llnl.gov/search/input4mips/ (last access: 7 January 2020), 2017a.

CEDS: v2017_10_05, https://esgf-node.llnl.gov/search/input4mips/ (last access: 7 January 2020), 2017b.

Chameides, W. L.: The photochemical role of tropospheric nitrogen oxides, Geophysical Research Letters, 5, 17-20, 10.1029/GL005i001p00017, 1978.

Chen, Y., Roden, C. A., and Bond, T. C.: Characterizing Biofuel Combustion with Patterns of Real-Time Emission Data (PaRTED), Environ. Sci. Technol., 46, 6110-6117, 10.1021/es3003348, 2012.

Commoner, B., Bartlett, P. W., Eisl, H., and Couchot, K.: Air Transport of Dioxin from North American Sources to Ecologically Vulnerable Receptors in Nunavut, Arctic Canada: Final Report to the North American Commission for Environmental Cooperation., http://www3.cec.org/islandora/en/item/1596-long-range-air-transport-dioxin-from-north-american-sources-ecologically-vulnerable-en.pdf (last access: 25 April, 2020), 2000.

Crippa, M., Guizzardi, D., Muntean, M., Schaaf, E., Dentener, F., van Aardenne, J. A., Monni, S., Doering, U., Olivier, J. G. J., Pagliari, V., and Janssens-Maenhout, G.: Gridded emissions of air pollutants for the period 1970–2012 within EDGAR v4.3.2, Earth Syst. Sci. Data, 10, 1987-2013, 10.5194/essd-10-1987-2018, 2018.

Crippa, M., Janssens-Maenhout, G., Guizzardi, D., Van Dingenen, R., and Dentener, F.: Contribution and uncertainty of sectorial and regional emissions to regional and global PM2.5 health impacts, Atmos. Chem. Phys., 19, 5165-5186, 10.5194/acp-19-5165-2019, 2019.

Crutzen, P. J.: The influence of nitrogen oxides on the atmospheric ozone content, Quarterly Journal of the Royal Meteorological Society, 96, 320-325, 10.1002/qj.49709640815, 1970.

de Gouw, J. A., Parrish, D. D., Frost, G. J., and Trainer, M.: Reduced emissions of CO2, NOx, and SO2 from U.S. power plants owing to switch from coal to natural gas with combined cycle technology, Earth's Future, 2, 75-82, 10.1002/2013EF000196, 2014.

Denier van der Gon, H. A. C., Bergström, R., Fountoukis, C., Johansson, C., Pandis, S. N., Simpson, D., and Visschedijk, A. J. H.: Particulate emissions from residential wood combustion in Europe – revised estimates and an evaluation, Atmos. Chem. Phys., 15, 6503-6519, 10.5194/acp-15-6503-2015, 2015.

DICE-Africa: DICE-Africa User Manual, https://www2.acom.ucar.edu/modeling/dice-africa(last access: 9 January 2020), 2016.

Doxsey-Whitfield, E., MacManus, K., Adamo, S. B., Pistolesi, L., Squires, J., Borkovska, O., and Baptista, S. R.: Taking Advantage of the Improved Availability of Census Data: A First Look at the Gridded Population of the World, Version 4, Papers in Applied Geography, 1, 226-234, 10.1080/23754931.2015.1014272, 2015.

Duncan, B. N., Yoshida, Y., de Foy, B., Lamsal, L. N., Streets, D. G., Lu, Z., Pickering, K. E., and Krotkov, N. A.: The observed response of Ozone Monitoring Instrument (OMI) NO2 columns to NOx emission controls on power plants in the United States: 2005–2011, Atmos. Environ., 81, 102-111, https://doi.org/10.1016/j.atmosenv.2013.08.068, 2013.

EC-JRC: Emissions Database for Global Atmospheric Research (EDGAR), release EDGARv4.3.2 https://edgar.jrc.ec.europa.eu/overview.php?v=432_AP, https://data.europa.eu/doi/10.2904/JRC_DATASET_EDGAR, (last access: 12 August 2019), 2018.

EC-JRC/PBL: Emission Database for Global Atmospheric Research (EDGAR), release EDGAR v4.2 FT2012, http://edgar.jrc.ec.europa.eu (last access: 15 January 2018), 2012.

EC-JRC/PBL: Emission Database for Global Atmospheric Research (EDGAR), release version 4.3.1, http://edgar.jrc.ec.europa.eu/overview.php?v=431 (last access: 15 January 2018), 2016.

ECCC: Environment and Climate Change Canada, EN_APEI-Canada, Canada's 2019 Air Pollutant Emissions Inventory, http://data.ec.gc.ca/data/substances/monitor/canada-s-air-pollutant-emissions-inventory/APEI_Tables_Canada_Provinces_Territories/?lang=en(last access: 13 August 2019), 2019.

EIA: U.S. Energy Information Administration: Table 10.2a: Renewable Energy Cnsumption, Residential and Commercial Sectors, https://www.eia.gov/totalenergy/data/monthly/#renewable (last access: 26 August 2019), 2019.

EIA: U.S. Energy Information Administration: Drilling Productivity Report, https://www.eia.gov/petroleum/drilling/ (last access: 7 April 2020), 2020.

Elguindi, N., Granier, C., Stavrakou, T., Darras, S., Bauwens, M., Cao, H., Chen, C., Denier van der Gon, H. A. C., Dubovik, O., Fu, T. M., Henze, D. K., Jiang, Z., Keita, S., Kuenen, J. J. P., Kurokawa, J., Liousse, C., Miyazaki, K., Müller, J. F., Qu, Z., Solmon, F., and Zheng, B.: Intercomparison of Magnitudes and Trends in Anthropogenic Surface Emissions From Bottom-Up Inventories, Top-Down Estimates, and Emission Scenarios, Earth's Future, 8, e2020EF001520, 10.1029/2020EF001520, 2020.

EMEP: Officially reported emission data to the European Monitoring and Evaluation Programme: EMEP_NFR14_LEVEL1 data, https://www.ceip.at/ms/ceip_home1/ceip_home/webdab_emepdatabase/reported_emissiondata/(last access: 19 December 2019), 2019.

FAOSTAT: FAOSTAT-Forestry database, http://www.fao.org/forestry/statistics/84922/en/ (last access: 15 January 2018), 2015.

Feng, L., Smith, S. J., Braun, C., Crippa, M., Gidden, M. J., Hoesly, R., Klimont, Z., van Marle, M., van den Berg, M., and van der Werf, G. R.: The generation of gridded emissions data for CMIP6, Geosci. Model Dev., 13, 461-482, 10.5194/gmd-13-461-2020, 2020.

FINN: Fire INventory from NCAR, Version 1.5, http://bai.acom.ucar.edu/Data/fire/ (last access: 4 March 2020), 2018.

GBD MAPS Working Group: Burden of Disease Attributable to Coal-Burning and Other Major Sources of Air Pollution in China. Special Report 20, Health Effects Institute [Available at: https://www.healtheffects.org/publication/burden-disease-attributable-coal-burning-and-other-air-pollution-sources-china], Boston, MA, 2016.

GBD MAPS Working Group: Burden of Disease Attributable to Major Air Pollution Sources in India. Special Report 21., Health Effects Institute [Available at: https://www.healtheffects.org/publication/gbd-air-pollution-india], Boston, MA, 2018.

GFED: Global Fire Emissions Database, http://globalfiredata.org/index.html (last access: 15 March 2020), 2019.

Gidden, M. J., Riahi, K., Smith, S. J., Fujimori, S., Luderer, G., Kriegler, E., van Vuuren, D. P., van den Berg, M., Feng, L., Klein, D., Calvin, K., Doelman, J. C., Frank, S., Fricko, O., Harmsen, M., Hasegawa, T., Havlik, P., Hilaire, J., Hoesly, R., Horing, J., Popp, A., Stehfest, E., and Takahashi, K.: Global emissions pathways under different socioeconomic scenarios for use in CMIP6: a dataset of harmonized emissions trajectories through the end of the century, Geosci. Model Dev., 12, 1443-1475, 10.5194/gmd-12-1443-2019, 2019.

Guan, D., Liu, Z., Geng, Y., Lindner, S., and Hubacek, K.: The gigatonne gap in China's carbon dioxide inventories, Nature Climate Change, 2, 672-675, 10.1038/nclimate1560, 2012.

Guenther, A. B., Jiang, X., Heald, C. L., Sakulyanontvittaya, T., Duhl, T., Emmons, L. K., and Wang, X.: The Model of Emissions of Gases and Aerosols from Nature version 2.1 (MEGAN2.1): an extended and updated framework for modeling biogenic emissions, Geosci. Model Dev., 5, 1471-1492, 10.5194/gmd-5-1471-2012, 2012.

Haywood, J., and Boucher, O.: Estimates of the direct and indirect radiative forcing due to tropospheric aerosols: A review, Reviews of Geophysics, 38, 513-543, 10.1029/1999RG000078, 2000.

Hoesly, R., O'Rourke, P., Braun, C., Feng, L., Smith, S. J., Pitkanen, T., Siebert, J., Vu, L., Presley, M., Bolt, R., Goldstein, B., and Kholod, N.: CEDS: Community Emissions Data System (Version Dec-23-2019), http://doi.org/10.5281/zenodo.3592073 (last access: March 15, 2020), 2019.

Hoesly, R. M., Smith, S. J., Feng, L., Klimont, Z., Janssens-Maenhout, G., Pitkanen, T., Seibert, J. J., Vu, L., Andres, R. J., Bolt, R. M., Bond, T. C., Dawidowski, L., Kholod, N., Kurokawa, J. I., Li, M., Liu, L., Lu, Z., Moura, M. C. P., O'Rourke, P. R., and Zhang, Q.: Historical (1750–2014) anthropogenic emissions of reactive gases and aerosols from the Community Emissions Data System (CEDS), Geosci. Model Dev., 11, 369-408, 10.5194/gmd-11-369-2018, 2018.

Hong, C., Zhang, Q., He, K., Guan, D., Li, M., Liu, F., and Zheng, B.: Variations of China's emission estimates: response to uncertainties in energy statistics, Atmos. Chem. Phys., 17, 1227-1239, 10.5194/acp-17-1227-2017, 2017.

HTAP2: RETRO NMVOC Ratio, http://iek8wikis.iek.fz-juelich.de/HTAPWiki/WP1.1?action=AttachFile&do=view&target=retro_nmvoc_ratio.zip(last access: 7 January 2020), 2013.

Huang, G., Brook, R., Crippa, M., Janssens-Maenhout, G., Schieberle, C., Dore, C., Guizzardi, D., Muntean, M., Schaaf, E., and Friedrich, R.: Speciation of anthropogenic emissions of non-methane volatile organic compounds: a global gridded data set for 1970–2012, Atmos. Chem. Phys., 17, 7683-7701, 10.5194/acp-17-7683-2017, 2017.

IEA: World Energy Statistics, http://www.iea.org/statistics/ (last access: 15 January 2018), 2015.

IEA: World Energy Statistics 2019 Edition, Database Documentation, http://wds.iea.org/wds/pdf/WORLDBES_Documentation.pdf (last access: 17 September 2019), 2019.

IIASA: GAINS - Sulfur content of fuels, http://gains.iiasa.ac.at/models/index.html, Scenario:TSAP_Consultation_2014, (last access: 15 January 2018), 2014.

IIASA: ECLIPSE v5a, https://www.iiasa.ac.at/web/home/research/researchPrograms/air/ECLIPSEv5a.html (last access: 7 January 2020), 2015.

IPCC: Summary for Policy Makers. In: *Climate Change 2013: The Physical Science Basis. Contribution of Working Group I to the Fifth Assessment Report of the Intergovernmental Panel on Climate Change*, edited by: Stocker, T. F., Qin, D., Plattner, G.-K., Tignor, M., Allen, S. K., Boschung, J., Nauels, Y., Xia, Y., Bex, V., and Midgley, P. M., Cambridge University Press, Cambridge, United Kingdom and New York, NY, USA., 2013.

Janssens-Maenhout, G., Crippa, M., Guizzardi, D., Dentener, F., Muntean, M., Pouliot, G., Keating, T., Zhang, Q., Kurokawa, J., Wankmüller, R., Denier van der Gon, H., Kuenen, J. J. P., Klimont, Z., Frost, G., Darras, S., Koffi, B., and Li, M.: HTAP_v2.2: a mosaic of regional and global emission grid maps for 2008 and 2010 to study hemispheric transport of air pollution, Atmos. Chem. Phys., 15, 11411-11432, 10.5194/acp-15-11411-2015, 2015.

Jayarathne, T., Stockwell, C. E., Bhave, P. V., Praveen, P. S., Rathnayake, C. M., Islam, M. R., Panday, A. K., Adhikari, S., Maharjan, R., Goetz, J. D., DeCarlo, P. F., Saikawa, E., Yokelson, R. J., and Stone, E. A.: Nepal Ambient Monitoring and Source Testing Experiment (NAMaSTE): emissions of particulate matter from wood- and dung-fueled cooking fires, garbage and crop residue burning, brick kilns, and other sources, Atmos. Chem. Phys., 18, 2259-2286, 10.5194/acp-18-2259-2018, 2018.

Jimenez, J. L., Canagaratna, M. R., Donahue, N. M., Prevot, A. S. H., Zhang, Q., Kroll, J. H., DeCarlo, P. F., Allan, J. D., Coe, H., Ng, N. L., Aiken, A. C., Docherty, K. S., Ulbrich, I. M., Grieshop, A. P., Robinson, A. L., Duplissy, J., Smith, J. D., Wilson, K. R., Lanz, V. A., Hueglin, C., Sun, Y. L., Tian, J., Laaksonen, A., Raatikainen, T., Rautiainen, J., Vaattovaara, P., Ehn, M., Kulmala, M., Tomlinson, J. M., Collins, D. R., Cubison, M. J., Dunlea, J., Huffman, J. A., Onasch, T. B., Alfarra, M. R., Williams, P. I., Bower, K., Kondo, Y., Schneider, J., Drewnick, F., Borrmann, S., Weimer, S., Demerjian, K., Salcedo, D., Cottrell, L., Griffin, R., Takami, A., Miyoshi, T., Hatakeyama, S., Shimono, A., Sun, J. Y., Zhang, Y. M., Dzepina, K., Kimmel, J. R., Sueper, D., Jayne, J. T., Herndon, S. C., Trimborn, A. M., Williams, L. R., Wood, E. C., Middlebrook, A. M., Kolb, C. E., Baltensperger, U., and Worsnop, D. R.: Evolution of Organic Aerosols in the Atmosphere, Science, 326, 1525, 10.1126/science.1180353, 2009.

Klein Goldewijk, K., Beusen, A., van Drecht, G., and de Vos, M.: The HYDE 3.1 spatially explicit database of human-induced global land-use change over the past 12,000 years, Global Ecology and Biogeography, 20, 73-86, 10.1111/j.1466-8238.2010.00587.x, 2011.

Klimont, Z., Kupiainen, K., Heyes, C., Purohit, P., Cofala, J., Rafaj, P., Borken-Kleefeld, J., and Schöpp, W.: Global anthropogenic emissions of particulate matter including black carbon, Atmos. Chem. Phys., 17, 8681-8723, 10.5194/acp-17-8681-2017, 2017.

Krotkov, N. A., McLinden, C. A., Li, C., Lamsal, L. N., Celarier, E. A., Marchenko, S. V., Swartz, W. H., Bucsela, E. J., Joiner, J., Duncan, B. N., Boersma, K. F., Veefkind, J. P., Levelt, P. F., Fioletov, V. E., Dickerson, R. R., He, H., Lu, Z., and Streets, D. G.: Aura OMI observations of regional SO2 and NO2 pollution changes from 2005 to 2015, Atmos. Chem. Phys., 16, 4605-4629, 10.5194/acp-16-4605-2016, 2016.

Kurokawa, J., Ohara, T., Morikawa, T., Hanayama, S., Janssens-Maenhout, G., Fukui, T., Kawashima, K., and Akimoto, H.: Emissions of air pollutants and greenhouse gases over Asian regions during 2000–2008: Regional Emission inventory in ASia (REAS) version 2, Atmos. Chem. Phys., 13, 11019-11058, 10.5194/acp-13-11019-2013, 2013.

Lacey, F., and Henze, D.: Global climate impacts of country-level primary carbonaceous aerosol from solid-fuel cookstove emissions, Environmental Research Letters, 10, 114003, 10.1088/1748-9326/10/11/114003, 2015.

Lacey, F. G., Marais, E. A., Henze, D. K., Lee, C. J., van Donkelaar, A., Martin, R. V., Hannigan, M. P., and Wiedinmyer, C.: Improving present day and future estimates of anthropogenic sectoral emissions and the resulting air quality impacts in Africa, Faraday Discussions, 200, 397-412, 10.1039/C7FD00011A, 2017.

Lamsal, L. N., Martin, R. V., Padmanabhan, A., van Donkelaar, A., Zhang, Q., Sioris, C. E., Chance, K., Kurosu, T. P., and Newchurch, M. J.: Application of satellite observations for timely updates to global anthropogenic NOx emission inventories, Geophysical Research Letters, 38, 10.1029/2010GL046476, 2011.

Lei, Y., Zhang, Q., He, K. B., and Streets, D. G.: Primary anthropogenic aerosol emission trends for China, 1990–2005, Atmos. Chem. Phys., 11, 931-954, 10.5194/acp-11-931-2011, 2011.

Lelieveld, J., Klingmüller, K., Pozzer, A., Burnett, R. T., Haines, A., and Ramanathan, V.: Effects of fossil fuel and total anthropogenic emission removal on public health and climate, P. Natl. Acad. Sci., 116, 7192, 10.1073/pnas.1819989116, 2019.

Li, C., McLinden, C., Fioletov, V., Krotkov, N., Carn, S., Joiner, J., Streets, D., He, H., Ren, X., Li, Z., and Dickerson, R. R.: India Is Overtaking China as the World's Largest Emitter of Anthropogenic Sulfur Dioxide, Scientific Reports, 7, 14304, 10.1038/s41598-017-14639-8, 2017a.

Li, M., Liu, H., Geng, G., Hong, C., Liu, F., Song, Y., Tong, D., Zheng, B., Cui, H., Man, H., Zhang, Q., and He, K.: Anthropogenic emission inventories in China: a review, National Science Review, 4, 834-866, 10.1093/nsr/nwx150, 2017b.

Li, M., Zhang, Q., Kurokawa, J. I., Woo, J. H., He, K., Lu, Z., Ohara, T., Song, Y., Streets, D. G., Carmichael, G. R., Cheng, Y., Hong, C., Huo, H., Jiang, X., Kang, S., Liu, F., Su, H., and Zheng, B.: MIX: a mosaic Asian anthropogenic emission inventory under the international collaboration framework of the MICS-Asia and HTAP, Atmos. Chem. Phys., 17, 935-963, 10.5194/acp-17-935-2017, 2017c.

Liang, C. K., West, J. J., Silva, R. A., Bian, H., Chin, M., Davila, Y., Dentener, F. J., Emmons, L., Flemming, J., Folberth, G., Henze, D., Im, U., Jonson, J. E., Keating, T. J., Kucsera, T., Lenzen, A., Lin, M., Lund, M. T., Pan, X., Park, R. J., Pierce, R. B., Sekiya, T., Sudo, K., and Takemura, T.: HTAP2 multi-model estimates of premature human mortality due to intercontinental transport of air pollution and emission sectors, Atmos. Chem. Phys., 18, 10497-10520, 10.5194/acp-18-10497-2018, 2018.

Liu, Z., Guan, D., Wei, W., Davis, S. J., Ciais, P., Bai, J., Peng, S., Zhang, Q., Hubacek, K., Marland, G., Andres, R. J., Crawford-Brown, D., Lin, J., Zhao, H., Hong, C., Boden, T. A., Feng, K., Peters, G. P., Xi, F., Liu, J., Li, Y., Zhao, Y., Zeng, N., and He, K.: Reduced carbon emission estimates from fossil fuel combustion and cement production in China, Nature, 524, 335-338, 10.1038/nature14677, 2015.

Lu, Z., Zhang, Q., and Streets, D. G.: Sulfur dioxide and primary carbonaceous aerosol emissions in China and India, 1996–2010, Atmos. Chem. Phys., 11, 9839-9864, 10.5194/acp-11-9839-2011, 2011.

Marais, E. A., and Wiedinmyer, C.: Air Quality Impact of Diffuse and Inefficient Combustion Emissions in Africa (DICE-Africa), Environ. Sci. Technol., 50, 10739-10745, 10.1021/acs.est.6b02602, 2016.

Marais, E. A., Silvern, R. F., Vodonos, A., Dupin, E., Bockarie, A. S., Mickley, L. J., and Schwartz, J.: Air Quality and Health Impact of Future Fossil Fuel Use for Electricity Generation and Transport in Africa, Environ. Sci. Technol., 53, 13524-13534, 10.1021/acs.est.9b04958, 2019.

Mauzerall, D. L., Sultan, B., Kim, N., and Bradford, D. F.: NOx emissions from large point sources: variability in ozone production, resulting health damages and economic costs, Atmos. Environ., 39, 2851-2866, https://doi.org/10.1016/j.atmosenv.2004.12.041, 2005.

McDonald, B. C., de Gouw, J. A., Gilman, J. B., Jathar, S. H., Akherati, A., Cappa, C. D., Jimenez, J. L., Lee-Taylor, J., Hayes, P. L., McKeen, S. A., Cui, Y. Y., Kim, S.-W., Gentner, D. R., Isaacman-VanWertz, G., Goldstein, A. H., Harley, R. A., Frost, G. J., Roberts, J. M., Ryerson, T. B., and Trainer, M.: Volatile chemical products emerging as largest petrochemical source of urban organic emissions, Science, 359, 760, 10.1126/science.aaq0524, 2018.

McDuffie, E. E., Hoesly, R., O'Rourke, P., Braun, C., Feng, L., Smith, S. J., Pitkanen, T., Seibert, J. J., Vu, L., Presley, M., Bolt, R., Goldstein, B., and Kholod, N.: CEDS_GBD-MAPS_SourceCode_2020_v1.0, https://doi.org/10.5281/zenodo.3865670, (last access: June 2, 2020), 2020a.

McDuffie, E. E., Smith, S. J., O'Rourke, P., Tibrewal, K., Venkataraman, C., Marais, E. A., Zheng, B., Crippa, M., Brauer, M., and Martin, R. V.: CEDS_GBD-MAPS: Data Snapshot (2014-2015), https://doi.org/10.5281/zenodo.3833935, (last access: June 2, 2020), 2020b.

McDuffie, E. E., Smith, S. J., O'Rourke, P., Tibrewal, K., Venkataraman, C., Marais, E. A., Zheng, B., Crippa, M., Brauer, M., and Martin, R. V.: CEDS_GBD-MAPS: Global Anthropogenic Emission Inventory of NOx, SO2, CO, NH3, NMVOCs, BC, and OC from 1970-2017 (Version 2020_v1.0), https://doi.org/10.5281/zenodo.3754964 (last access: April 26, 2020), 2020c.

McLinden, C. A., Fioletov, V., Boersma, K. F., Krotkov, N., Sioris, C. E., Veefkind, J. P., and Yang, K.: Air quality over the Canadian oil sands: A first assessment using satellite observations, Geophysical Research Letters, 39, 10.1029/2011GL050273, 2012.

McLinden, C. A., Fioletov, V., Shephard, M. W., Krotkov, N., Li, C., Martin, R. V., Moran, M. D., and Joiner, J.: Space-based detection of missing sulfur dioxide sources of global air pollution, Nature Geoscience, 9, 496, 10.1038/ngeo2724 https://www.nature.com/articles/ngeo2724#supplementary-information, 2016.

MEGAN: The Model of Emissions of Gases and Aerosols from Nature, Version 3.1, https://sites.google.com/uci.edu/bai/megan/data-and-code (last access: 4 March 2020), 2019.

Meidiana, C., and Gamse, T.: Development of Waste Management Practices in Indonesia, European Journal of Scientific Research, 40, 199-210, 2010.

Mickley, L. J., Jacob, D. J., Field, B. D., and Rind, D.: Effects of future climate change on regional air pollution episodes in the United States, Geophysical Research Letters, 31, 10.1029/2004GL021216, 2004.

Moravek, A., Murphy, J. G., Hrdina, A., Lin, J. C., Pennell, C., Franchin, A., Middlebrook, A. M., Fibiger, D. L., Womack, C. C., McDuffie, E. E., Martin, R., Moore, K., Baasandorj, M., and Brown, S. S.: Wintertime spatial distribution of ammonia and its emission sources in the Great Salt Lake region, Atmos. Chem. Phys., 19, 15691-15709, 10.5194/acp-19-15691-2019, 2019.

Mozurkewich, M.: The dissociation constant of ammonium nitrate and its dependence on temperature, relative humidity and particle size, Atmospheric Environment. Part A. General Topics, 27, 261-270, https://doi.org/10.1016/0960-1686(93)90356-4, 1993.

Nagpure, A. S., Ramaswami, A., and Russell, A.: Characterizing the Spatial and Temporal Patterns of Open Burning of Municipal Solid Waste (MSW) in Indian Cities, Environ. Sci. Technol., 49, 12904-12912, 10.1021/acs.est.5b03243, 2015.

NEI: 2011 National Emissions Inventory (NEI) Data, https://www.epa.gov/air-emissions-inventories/2011-national-emissions-inventory-nei-data(last), 2013.

Paulot, F., Jacob, D. J., Pinder, R. W., Bash, J. O., Travis, K., and Henze, D. K.: Ammonia emissions in the United States, European Union, and China derived by high-resolution inversion of ammonium wet deposition data: Interpretation with a new agricultural emissions inventory (MASAGE_NH3), J. Geophys. Res. Atmos., 119, 4343-4364, 10.1002/2013JD021130, 2014.

Philip, S., Martin, R. V., Snider, G., Weagle, C. L., van Donkelaar, A., Brauer, M., Henze, D. K., Klimont, Z., Venkataraman, C., Guttikunda, S. K., and Zhang, Q.: Anthropogenic fugitive, combustion and industrial dust is a significant, underrepresented fine particulate matter source in global atmospheric models, Environmental Research Letters, 12, 044018, 10.1088/1748-9326/aa65a4, 2017.

RAQC: Regional Air Quality Council: Summary of State Implementation Plans, https://raqc.egnyte.com/dl/KZXQmQtFaQ/2019_SIP_Summaries_Update.pdf_(last access: January 23, 2020), 2019.

Reyna-Bensusan, N., Wilson, D. C., and Smith, S. R.: Uncontrolled burning of solid waste by households in Mexico is a significant contributor to climate change in the country, Environmental Research, 163, 280-288, https://doi.org/10.1016/j.envres.2018.01.042, 2018.

Sadavarte, P., and Venkataraman, C.: Trends in multi-pollutant emissions from a technology-linked inventory for India: I. Industry and transport sectors, Atmos. Environ., 99, 353-364, https://doi.org/10.1016/j.atmosenv.2014.09.081, 2014.

Saxena, P., and Seigneur, C.: On the oxidation of SO2 to sulfate in atmospheric aerosols, Atmospheric Environment (1967), 21, 807-812, https://doi.org/10.1016/0004-6981(87)90077-1, 1987.

Schöpp, W., Klimont, Z., Suutari, R., and Cofala, J.: Uncertainty analysis of emission estimates in the RAINS integrated assessment model, Environmental Science & Policy, 8, 601-613, https://doi.org/10.1016/j.envsci.2005.06.008, 2005.

Sharma, G., Sinha, B., Pallavi, Hakkim, H., Chandra, B. P., Kumar, A., and Sinha, V.: Gridded Emissions of CO, NOx, SO2, CO2, NH3, HCl, CH4, PM2.5, PM10, BC, and NMVOC from Open Municipal Waste Burning in India, Environ. Sci. Technol., 53, 4765-4774, 10.1021/acs.est.8b07076, 2019.

Shindell, D., and Smith, C. J.: Climate and air-quality benefits of a realistic phase-out of fossil fuels, Nature, 573, 408-411, 10.1038/s41586-019-1554-z, 2019.

SMoG-India: Speciated Multi-pollutant Generator, https://sites.google.com/view/smogindia (last access: 28 February 2020), 2019.

South Korea National Institute of Environmental Research: National air pollutants emission service, http://airemiss.nier.go.kr/ (last access: 15 Janurary 2018), 2016.

Stanaway, J. D., Afshin, A., Gakidou, E., Lim, S. S., Abate, D., Abate, K. H., Abbafati, C., Abbasi, N., Abbastabar, H., Abd-Allah, F., Abdela, J., Abdelalim, A., Abdollahpour, I., Abdulkader, R. S., Abebe, M., Abebe, Z., Abera, S. F., Abil, O. Z., Abraha, H. N., Abrham, A. R., Abu-Raddad, L. J., Abu-Rmeileh, N. M. E., Accrombessi, M. M. K., Acharya, D., Acharya, P., Adamu, A. A., Adane, A. A., Adebayo, O. M., Adedoyin, R. A., Adekanmbi, V., Ademi, Z., Adetokunboh, O. O., Adib, M. G., Admasie, A., Adsuar, J. C., Afanvi, K. A., Afarideh, M., Agarwal, G., Aggarwal, A., Aghayan, S. A., Agrawal, A., Agrawal, S., Ahmadi, A., Ahmadi, M., Ahmadieh, H., Ahmed, M. B., Aichour, A. N., Aichour, I., Aichour, M. T. E., Akbari, M. E., Akinyemiju, T., Akseer, N., Al-Aly, Z., Al-Eyadhy, A., Al-Mekhlafi, H. M., Alahdab, F., Alam, K., Alam, S., Alam, T., Alashi, A., Alavian, S. M., Alene, K. A., Ali, K., Ali, S. M., Alijanzadeh, M., Alizadeh-Navaei, R., Aljunid, S. M., Alkerwi, A. a., Alla, F., Alsharif, U., Altirkawi, K., Alvis-Guzman, N., Amare, A. T., Ammar, W., Anber, N. H., Anderson, J. A., Andrei, C. L., Androudi, S., Animut, M. D., Anjomshoa, M., Ansha, M. G., Antó, J. M., Antonio, C. A. T., Anwari, P., Appiah, L. T., Appiah, S. C. Y., Arabloo, J., Aremu, O., Ärnlöv, J., Artaman, A., Aryal, K. K., Asayesh, H., Ataro, Z., Ausloos, M., Avokpaho, E. F. G. A., Awasthi, A., Ayala Quintanilla, B. P., Ayer, R., Ayuk, T. B., Azzopardi, P. S., Babazadeh, A., Badali, H., Badawi, A., Balakrishnan, K., Bali, A. G., Ball, K., Ballew, S. H., Banach, M., Banoub, J. A. M., Barac, A., Barker-Collo, S. L., Bärnighausen, T. W., Barrero, L. H., Basu, S., Baune, B. T., Bazargan-Hejazi, S., Bedi, N., Beghi, E., Behzadifar, M., Behzadifar, M., Béjot, Y., Bekele, B. B., Bekru, E. T., Belay, E., Belay, Y. A., Bell, M. L., Bello, A. K., Bennett, D. A., Bensenor, I. M., Bergeron, G., Berhane, A., Bernabe, E., Bernstein, R. S., Beuran, M., Beyranvand, T., Bhala, N., Bhalla, A., Bhattarai, S., Bhutta, Z. A., Biadgo, B., Bijani, A., Bikbov, B., Bilano, V., Bililign, N., Bin Sayeed, M. S., Bisanzio, D., Biswas, T., Bjørge, T., Blacker, B. F., Bleyer, A., Borschmann, R., Bou-Orm, I. R., Boufous, S., Bourne, R., Brady, O. J., Brauer, M., Brazinova, A., Breitborde, N. J. K., Brenner, H., Briko, A. N., Britton, G., Brugha, T., Buchbinder, R., Burnett, R. T., Busse, R., Butt, Z. A., Cahill, L. E., Cahuana-Hurtado, L., Campos-Nonato, I. R., Cárdenas, R., Carreras, G., Carrero, J. J., Carvalho, F., Castañeda-Orjuela, C. A., Castillo Rivas, J., Castro, F., Catalá-López, F., Causey, K., Cercy, K. M., Cerin, E., Chaiah, Y., Chang, H.-Y., Chang, J.-C., Chang, K.-L., Charlson, F. J., Chattopadhyay, A., Chattu, V. K., Chee, M. L., Cheng, C.-Y., Chew, A., Chiang, P. P.-C., Chimed-Ochir, O., Chin, K. L., Chitheer, A., Choi, J.-Y. J., Chowdhury, R., Christensen, H., Christopher, D. J., Chung, S.-C., Cicuttini, F. M., Cirillo, M., Cohen, A. J., Collado-Mateo, D., Cooper, C., Cooper, O. R., Coresh, J., Cornaby, L., Cortesi, P. A., Cortinovis, M., Costa, M., Cousin, E., Criqui, M. H., Cromwell, E. A., Cundiff, D. K., Daba, A. K., Dachew, B. A., Dadi, A. F., Damasceno, A. A. M., Dandona, L., Dandona, R., Darby, S. C., Dargan, P. I., Daryani, A., Das Gupta, R., Das Neves, J., Dasa, T. T., Dash, A. P., Davitoiu, D. V., Davletov, K., De la Cruz-Góngora, V., De La Hoz, F. P., De Leo, D., De Neve, J.-W., Degenhardt, L., Deiparine, S., Dellavalle, R. P., Demoz, G. T., Denova-Gutiérrez, E., Deribe, K., Dervenis, N., Deshpande, A., Des Jarlais, D. C., Dessie, G. A., Deveber, G. A., Dey, S., Dharmaratne, S. D., Dhimal, M., Dinberu, M. T., Ding, E. L., Diro, H. D., Djalalinia, S., Do, H. P., Dokova, K., Doku, D. T., Doyle, K. E., Driscoll, T. R., Dubey, M., Dubljanin, E., Duken, E. E., Duncan, B. B., Duraes, A. R., Ebert, N., Ebrahimi, H., Ebrahimpour, S., Edvardsson, D., Effiong, A., Eggen, A. E., El Bcheraoui, C., El-Khatib, Z., Elyazar, I. R., Enayati, A., Endries, A. Y., Er, B., Erskine, H. E., Eskandarieh, S., Esteghamati, A., Estep, K., Fakhim, H., Faramarzi, M., Fareed, M., Farid, T. A., Farinha, C. S. E. s., Farioli, A., Faro, A., Farvid, M. S., Farzaei, M. H., Fatima, B., Fay, K. A., Fazaeli, A. A., Feigin, V. L., Feigl, A. B., Fereshtehnejad, S.-M., Fernandes, E., Fernandes, J. C., Ferrara, G., Ferrari, A. J., Ferreira, M. L., Filip, I., Finger, J. D., Fischer, F., Foigt, N. A., Foreman, K. J., Fukumoto, T., Fullman, N., Fürst, T., Furtado, J. M., Futran, N. D., Gall, S., Gallus, S., Gamkrelidze, A., Ganji, M., Garcia-Basteiro, A. L., Gardner, W. M., Gebre, A. K., Gebremedhin, A. T., Gebremichael, T. G., Gelano, T. F., Geleijnse, J. M., Geramo, Y. C. D., Gething, P. W., Gezae, K. E., Ghadimi, R., Ghadiri, K., Ghasemi Falavarjani, K., Ghasemi-Kasman, M., Ghimire, M., Ghosh, R., Ghoshal, A. G., Giampaoli, S., Gill, P. S., Gill, T. K., Gillum, R. F., Ginawi, I. A., Giussani, G., Gnedovskaya, E. V., Godwin, W. W., Goli, S., Gómez-Dantés, H., Gona, P. N., Gopalani, S. V., Goulart, A. C., Grada, A., Grams, M. E., Grosso, G., Gugnani, H. C., Guo, Y., Gupta, R., Gupta, R., Gupta, T., Gutiérrez, R. A., Gutiérrez-Torres, D. S., Haagsma, J. A., Habtewold, T. D., Hachinski, V., Hafezi-Nejad, N., Hagos, T. B., Hailegiyorgis, T. T., Hailu, G. B., Haj-Mirzaian, A., Haj-Mirzaian, A., Hamadeh, R. R., Hamidi, S., Handal, A. J., Hankey, G. J., Hao, Y., Harb, H. L., Harikrishnan, S., Haro, J. M., Hassankhani, H., Hassen, H. Y., Havmoeller, R., Hawley, C. N., Hay, S. I., Hedayatizadeh-Omran, A., Heibati, B., Heidari, B., Heidari, M., Hendrie, D., Henok, A., Heredia-Pi, I., Herteliu, C., Heydarpour, F., Heydarpour, S., Hibstu, D. T., Higazi, T. B., Hilawe, E. H., Hoek, H. W., Hoffman, H. J., Hole, M. K., Homaie Rad, E., Hoogar, P., Hosgood, H. D., Hosseini, S. M., Hosseinzadeh, M., Hostiuc, M., Hostiuc, S., Hoy, D. G., Hsairi, M.,

Hsiao, T., Hu, G., Hu, H., Huang, J. J., Hussen, M. A., Huynh, C. K., Iburg, K. M., Ikeda, N., Ilesanmi, O. S., Iqbal, U., Irvani, S. S. N., Irvine, C. M. S., Islam, S. M. S., Islami, F., Jackson, M. D., Jacobsen, K. H., Jahangiry, L., Jahanmehr, N., Jain, S. K., Jakovljevic, M., James, S. L., Jassal, S. K., Jayatilleke, A. U., Jeemon, P., Jha, R. P., Jha, V., Ji, J. S., Jonas, J. B., Jonnagaddala, J., Jorjoran Shushtari, Z., Joshi, A., Jozwiak, J. J., Jürisson, M., Kabir, Z., Kahsay, A., Kalani, R., Kanchan, T., Kant, S., Kar, C., Karami, M., Karami Matin, B., Karch, A., Karema, C., Karimi, N., Karimi, S. M., Kasaeian, A., Kassa, D. H., Kassa, G. M., Kassa, T. D., Kassebaum, N. J., Katikireddi, S. V., Kaul, A., Kawakami, N., Kazemi, Z., Karyani, A. K., Kefale, A. T., Keiyoro, P. N., Kemp, G. R., Kengne, A. P., Keren, A., Kesavachandran, C. N., Khader, Y. S., Khafaei, B., Khafaie, M. A., Khajavi, A., Khalid, N., Khalil, I. A., Khan, G., Khan, M. S., Khan, M. A., Khang, Y.-H., Khater, M. M., Khazaei, M., Khazaie, H., Khoja, A. T., Khosravi, A., Khosravi, M. H., Kiadaliri, A. A., Kiirithio, D. N., Kim, C.-I., Kim, D., Kim, Y.-E., Kim, Y. J., Kimokoti, R. W., Kinfu, Y., Kisa, A., Kissimova-Skarbek, K., Kivimäki, M., Knibbs, L. D., Knudsen, A. K. S., Kochhar, S., Kokubo, Y., Kolola, T., Kopec, J. A., Kosen, S., Koul, P. A., Koyanagi, A., Kravchenko, M. A., Krishan, K., Krohn, K. J., Kromhout, H., Kuate Defo, B., Kucuk Bicer, B., Kumar, G. A., Kumar, M., Kuzin, I., Kyu, H. H., Lachat, C., Lad, D. P., Lad, S. D., Lafranconi, A., Lalloo, R., Lallukka, T., Lami, F. H., Lang, J. J., Lansingh, V. C., Larson, S. L., Latifi, A., Lazarus, J. V., Lee, P. H., Leigh, J., Leili, M., Leshargie, C. T., Leung, J., Levi, M., Lewycka, S., Li, S., Li, Y., Liang, J., Liang, X., Liao, Y., Liben, M. L., Lim, L.-L., Linn, S., Liu, S., Lodha, R., Logroscino, G., Lopez, A. D., Lorkowski, S., Lotufo, P. A., Lozano, R., Lucas, T. C. D., Lunevicius, R., Ma, S., Macarayan, E. R. K., Machado, I. E., Madotto, F., Mai, H. T., Majdan, M., Majdzadeh, R., Majeed, A., Malekzadeh, R., Malta, D. C., Mamun, A. A., Manda, A.-L., Manguerra, H., Mansournia, M. A., Mantovani, L. G., Maravilla, J. C., Marcenes, W., Marks, A., Martin, R. V., Martins, S. C. O., Martins-Melo, F. R., März, W., Marzan, M. B., Massenburg, B. B., Mathur, M. R., Mathur, P., Matsushita, K., Maulik, P. K., Mazidi, M., McAlinden, C., McGrath, J. J., McKee, M., Mehrotra, R., Mehta, K. M., Mehta, V., Meier, T., Mekonnen, F. A., Melaku, Y. A., Melese, A., Melku, M., Memiah, P. T. N., Memish, Z. A., Mendoza, W., Mengistu, D. T., Mensah, G. A., Mensink, G. B. M., Mereta, S. T., Meretoja, A., Meretoja, T. J., Mestrovic, T., Mezgebe, H. B., Miazgowski, B., Miazgowski, T., Millear, A. I., Miller, T. R., Miller-Petrie, M. K., Mini, G. K., Mirarefin, M., Mirica, A., Mirrakhimov, E. M., Misganaw, A. T., Mitiku, H., Moazen, B., Mohajer, B., Mohammad, K. A., Mohammadi, M., Mohammadifard, N., Mohammadnia-Afrouzi, M., Mohammed, S., Mohebi, F., Mokdad, A. H., Molokhia, M., Momeniha, F., Monasta, L., Moodley, Y., Moradi, G., Moradi-Lakeh, M., Moradinazar, M., Moraga, P., Morawska, L., Morgado-Da-Costa, J., Morrison, S. D., Moschos, M. M., Mouodi, S., Mousavi, S. M., Mozaffarian, D., Mruts, K. B., Muche, A. A., Muchie, K. F., Mueller, U. O., Muhammed, O. S., Mukhopadhyay, S., Muller, K., Musa, K. I., Mustafa, G., Nabhan, A. F., Naghavi, M., Naheed, A., Nahvijou, A., Naik, G., Naik, N., Najafi, F., Nangia, V., Nansseu, J. R., Nascimento, B. R., Neal, B., Neamati, N., Negoi, I., Negoi, R. I., Neupane, S., Newton, C. R. J., Ngunjiri, J. W., Nguyen, A. Q., Nguyen, G., Nguyen, H. T., Nguyen, H. L. T., Nguyen, H. T., Nguyen, M., Nguyen, N. B., Nichols, E., Nie, J., Ningrum, D. N. A., Nirayo, Y. L., Nishi, N., Nixon, M. R., Nojomi, M., Nomura, S., Norheim, O. F., Noroozi, M., Norrving, B., Noubiap, J. J., Nouri, H. R., Nourollahpour Shiadeh, M., Nowroozi, M. R., Nsoesie, E. O., Nyasulu, P. S., Obermeyer, C. M., Odell, C. M., Ofori-Asenso, R., Ogbo, F. A., Oh, I.-H., Oladimeji, O., Olagunju, A. T., Olagunju, T. O., Olivares, P. R., Olsen, H. E., Olusanya, B. O., Olusanya, J. O., Ong, K. L., Ong, S. K., Oren, E., Orpana, H. M., Ortiz, A., Ota, E., Otstavnov, S. S., Øverland, S., Owolabi, M. O., P A, M., Pacella, R., Pakhare, A. P., Pakpour, A. H., Pana, A., Panda-Jonas, S., Park, E.-K., Parry, C. D. H., Parsian, H., Patel, S., Pati, S., Patil, S. T., Patle, A., Patton, G. C., Paudel, D., Paulson, K. R., Paz Ballesteros, W. C., Pearce, N., Pereira, A., Pereira, D. M., Perico, N., Pesudovs, K., Petzold, M., Pham, H. Q., Phillips, M. R., Pillay, J. D., Piradov, M. A., Pirsaheb, M., Pischon, T., Pishgar, F., Plana-Ripoll, O., Plass, D., Polinder, S., Polkinghorne, K. R., Postma, M. J., Poulton, R., Pourshams, A., Poustchi, H., Prabhakaran, D., Prakash, S., Prasad, N., Purcell, C. A., Purwar, M. B., Qorbani, M., Radfar, A., Rafay, A., Rafiei, A., Rahim, F., Rahimi, Z., Rahimi-Movaghar, A., Rahimi-Movaghar, V., Rahman, M., Rahman, M. H. u., Rahman, M. A., Rai, R. K., Rajati, F., Rajsic, S., Raju, S. B., Ram, U., Ranabhat, C. L., Ranjan, P., Rath, G. K., Rawaf, D. L., Rawaf, S., Reddy, K. S., Rehm, C. D., Rehm, J., Reiner, R. C., Reitsma, M. B., Remuzzi, G., Renzaho, A. M. N., Resnikoff, S., Reynales-Shigematsu, L. M., Rezaei, S., Ribeiro, A. L. P., Rivera, J. A., Roba, K. T., Rodríguez-Ramírez, S., Roever, L., Román, Y., Ronfani, L., Roshandel, G., Rostami, A., Roth, G. A., Rothenbacher, D., Roy, A., Rubagotti, E., Rushton, L., Sabanayagam, C., Sachdev, P. S., Saddik, B., Sadeghi, E., Saeedi Moghaddam, S., Safari, H., Safari, Y., Safari-Faramani, R., Safdarian, M., Safi, S., Safiri, S., Sagar, R., Sahebkar, A., Sahraian, M. A., Sajadi, H. S., Salam, N., Salamati, P., Saleem, Z., Salimi, Y., Salimzadeh, H., Salomon, J. A., Salvi, D. D., Salz, I., Samy, A. M., Sanabria, J., Sanchez-Niño, M. D., Sánchez-Pimienta, T. G., Sanders, T., Sang, Y., Santomauro, D. F., Santos, I. S., Santos, J. V., Santric Milicevic, M. M., Sao Jose, B. P., Sardana, M., Sarker, A. R., Sarmiento-Suárez, R., Sarrafzadegan, N., Sartorius, B., Sarvi, S., Sathian, B., Satpathy, M., Sawant, A. R., Sawhney, M., Saylan, M., Sayyah, M., Schaeffner, E.,

Schmidt, M. I., Schneider, I. J. C., Schöttker, B., Schutte, A. E., Schwebel, D. C., Schwendicke, F., Scott, J. G., Seedat, S., Sekerija, M., Sepanlou, S. G., Serre, M. L., Serván-Mori, E., Seyedmousavi, S., Shabaninejad, H., Shaddick, G., Shafieesabet, A., Shahbazi, M., Shaheen, A. A., Shaikh, M. A., Shamah Levy, T., Shams-Beyranvand, M., Shamsi, M., Sharafi, H., Sharafi, K., Sharif, M., Sharif-Alhoseini, M., Sharifi, H., Sharma, J., Sharma, M., Sharma, R., She, J., Sheikh, A., Shi, P., Shibuya, K., Shiferaw, M. S., Shigematsu, M., Shin, M.-J., Shiri, R., Shirkoohi, R., Shiue, I., Shokraneh, F., Shoman, H., Shrime, M. G., Shupler, M. S., Si, S., Siabani, S., Sibai, A. M., Siddiqi, T. J., Sigfusdottir, I. D., Sigurvinsdottir, R., Silva, D. A. S., Silva, J. P., Silveira, D. G. A., Singh, J. A., Singh, N. P., Singh, V., Sinha, D. N., Skiadaresi, E., Skirbekk, V., Smith, D. L., Smith, M., Sobaih, B. H., Sobhani, S., Somayaji, R., Soofi, M., Sorensen, R. J. D., Soriano, J. B., Soyiri, I. N., Spinelli, A., Sposato, L. A., Sreeramareddy, C. T., Srinivasan, V., Starodubov, V. I., Steckling, N., Stein, D. J., Stein, M. B., Stevanovic, G., Stockfelt, L., Stokes, M. A., Sturua, L., Subart, M. L., Sudaryanto, A., Sufiyan, M. a. B., Sulo, G., Sunguya, B. F., Sur, P. J., Sykes, B. L., Szoeke, C. E. I., Tabarés-Seisdedos, R., Tabuchi, T., Tadakamadla, S. K., Takahashi, K., Tandon, N., Tassew, S. G., Tavakkoli, M., Taveira, N., Tehrani-Banihashemi, A., Tekalign, T. G., Tekelemedhin, S. W., Tekle, M. G., Temesgen, H., Temsah, M.-H., Temsah, O., Terkawi, A. S., Tessema, B., Teweldemedhin, M., Thankappan, K. R., Theis, A., Thirunavukkarasu, S., Thomas, H. J., Thomas, M. L., Thomas, N., Thurston, G. D., Tilahun, B., Tillmann, T., To, Q. G., Tobollik, M., Tonelli, M., Topor-Madry, R., Torre, A. E., Tortajada-Girbés, M., Touvier, M., Tovani-Palone, M. R., Towbin, J. A., Tran, B. X., Tran, K. B., Truelsen, T. C., Truong, N. T., Tsadik, A. G., Tudor Car, L., Tuzcu, E. M., Tymeson, H. D., Tyrovolas, S., Ukwaja, K. N., Ullah, I., Updike, R. L., Usman, M. S., Uthman, O. A., Vaduganathan, M., Vaezi, A., Valdez, P. R., Van Donkelaar, A., Varavikova, E., Varughese, S., Vasankari, T. J., Venkateswaran, V., Venketasubramanian, N., Villafaina, S., Violante, F. S., Vladimirov, S. K., Vlassov, V., Vollset, S. E., Vos, T., Vosoughi, K., Vu, G. T., Vujcic, I. S., Wagnew, F. S., Waheed, Y., Waller, S. G., Walson, J. L., Wang, Y., Wang, Y., Wang, Y.-P., Weiderpass, E., Weintraub, R. G., Weldegebreal, F., Werdecker, A., Werkneh, A. A., West, J. J., Westerman, R., Whiteford, H. A., Widecka, J., Wijeratne, T., Winkler, A. S., Wiyeh, A. B., Wiysonge, C. S., Wolfe, C. D. A., Wong, T. Y., Wu, S., Xavier, D., Xu, G., Yadgir, S., Yadollahpour, A., Yahyazadeh Jabbari, S. H., Yamada, T., Yan, L. L., Yano, Y., Yaseri, M., Yasin, Y. J., Yeshaneh, A., Yimer, E. M., Yip, P., Yisma, E., Yonemoto, N., Yoon, S.-J., Yotebieng, M., Younis, M. Z., Yousefifard, M., Yu, C., Zaidi, Z., Zaman, S. B., Zamani, M., Zavala-Arciniega, L., Zhang, A. L., Zhang, H., Zhang, K., Zhou, M., Zimsen, S. R. M., Zodpey, S., and Murray, C. J. L.: Global, regional, and national comparative risk assessment of 84 behavioural, environmental and occupational, and metabolic risks or clusters of risks for 195 countries and territories, 1990–2017: a systematic analysis for the Global Burden of Disease Study 2017, The Lancet, 392, 1923-1994, https://doi.org/10.1016/S0140-6736(18)32225-6, 2018.

Stevens, C. J., Dise, N. B., Mountford, J. O., and Gowing, D. J.: Impact of Nitrogen Deposition on the Species Richness of Grasslands, Science, 303, 1876, 10.1126/science.1094678, 2004.

Stohl, A., Aamaas, B., Amann, M., Baker, L. H., Bellouin, N., Berntsen, T. K., Boucher, O., Cherian, R., Collins, W., Daskalakis, N., Dusinska, M., Eckhardt, S., Fuglestvedt, J. S., Harju, M., Heyes, C., Hodnebrog, Ø., Hao, J., Im, U., Kanakidou, M., Klimont, Z., Kupiainen, K., Law, K. S., Lund, M. T., Maas, R., MacIntosh, C. R., Myhre, G., Myriokefalitakis, S., Olivié, D., Quaas, J., Quennehen, B., Raut, J. C., Rumbold, S. T., Samset, B. H., Schulz, M., Seland, Ø., Shine, K. P., Skeie, R. B., Wang, S., Yttri, K. E., and Zhu, T.: Evaluating the climate and air quality impacts of short-lived pollutants, Atmos. Chem. Phys., 15, 10529-10566, 10.5194/acp-15-10529-2015, 2015.

Streets, D. G., Canty, T., Carmichael, G. R., de Foy, B., Dickerson, R. R., Duncan, B. N., Edwards, D. P., Haynes, J. A., Henze, D. K., Houyoux, M. R., Jacob, D. J., Krotkov, N. A., Lamsal, L. N., Liu, Y., Lu, Z., Martin, R. V., Pfister, G. G., Pinder, R. W., Salawitch, R. J., and Wecht, K. J.: Emissions estimation from satellite retrievals: A review of current capability, Atmos. Environ., 77, 1011-1042, https://doi.org/10.1016/j.atmosenv.2013.05.051, 2013.

TEPA: Taiwan Emission Data System, https://erdb.epa.gov.tw/eng/DataRepository/EnvMonitor/ReportInspectAirTEDS.aspx?topic1=Environmental_and_Biological_Monitoring&topic2=Air&subject=Air_Quality (last access: 15 January 2018), 2016.

The World Bank: World Development Indicators, databank.worldbank.org/data/download/WDI_excel.zip (last access: 15 January 2018), 2016.

Travis, K. R., Jacob, D. J., Fisher, J. A., Kim, P. S., Marais, E. A., Zhu, L., Yu, K., Miller, C. C., Yantosca, R. M., Sulprizio, M. P., Thompson, A. M., Wennberg, P. O., Crounse, J. D., St. Clair, J. M., Cohen, R. C., Laughner, J. L., Dibb, J. E., Hall, S. R., Ullmann, K., Wolfe, G. M., Pollack, I. B., Peischl, J., Neuman, J. A., and Zhou, X.: Why do models overestimate surface ozone in the Southeast United States?, Atmos. Chem. Phys., 16, 13561-13577, 10.5194/acp-16-13561-2016, 2016.

UN: World Urbanization Prospects: The 2014 Revision, https://esa.un.org/unpd/wup/CD-ROM/WUP2014_XLS_CD_FILES/WUP2014-F01-Total_Urban_Rural.xls (last access: 15 January 2018), 2014.

UN: UN World Population Prospects: The 2015 Revision, http://esa.un.org/unpd/wpp/DVD/ (last access: 15 January 2018), 2015.

UN: World urbanization prospects: The 2018 revision, annual percentage of population at mid-year residing in urban areas by region, subregion, country and area, 1950-2050, https://population.un.org/wup/Download/(last access: 24 July 2019), 2018.

UN: World Population Prospects 2019: Total population (both sexes combined) by region, subregion and country, annually for 1950 to 2100, https://esa.un.org/unpd/wpp/Download/Standard/Population/(last), 2019.

UNFCCC: National Inventory Submissions of Annex I Parties to the UNFCCC, https://di.unfccc.int/(last access: 12 August 2019), 2019.

US EPA: An inventory of sources and environmental releases of dioxin-like compounds in the U.S. for the years 1987, 1995, and 2000, U.S. Environmental Protection Agency, Washington DC, EPA/600/P-03/002F, 2006.

US EPA: Criteria Air Pollutants, https://www.epa.gov/criteria-air-pollutants (last access: January 23, 2020), 2018.

US EPA: National Annual Emissions Trend: 1970-2018, https://www.epa.gov/air-emissions-inventories/air-pollutant-emissions-trends-data(last access: 26 August 2019), 2019.

van der Werf, G. R., Randerson, J. T., Giglio, L., van Leeuwen, T. T., Chen, Y., Rogers, B. M., Mu, M., van Marle, M. J. E., Morton, D. C., Collatz, G. J., Yokelson, R. J., and Kasibhatla, P. S.: Global fire emissions estimates during 1997–2016, Earth Syst. Sci. Data, 9, 697-720, 10.5194/essd-9-697-2017, 2017.

Venkataraman, C., Brauer, M., Tibrewal, K., Sadavarte, P., Ma, Q., Cohen, A., Chaliyakunnel, S., Frostad, J., Klimont, Z., Martin, R. V., Millet, D. B., Philip, S., Walker, K., and Wang, S.: Source influence on emission pathways and ambient $PM_{2.5}$ pollution over India (2015–2050), Atmos. Chem. Phys., 18, 8017-8039, 10.5194/acp-18-8017-2018, 2018.

Venkataraman, C., Bhushan, M., Dey, S., Ganguly, D., Gupta, T., Habib, G., Kesarkar, A., Phuleria, H., and Sunder Raman, R.: Indian network project on Carbonaceous Aerosol Emissions, Source Apportionment and Climate Impacts (COALESCE), Bulletin of the American Meteorological Society, 10.1175/BAMS-D-19-0030.1, 2020.

Wang, S., Zhang, Q., Martin, R. V., Philip, S., Liu, F., Li, M., Jiang, X., and He, K.: Satellite measurements oversee China's sulfur dioxide emission reductions from coal-fired power plants, Environmental Research Letters, 10, 114015, 10.1088/1748-9326/10/11/114015, 2015.

Wiedinmyer, C., Akagi, S. K., Yokelson, R. J., Emmons, L. K., Al-Saadi, J. A., Orlando, J. J., and Soja, A. J.: The Fire INventory from NCAR (FINN): a high resolution global model to estimate the emissions from open burning, Geosci. Model Dev., 4, 625-641, 10.5194/gmd-4-625-2011, 2011.

Wiedinmyer, C., Yokelson, R. J., and Gullett, B. K.: Global Emissions of Trace Gases, Particulate Matter, and Hazardous Air Pollutants from Open Burning of Domestic Waste, Environ. Sci. Technol., 48, 9523-9530, 10.1021/es502250z, 2014.

Zhang, Q., Streets, D. G., Carmichael, G. R., He, K. B., Huo, H., Kannari, A., Klimont, Z., Park, I. S., Reddy, S., Fu, J. S., Chen, D., Duan, L., Lei, Y., Wang, L. T., and Yao, Z. L.: Asian emissions in 2006 for the NASA INTEX-B mission, Atmos. Chem. Phys., 9, 5131-5153, 10.5194/acp-9-5131-2009, 2009.

Zhao, Y., Nielsen, C. P., Lei, Y., McElroy, M. B., and Hao, J.: Quantifying the uncertainties of a bottom-up emission inventory of anthropogenic atmospheric pollutants in China, Atmos. Chem. Phys., 11, 2295-2308, 10.5194/acp-11-2295-2011, 2011.

Zheng, B., Tong, D., Li, M., Liu, F., Hong, C., Geng, G., Li, H., Li, X., Peng, L., Qi, J., Yan, L., Zhang, Y., Zhao, H., Zheng, Y., He, K., and Zhang, Q.: Trends in China's anthropogenic emissions since 2010 as the consequence of clean air actions, Atmos. Chem. Phys., 18, 14095-14111, 10.5194/acp-18-14095-2018, 2018.

Zheng, B., Chevallier, F., Yin, Y., Ciais, P., Fortems-Cheiney, A., Deeter, M. N., Parker, R. J., Wang, Y., Worden, H. M., and Zhao, Y.: Global atmospheric carbon monoxide budget 2000–2017 inferred from multi-species atmospheric inversions, Earth Syst. Sci. Data, 11, 1411-1436, 10.5194/essd-11-1411-2019, 2019.

Tables

Table 1. Comparison of three historical, gridded, source-specific emission inventories of atmospheric pollutants (NO_x, SO_2, CO, NMVOCs, NH_3, BC, OC).

Inventory Name (version)	Temporal Coverage	Number of Reported Gridded Sectors	Detailed Fuels	Spatial Resolution	Reference
CEDS (v2016_07_26)	1750 – 2014	9	Total only	0.5°×0.5°	(Hoesly et al., 2018)
EDGAR (v4.3.2)	1970 – 2012	26	Biofuel (Europe only)[b]	0.1°×0.1°	(Crippa et al., 2018)
ECLIPSE (v5a)	1990, 1995, 2000, 2005, 2010 (projections to 2050)[a]	8	Total only	0.5°×0.5°	(Klimont et al., 2017;Amann et al., 2011)

[a]Projections assume current air pollution legislation (CLE) in the GAINS model
[b]Described in Crippa et al. (2019)

Table 2. CEDS sector and fuel-type definitions. Aggregate sectors and fuel-types in the **$CEDS_{Hoesly}$** and ***$CEDS_{GBD\text{-}MAPS}$*** inventories, as well as the system's *intermediate gridding sectors*, and detailed working sectors/fuel-types (consistent between $CEDS_{Hoesly}$ and $CEDS_{GBD\text{-}MAPS}$ inventories). CEDS working sectors are methodologically treated as two different categories: combustion sectors (c) and 'process' sectors (p). As described in text, combustion sector emissions are calculated as a function of CEDS working fuels while process emissions assigned to the single 'process' fuel-type.

CEDS Emission Sectors

Energy Production (ENE)
- ***Energy Production (ENE)***
  - *Electricity and heat production*
    - 1A1a_Electricity-public (c)
    - 1A1a_Electricity-autoproducer (c)
    - 1A1a_Heat-production (c)
  - *Fuel Production and Transformation*
    - 1A1bc_Other-transformation (p)
    - 1B1_Fugitive-solid-fuels (p)
  - *Oil and Gas Fugitive/Flaring*
    - 1B2_Fugitive-petr-and-gas (p)
  - *Fuel Production and Transformation*
    - 1B2d_Fugitive-other-energy (p)
  - *Fossil Fuel Fires*
    - 7A_Fossil-fuel-fires (p)

Industry (IND)
- ***Industry (IND)***
  - *Industrial combustion*
    - 1A2a_Ind-Comb-Iron-steel (c)
    - 1A2b_Ind-Comb-Non-ferrous-metals (c)
    - 1A2c_Ind-Comb-Chemicals (c)
    - 1A2d_Ind-Comb-Pulp-paper (c)
    - 1A2e_Ind-Comb-Food-tobacco (c)
    - 1A2f_Ind-Comb-Non-metalic-minerals (c)
    - 1A2g_Ind-Comb-Construction (c)
    - 1A2g_Ind-Comb-transpequip (c)
    - 1A2g_Ind-Comb-machinery (c)
    - 1A2g_Ind-Comb-mining-quarying (c)
    - 1A2g_Ind-Comb-wood-products (c)
    - 1A2g_Ind-Comb-textile-leather (c)
    - 1A2g_Ind-Comb-other (c)
    - 1A5_Other-unspecified (c)
  - *Industrial process and product use*
    - 2A1_Cement-production (p)
    - 2A2_Lime-production (p)
    - 2A6_Other-minerals (p)
    - 2B_Chemical-industry (p)
    - 2C_Metal-production (p)
    - 2H_Pulp-and-paper-food-beverage-wood (p)
    - 2L_Other-process-emissions (p)
    - 6A_Other-in-total (p)

Transportation (TRA)
- ***Road Transportation (ROAD)***
  - *Road transportation*
    - 1A3b_Road (c)

Residential, Commercial, Other (RCO)
- ***Residential (RCOR)***
  - *Res., Comm., Other - Residential*
    - 1A4b_Residential (c)
- ***Commercial (RCOC)***
  - *Res., Comm., Other - Commercial*
    - 1A4a_Commercial-institutional (c)
- ***Other (RCOO)***
  - *Res., Comm., Other - Other*
    - 1A4c_Agriculture-forestry-fishing (c)

Solvents (SLV)
- ***Solvents (SLV)***
  - *Solvents production and application*
    - 2D_Degreasing-Cleaning (p)
    - 2D3_Other-product-use (p)
    - 2D_Paint-application (p)
    - 2D3_Chemical-products-manufacture-processing (p)

Agriculture (AGR)
- ***Agriculture (AGR)***
  - *Agriculture*
    - 3B_Manure-management (p)
    - 3D_Soil-emissions (p)
    - 3I_Agriculture-other (p)
    - 3D_Rice-Cultivation (p)
    - 3E_Enteric-fermentation (p)

Waste (WST)
- ***Waste (WST)***
  - *Waste*
    - 5A_Solid-waste-disposal (p)
    - 5E_Other-waste-handling (p)
    - 5C_Waste-incineration (p)
    - 5D_Wastewater-handling (p)

Shipping (SHP)
- ***Shipping (SHP)***
  - *International shipping*
    - 1A3di_International-shipping (c)
  - *Tanker Loading*
    - 1A3di_Oil_Tanker_Loading (p)

Transportation Cont. (TRA)
- ***Non-Road Transportation (NRTR)***
  - *Non-road Transport*ation
    - 1A3c_Rail (c)
    - 1A3dii_Domestic-navigation (c)
    - 1A3eii_Other-transp (c)

CEDS Fuels

Total
- ***Coal***
  - Brown coal
  - Coal coke
  - Hard coal
- ***Biofuel***
  - Biofuel
- ***Liquid Fuel & Natural Gas***
  - Heavy oil
  - Diesel oil
  - Light oil
  - Natural Gas
- ***Process***
  - Process

1735

Table 3. Scaling Inventories

Inventory Name	Scaled Inventory Years	Scaled Species	Reference
EDGAR v4.3.2	1992 – 2012	CO, NH_3, NMVOCs, NO_x	(EC-JRC, 2018)
EMEP NFR14	1990 – 2017	CO, NH_3, NMVOCs, NO_x, SO_2, BC	(EMEP, 2019)
UNFCCC	1990 – 2017	CO, NMVOCs, NO_x, SO_2	(UNFCCC, 2019)
REAS 2.1[a]	2000 – 2008	CO, NH_3, NMVOCs, NO_x, SO_2, BC	(Kurokawa et al., 2013)
APEI (Canada)	1990 – 2017	CO, NH_3, NMVOCs, NO_x, SO_2	(ECCC, 2019)
US EPA	1970, 1975, 1980, 1985, 1990 – 2017	CO, NH_3, NMVOCs, NO_x, SO_2	(US EPA, 2019)
MEIC (China)	2008, 2010 – 2017	CO, NH_3, NMVOCs, NO_x, SO_2, BC, OC	(Zheng et al., 2018;Li et al., 2017c)
Argentina[a]	1990 – 1999, 2011 – 2009, 2011	CO, NMVOCs, NO_x, SO_2	(Argentina UNFCCC Submission, 2016)
Japan[a]	1960 – 2010	CO, NH_3, NMVOCs, NO_x, SO_2, BC, OC	(preliminary update from Kurokawa et al., 2013)[a]
NEIR (South Korea)[a]	1999 –2012	CO, NMVOCs, NO_x, SO_2	(South Korea National Institute of Environmental Research, 2016)
Taiwan[a]	2003, 2006, 2010	CO, NMVOCs, NO_x, SO_2	(TEPA, 2016)
NPI (Australia)	2000 – 2017	CO, NMVOCs, NO_x, SO_2	(ADE, 2019)
DICE-Africa[b]	2006, 2013	CO, NMVOCs, NO_x, SO_2, BC, OC	(Marais and Wiedinmyer, 2016)
SMoG-India[b]	2015	CO, NMVOCs, NO_x, SO_2, BC, OC	(Venkataraman et al., 2018)

[a]Not updated from CEDS v2019-12-23, details in Hoesly et al. (2018).

[b]Emissions scaled as a function of sector and fuel-type

Deleted: Calibration

Deleted: calibrated

Figures

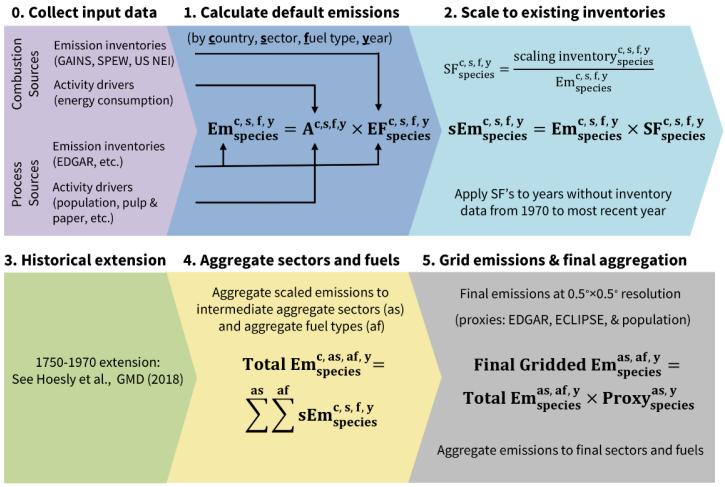

Figure 1: Default CEDS System Summary, adapted from Fig. 1 in Hoesly et al. (2018). Key steps include: (0) collecting activity driver (A) and emission factor (EF) input data for non-combustion and combustion emission sources, (1) calculating default emissions (Em) as a function of chemical species, country, emission sector, fuel-type, and year, (2) calculating scaling factors (SFs) for overlapping years with existing inventories in order to scale default estimates (sEm) and extending SFs for non-overlapping years between 1970 – 2017 (for earlier emissions, see Hoesly et al. (2018)), (4) aggregating scaled emissions to intermediate sectors and fuel-types, and (5) using source and compound-specific spatial proxies to calculate final gridded emissions and aggregating them to the final sectors and fuels. A list of intermediate and final sectors and fuels are in Table 2.

Deleted: calibrate

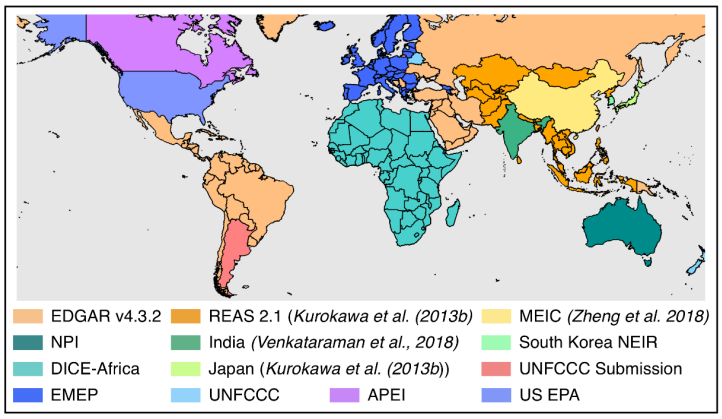

Figure 2: Final scaling inventories used for $CEDS_{GBD\text{-}MAPS}$ NO_x emissions, inventory details in Table 3.

Deleted: calibration

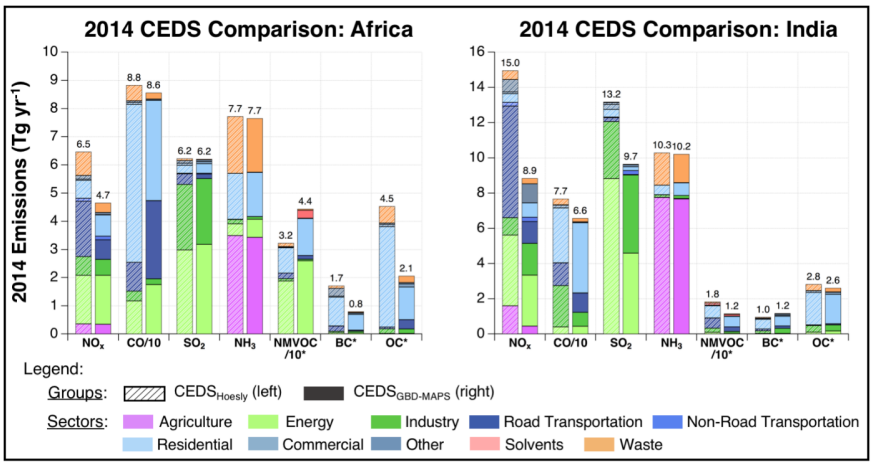

Figure 3: Sectoral contributions to total annual emissions for 2014 of $CEDS_{Hoesly}$ (left) and $CEDS_{GBD\text{-}MAPS}$ (right) emissions after scaling to DICE-Africa and SMoG-India regional inventories. The total annual emissions are given by the values above each bar, bar colors represent absolute sectoral contributions to emissions of each chemical compound. CO and NMVOC emissions are divided by 10 for clarity. Stars indicate that NMVOCs, BC, and OC emissions are in units of TgC yr^{-1}. NO_x is in units of Tg NO_2 yr^{-1}

Deleted: calibration

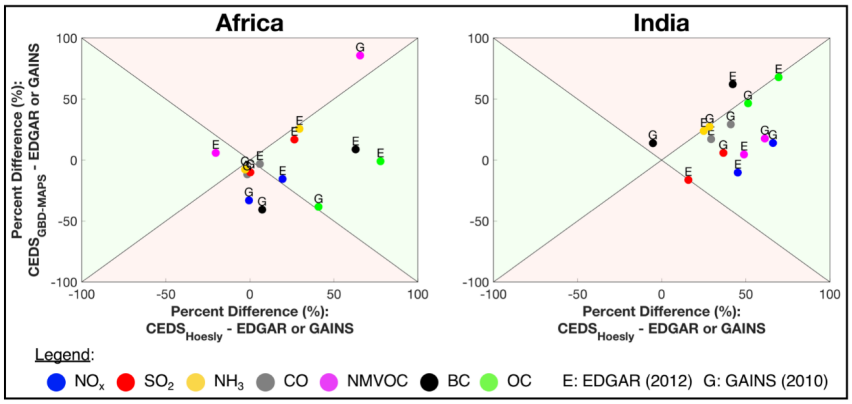

Figure 4: Comparison of the percent difference between $CEDS_{GBD\_MAPS}$. X and Y-axes show the percent difference between the CEDS emission inventories (y-axis: $CEDS_{GBD\text{-}MAPS}$, x-axis: $CEDS_{Hoesly}$) for each compound and the GAINS (ECLIPSE v5a) or EDGARv4.3.2 inventories from Africa and India (i.e., 100*(CEDS – EDGAR)/(CEDS – EDGAR)/2)). Comparisons are conducted with the most recent available year, 2010 for the comparison with GAINS and 2012 for the comparison with EDGAR. Green regions indicate areas where the $CEDS_{GBD\text{-}MAPS}$ emissions have improved agreement with EDGAR and GAINS relative to the $CEDS_{Hoesly}$ inventory. Red areas indicate regions where $CEDS_{GBD\text{-}MAPS}$ emissions have worse agreement with EDGAR or GAINS relative to the $CEDS_{Hoesly}$ inventory. The color of each point represents the chemical compound and each point is labeled with an 'E' or 'G' indicating that the percent difference was calculated using EDGAR or GAINS, respectively.

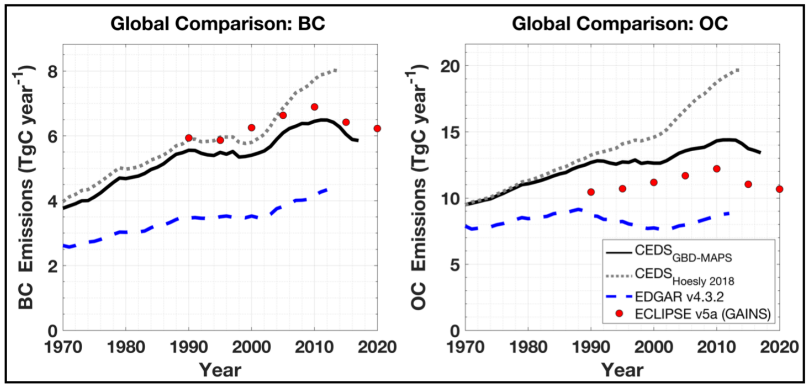

Figure 5: Comparison of global inventories of BC and OC emissions. Total EDGARv4.3.2 and GAINS (ECLIPSE v5a) emission inventories shown without agricultural waste burning and aviation emissions. $CEDS_{GBD\text{-}MAPS}$ emissions of BC and OC are not scaled to EDGAR or GAINS estimates.

Deleted: calibrated

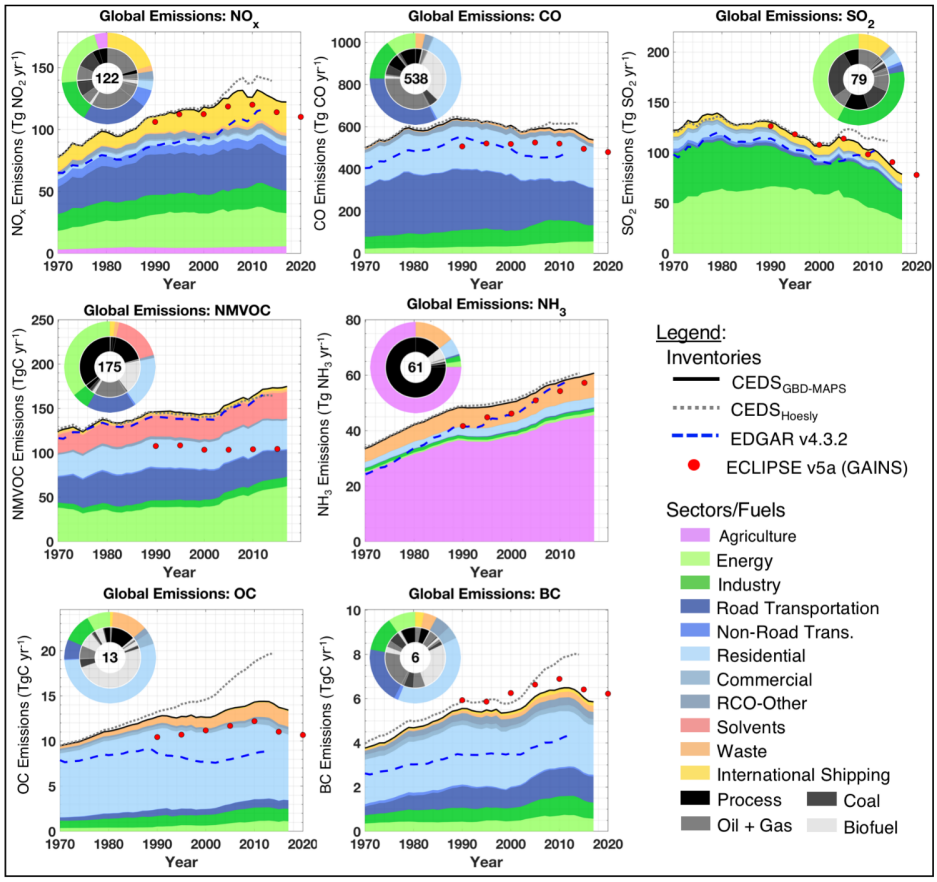

Figure 6. Time series of global annual emissions of NO_x (as NO_2), CO, SO_2, NMVOCs, NH_3, BC, and OC for all sectors and fuel types. Solid black lines are the $CEDS_{GBD-MAPS}$ inventory, with fractional sector contributions indicated by colors. Dashed gray lines are the $CEDS_{Hoesly}$ inventory. Dashed blue lines are the EDGAR v4.3.2 global inventory. Red markers are ECLIPSE v5a baseline 'current legislation' (CLE) emissions (from the GAINS model) with data in 2015 and 2020 from GAINS CLE projections. All inventories include international shipping but exclude aircraft emissions. Pie chart inserts show fractional contributions of emission sectors to total 2017 emissions (outer) and fuel type contributions to each sector (inner). Emission totals for 2017 (units: Tg yr^{-1}, TgC yr^{-1} for NMVOCs, OC, BC) are given inside each pie chart.

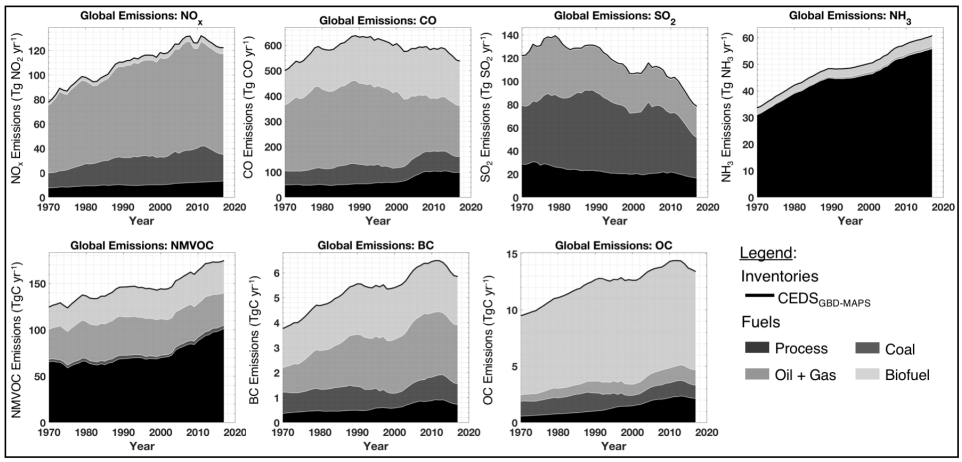

Figure 7. Time series of global annual emissions of NO_x, CO, SO_2, NH_3, NMVOCs, BC, and OC for all sectors, colored by fuel group.

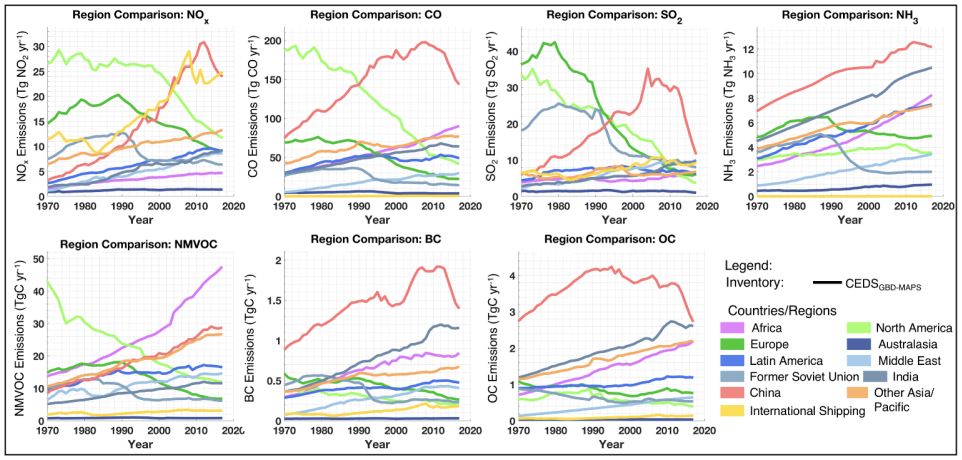

Figure 8. Time series of global annual $CEDS_{GBD-MAPS}$ emissions of NO_x, CO, SO_2, NH_3, NMVOCs, BC, and OC for all sectors and fuel types (excluding aircraft emissions), split into 11 countries/regions (defined in Table S9).

Deleted: nine